Comparison of *in vitro* high content screening methods for drug genotoxicity

Emmi Kuokkanen, 40086

ekuokkan@abo.fi

Master's Thesis in Cell Biology CB00BR56, Faculty of Science and Engineering, Åbo Akademi University

Instructors: Emma Kutvonen MSc, Mikko Karjalainen PhD, Orion Corporation Orion Pharma

Supervisor: Annika Meinander, PhD, Cell biology, Åbo Akademi University

2021

ÅBO AKADEMI

Master's Thesis in Cell Biology, 93 pages + 2 Appendix

Emmi Kuokkanen, 2021

Comparison of in vitro high content screening methods for drug genotoxicity

Keywords: DNA damage, Genotoxicity, γH2AX, pH3, p53, Flow cytometry, HCA, High content analysis, Imaging

ABSTRACT

Detection of chemicals that induce damage to the DNA is an important aspect in drug development. The recognition of these chemicals is based on *in vitro* studies followed by *in vivo* studies, the latter being both expensive and ethically questionable. An early, accurate prediction of the genotoxic properties of these chemicals is therefore highly desired.

The phosphorylated histones yH2AX and pH3 are well established genotoxicity markers, yH2AX expressed upon double-stranded DNA damage caused by clastogens, and pH3 accumulating as a cause of aneuploidy in mitosis caused by aneugens. The detection of these, in combination with a translocation of p53 to the nucleus in response to DNA damage, is one example of markers used for high content genotoxicity analyses. In this study, these three markers were used to evaluate the genotoxic predictivity of 16 reference compounds with known properties in TK6 and HepG2 cells by two different high content methods for genotoxicity screening. The cells were exposed to the compounds over a range of concentrations for 4 and 24 hours. The first method used was a validated flow cytometry-based DNA damage assay MultiFlow® which was used with both TK6 and HepG2 cells. The other method was an imaging-based high content analysis method that was set up in this study and tested on HepG2 cells only. The aim was to compare these two methods and see which method could predict the genotoxic potential more accurately.

Using the MultiFlow® method with TK6 cells and previously determined cut-off values for genotoxicity, 14 out of 16 compounds were predicted correctly. With the imaging-based method with HepG2 cells the corresponding predictivity was 15 out of 16. By adapting the imaging-based method to include a 48-hour incubation with the reference compounds all compounds could be predicted correctly. This prediction did, however, not include p53 as a criterion and it was therefore not considered as a significant marker in HepG2 cells in this study. Based on these results the imaging-based genotoxicity assay with HepG2 cells was considered a promising alternative for genotoxicity testing.

PREFACE

This Master's Thesis was conducted at the Molecular Profiling/Discovery Technologies department at Orion Pharma, Turku.

I would like to express my deepest appreciation to Emma Kutvonen, my preliminary instructor, for her valuable contribution in introducing me to the topic, guiding me through the project and all her upfront support and tuition despite being on maternity leave. I would also like to extend my deepest gratitude to Mikko Karjalainen, the head of our department, both for this opportunity and belief in my abilities as well as the patience, accessibility and helpfulness whenever needed. I'm extremely grateful to Annika Meinander, my supervisor at Åbo Akademi, for her valuable comments, insightful suggestions, and helpful contribution in revising my thesis.

I would like to collectively thank the whole Discovery Technologies team for the support and help I have received during this project. I would like to express my sincere thanks to Fanny Örn, who extended a great amount of assistance with the lab work and her helpful attitude throughout the whole project. A special thanks also to Rami Mäkelä for his expertise and helpful advice in data handling during this project. Thanks should also go to Anna-Reeta Virta for her encouraging contribution for guidance and instructions in the use of technologies and automation in the lab. I also had great pleasure to work with Paula Väyrynen, who has contributed with assistance and guidance in the lab.

I would also want to acknowledge the effort of my mother Katja, whose help in revising my thesis cannot be overestimated. Thank you for the invaluable contribution and your expertise in scientific writing. An especial appreciation also to my partner Lauri, with an admirable calmness and all the support during the whole writing process, thank you for being here for me.

Finally, as this thesis also marks the end of my studies for now, I would like to thank all the personnel at Åbo Akademi, for being both accessible and contributing to a warm supportive atmosphere at the university. I would also like to show my appreciation to all persons who were involved in the study organization Biologica, thank you for making this journey unforgettable. A special thanks also to all my nearest fellow students for the peer support during this project and the 6 past years.

Emmi Kuokkanen

Turku, 30.4.2021

ABBREVIATIONS

4NQO	4-Nitroquinoline N-oxide
ABS	Absolute value
ATM	Ataxia telangiectasia mutated
ATR	ATM and Rad3 related
BAP	Benzo[a]pyrene
BSA	Bovine Serum Albumin
CCCP	Carbonyl cyanide 3-chlorophenylhydrazone
CDK	Cyclin-dependent Ser/Thr kinase
DDR	DNA damage response
DMEM	Dulbecco's Modified Eagle Medium
DMSO	Dimethyl Sulfoxide
DNA	Deoxyribonucleic acid
DNA-PK	DNA dependent protein kinase
DSB	Double-stranded break
EEC	European Economic Community
EURL ECVAM	EU Reference Laboratory for alternatives to animal testing
FBS	Foetal bovine serum
FDA	Food and Drug Administration
FITC	Fluorescein isothiocyanate
FSC	Forward scatter
GEF	Global evaluation factor

HCA	High content analysis
HCI	High content imagining
HCS	High content screening
ICH	International Council for Harmonisation of Technical Requirements for Pharmaceuticals for Human Use
LEC	Lowest effective concentration
LPC	Lowest precipitating concentration
MAD	Median absolute deviation
MMS	Methyl methanesulfonate
MoA	Mechanism of action
MRN	MRE11-RAD50-NBS1
OECD	The Organisation for Economic Co-operation and Development
PARP	Poly (ADP-ribose) polymerase
PBS	Phosphate buffered saline
PBST	Triton + PBS
PE	Phycoerythrin
pH3	Phospho-Histone H3
PI	Propidium Iodide
QC	Quality control
RNC	Relative nuclei count
ROS	Reactive oxygen species
RT	Room Temperature
SSC	Side scatter
γH2AX	Phospho-Histone H2A.X

TABLE OF CONTENTS

I INTRODUCTION

Toxicological analysis is an important aspect in safety for all chemical substances (Corvi & Madia, 2017). In all industries, including the pharma, all chemicals intended for animal or human use are required to be tested for their toxicological properties (Custer & Sweder, 2008). The toxicological testing is regulated by the authorities and all drugs under development are screened for a variety of toxicological properties (Whitebread, Hamon, Bojanic, & Urban, 2005). A drug candidate that induces toxicity in a cell or organism is highly undesirable and a common reason for rejection from the drug development process (Whitebread et al., 2005). Therefore, it is desirable to be able to detect the toxicological effects of the compounds as early as possible in the development. To avoid extensive *in vivo* testing, which may lead to unnecessary costs and animal suffering, improvement in precision and accuracy of *in vitro* tests is an important aspect in drug development (Custer & Sweder, 2008).

The toxicological effects of chemicals can be classified into different categories. A compound at a certain concentration is considered cytotoxic if it causes cell death (Ramakrishna, Tian, Wang, Liao, & Teo, 2015). All chemicals are cytotoxic at a high concentration and cytotoxicity can, in some cases, be observed as an outcome of other types of toxicity. For example, mitochondrial toxins can cause depletion in the energy of the cell which ultimately leads to apoptosis (Ramakrishna et al., 2015). Genotoxicity, in contrast, is the mechanism where a compound induces damage to the DNA (Custer & Sweder, 2008). Severe damage to the DNA may also lead to cell cycle arrest and cause apoptosis (Niida & Nakanishi, 2006). As a consequence, the range of concentrations in genotoxicity testing lies around and below the concentrations where the compound shows cytotoxic properties.

Determination of genotoxic properties of chemicals is used to predict carcinogenic and mutagenic effects in humans and animals. Damage to the DNA may lead to mutations which give rise to cancer or otherwise damage the inheritance (Corvi & Madia, 2017). Currently there are several approved *in vitro* methods for genotoxicity testing, but new methods are of high interest for more accurate, efficient, cost effective and precise determinations. Genotoxic testing is highly regulated to ensure the safety and protection of human and animal health. Legislation covers several areas such as pharmaceuticals, veterinary products, industrial chemistry, cosmetics, food additives, pesticides and many more. (Corvi & Madia, 2017). Testing of compounds is primarily

based on *in vitro* testing, followed by *in vivo* testing. Guidelines for testing is both dependant on the purpose of use of the product and the country where marketing authorisations is sought. For pharmaceuticals the guidelines for genotoxicity testing are regulated by the European community EEC in Europe, the Japanese ministry of health and welfare in Japan and FDA in the USA (European Medicines Agency, 2012). The guidelines for testing are based on Organisation for Economic Co-operation and Development (OECD) guidelines (*OECD home.*). One of the current challenges is to develop methods that have a high sensitivity and specificity *in vitro*, which would reduce the burden of expensive and ethically questionable *in vivo* testing. (Corvi & Madia, 2017)

II LITERATURE REVIEW

1. DNA Damage

1.1 DNA damage pathway

The DNA is located in the nucleus of the cell and serves as the storage of genetic information. It is continuously interacting with several different molecules and substances, which are e.g., involved in transcription and replication. The DNA molecule is highly dynamic and therefore also prone to errors and damages. (Chatterjee & Walker, 2017) To be able to preserve and carry on the genetic information the cell is continuously repairing damages that occur on the DNA. This mechanism is collectively called the DNA damage response (DDR), which consists of sensors that recognise the damage, and mediators and transducers which signal the damage to effectors. There are several different types of DNA damage, commonly classified as endogenous and exogenous damage (Chatterjee & Walker, 2017). The endogenous damage is caused by biochemical reactions where the DNA molecule reacts with factors naturally present in the cell, such as reactive oxygen species (ROS) or oxidative reactions with water (Chatterjee & Walker, 2017). The exogenous damage is caused by external factors, such as radiation and chemical agents (Chatterjee & Walker, 2017). The type of damage caused steers the DDR. Different types of sensors recognise specific types of damage and mediate the signal through various signalling cascades.

The DDR response reacts to the DNA damage and leads to a cascade of signalling events that may cause cell cycle delay or arrest in an attempt to repair the damage to the DNA. The final outcome is dependent on DNA damage checkpoint molecules that consist of sensors, mediators, transducers and effectors, which will determine the actions of the cell and guide it through cell cycle arrest, DNA repair or apoptosis (figure 1). (Niida & Nakanishi, 2006)

The DNA damage sensors consists of a group of proteins that are involved in identifying different types of damage of DNA and mediate the signal of a damage via transducer and mediator proteins. The sensor proteins accumulate at the sites of the DNA damage, promoting the phosphorylation of the mediator proteins. The kinases that mediate the phosphorylation of proteins in the DDR and cell cycle progression

are collectively called checkpoint kinases. (Niida & Nakanishi, 2006) The mediators and transducers amplify the signal from the damage and mediate it to different types of effector proteins, which regulate intracellular processes (Wan, Liu, Han, Zhang, & Lu, 2014). The effectors are in many cases proteins that control the cell cycle which allows the cells to repair the damage. Only when damage is repaired cell cycle progression is continued. Otherwise, signals will mediate the cell to commit the apoptotic pathway. (Niida & Nakanishi, 2006)

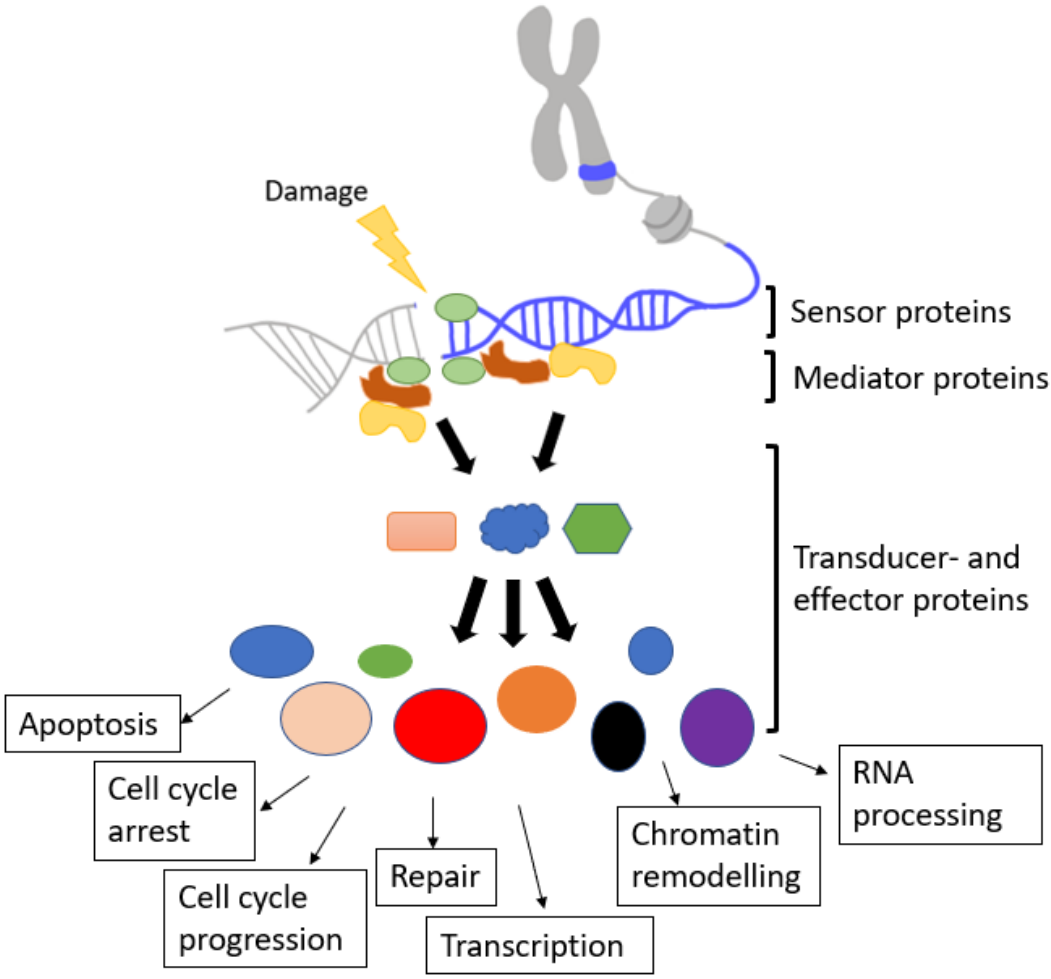

Figure 1, DNA damage response. Damage to the DNA or stalled replication leads to a signalling cascade. The DNA damage sensors (green spheres on the DNA) identify the damage and recruit mediator proteins (yellow and orange in close proximity to the DNA) to the site of the damage. The mediators amplify the signal and mediate the signal to various transducer and effector proteins. The effectors induce the cellular responses which may include changes in transcription, RNA processing, chromatin remodelling and cell cycle arrest or progression. These changes contribute to either DNA repair or apoptosis. (Jackson & Bartek, 2009)

1.2 Cell cycle progression and DNA damage

The most important function of the cell cycle is to replicate and to transfer the genetic material of a cell intactly to both daughter cells. The cell cycle progress and DNA damage response are, therefore, tightly coupled processes to avoid damages being inherited to daughter cells. The cell cycle is divided into four stages: G1, S, G2 and M phase (figure 2). The S phase stands for synthesis and represents the phase where the DNA is replicated. The M phase stands for mitosis and is the stage where the chromosomes condense and the cell divides. In between these phases the G1 and G2 "gap" phases take place, in which regulation of several cell cycle proteins and cell cycle progression checkpoints is activated. One of the most important type of cell cycle progression proteins are the cyclin-dependent serine/threonine kinases (CDKs) which interact with cyclins and control the cell cycle by periodic activation and deactivation. In general, the activity of different CDKs vary from the G1 phase throughout to the M phase, with different CDKs being active at different stages of the cell cycle. In addition, for the cells to be able to progress from one phase to another, certain checkpoint proteins need to be activated or deactivated. In the case of DNA damage, the signalling molecules interact with these checkpoints and inhibit the cell cycle progression until the damage has been corrected. The phase of the cell cycle can also affect which type of result the DNA damage response has on the repair process. (Hustedt & Durocher, 2016)

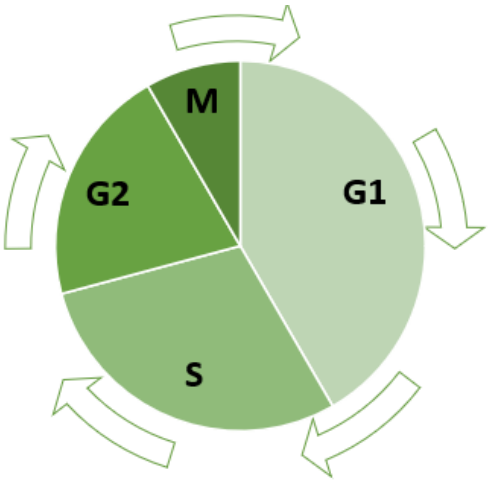

Figure 2, Cell cycle progression. In the G1 phase the cell prepares for division. At the transition from the G1 to the S phase, certain regulatory CDKs need to become activated to allow the cells to enter the S phase. In the S phase, the DNA is replicated to transition to the G2 phase, where another set of checkpoint molecules are activated, which certify that the DNA is fully replicated and the cell is ready to progress to the next phase. Likewise, at the G2 to M transition checkpoint molecules allow transition when the cell is ready to divide. The M phase when the cell divides is the shortest of the phases. As the division is successfully established, the CDKs become inactivated resulting in that the daughter cells are shifted back to the G1 phase.

1.3 Histones in DNA damage

DNA architecture is highly dependent on all DNA-associated proteins. The histones are one of these. The histone proteins form nucleosomes which have the DNA wrapped around them. Nucleosomes are highly dynamic structures that, in addition to chromosome condensation, allow the replication, transcription and repair of DNA. (Bartova, Krejci, Harnicarova, Galiova, & Kozubek, 2008)

1.3.1 Structure of the nucleosomes

The nucleosomes consist of four main categories of histones, H2A, H2B, H3 and H4. The histones assemble as illustrated in figure 3. H2A and H2B form two dimers which associate with a H3-H4 tetramer, consisting of two H3-H4 dimers. (Chen, Kang, Fan, & Tang, 2014) The core histones share similar structures which consist of the core and a tail-like structure that extends out of the nucleosome and is a site for several posttranslational modifications (Chen et al., 2014). Histones can be modified by acetylation, methylation, phosphorylation and sumoylation, altering the structure and activity of histones and the nucleosome formation. In addition, histones serve as docking sites for other regulatory proteins (Chen et al., 2014).

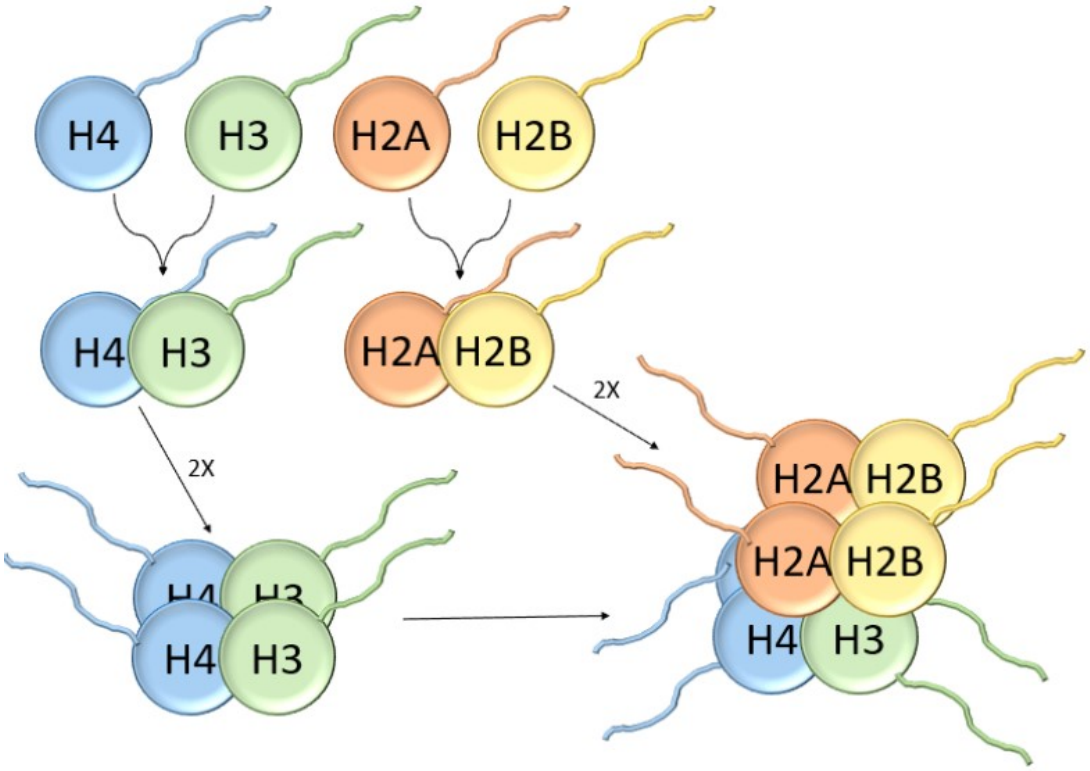

Figure 3, Histone structure and histone assembly. The nucleosome consists of eight core histones. The histones H3 and H4 form two dimers which form a tetramer. The H3-H4 tetramer then serves as a binding site for two H2A-H2B dimers.

1.3.2 H2AX in DNA damage response

The H2AX protein is one variant of the H2A family with an abundancy of about 10% in human fibroblasts (Kopp, Khoury, & Audebert, 2019a). Since each nucleosome consists of two H2A proteins, the H2AX is found approximately in every fifth nucleosome. H2AX differs from other H2A subtypes with a unique C terminal tail containing a highly conserved Serine139, located four residues from the end of the C terminal tail (Dickey et al., 2009). This serine is rapidly phosphorylated in response to DNA damage. The phosphorylated form of the histone is called γH2AX (Podhorecka, Skladanowski, & Bozko, 2010).

The phosphorylation of H2AX is triggered at an early stage of DNA damage by proteins of the PI3-kinase family which include ataxia telangiectasia mutated (ATM), ATM and Rad3-related (ATR) or DNA-dependent protein kinase (DNA-PK) (figure 4) (Dickey et al., 2009). The type of DNA damage controls the expression and phosphorylation of DNA damage response proteins. The signalling pathway that follows is determined by the proteins that bind to the site of the break and which molecules they interact with.

In case of a double-stranded break (DSB) ATM is autophosphorylated which is followed by increased kinase activity and γH2AX phosphorylation. The autophosphorylation of ATM is mediated by the DSB recognising MRE11-RAD50-NBS1 (MRN)-complex which recruits both the kinase and its other targets to the site of the damage. (Podhorecka et al., 2010) In addition, the γH2AX serves as a docking site for several other proteins included in the DNA damage and signalling process. Upon DSB, the complex mediates a positive feedback loop where the mediator of DNA damage checkpoint protein 1 (MDC1) binds to γH2AX and interacts with parts of the MDR complex. Since the complex promotes the ATM autophosphorylation, it leads to the spreading of the H2AX phosphorylation on the length of the DNA. (Podhorecka et al., 2010) The ATR and DNA-PK mediated responses are coupled to other types of DNA damage and also lead to H2AX phosphorylation. ATR becomes activated upon damage or failure of DNA replication, such as lagging replication forks or single-stranded DNA breaks (Menolfi & Zha, 2020). Activation of DNA-PK is mediated by the presence of double-stranded DNA ends (Menolfi & Zha, 2020). These mechanisms result in H2AX phosphorylation upon DNA damage and the positive feedback loop causes a significant expression of γH2AX in cells which have been

exposed to DNA damage. The dephosphorylation of γH2AX is also critical for DNA damage response and cell cycle progression. One main protein involved in the dephosphorylation of γH2AX is the Wip1 which is a chromatin-associated phosphatase (Banerjee & Chakravarti, 2011). Several other phosphatases have been identified to dephosphorylate γH2AX, some of them mediated by the same ATM kinase involved in H2AX phosphorylation (Tu et al., 2013)

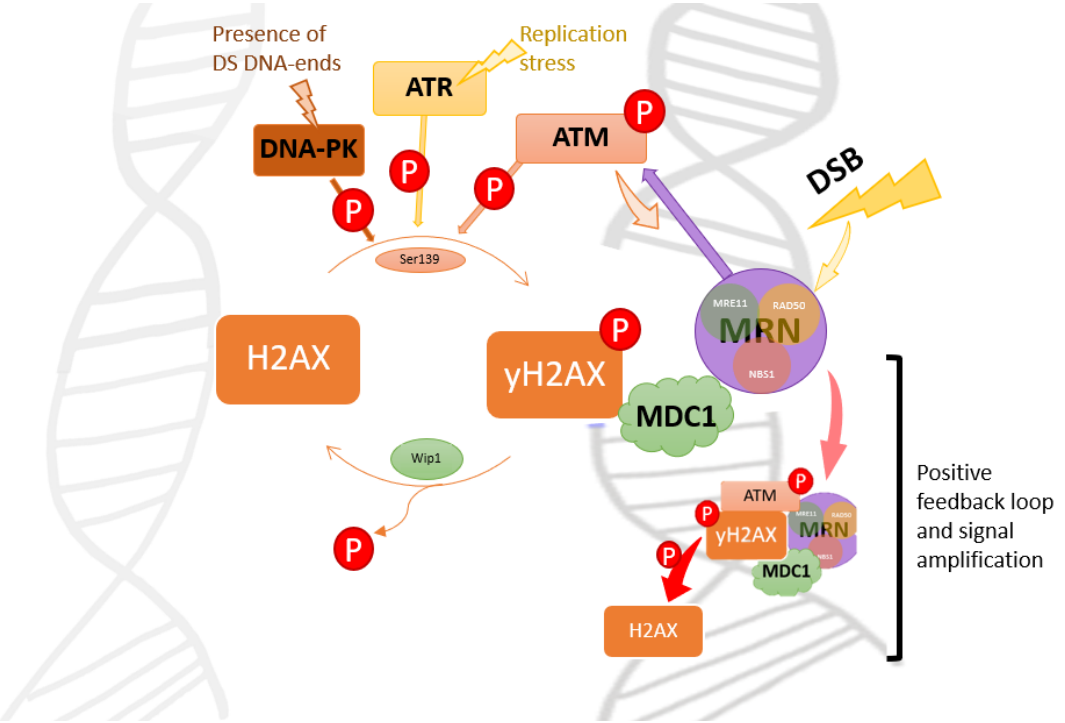

Figure 4, H2AX phosphorylation and dephosphorylation. The phosphorylation of H2AX is mediated by one or several of PI-3 family kinases. DNA-PK is activated upon recognition of DS-DNA ends, ATR is activated upon replication stress and ATM as a consequence of DSB. Upon DNA damage the MRN complex (see text for further details) is assembled on the site of the break and recruits ATM to the site, promoting its autophosphorylation. ATM phosphorylates H2AX on Ser139 and the phosphorylated γH2AX mediates the binding of MDC1, which further interacts with the MRN complex. This interaction between the proteins creates a feedback loop where γH2AX interacts with MDC1 which interacts with MRN resulting in recruitment of ATM which spreads the phosphorylation of γH2AX.

1.3.3 Phosphorylation of H3 mediates chromosome condensation

Like the other histones, histone H3 has a tail that is highly prone to posttranslational modifications. Upon progression through the cell cycle, the chromatin is remodelled where one important aspect is the condensation and decondensation of the chromatin. One well-established modification is the phosphorylation of H3 at Serine10, which is mediated by the Aurora family of kinases, mainly Aurora B (Khoury, Zalko, & Audebert, 2016a). The phosphorylated form of H3 is called pH3 which is present in cells during metaphase when the chromatin is condensed (Hans & Dimitrov, 2001). When the cell exits metaphase and the cell cycle progresses, the pH3 is dephosphorylated and the chromatin returns to a less condensed form. The phosphorylated form of H3 is, therefore, present only during mitosis. In a situation where chromosome separation is damaged or interrupted the cell cycle arrests and pH3 stays in a phosphorylated state until the cell continues the cell division, or apoptosis is mediated. (Kopp et al., 2019)

1.4 p53 in DNA damage

The tumor suppressor p53 is recognised as “the guardian of the genome”. It is present in several processes concerning cell cycle progression and DNA damage (Williams & Schumacher, 2016). p53 plays a central role in the signalling pathways of DNA damage, controlling both cell cycle progression and apoptosis. The concentration and localisation of p53 in the cell is regulated by posttranslational modifications. In the normal state ubiquitination leads to degradation of p53 but upon DNA damage p53 becomes phosphorylated by ATR and ATM kinases which are also involved in H2AX phosphorylation (Niida & Nakanishi, 2006). The phosphorylation of p53 promotes its nuclear localisation by inhibiting nuclear export, as well as by inhibiting ubiquitination and degradation (Niida & Nakanishi, 2006). Therefore, upon DNA damage p53 may localise and accumulate in the nucleus where it acts as a transcription factor for proteins involved in the DDR (Reaves et al., 2000).

1.5 Chemicals induce genotoxicity by several mechanisms

1.5.1 The mechanism of action classifies the type of damage

Different chemicals can cause genotoxic effects in several ways. A straightforward DNA damage is when the compound itself interacts with the DNA causing DNA damage or cell division errors. In other cases, the compound is metabolised by the cell and the metabolites of the compound cause the damage. A chemical can also disturb other processes within the cell which ultimately leads to a toxic effect. In addition, the chemical or its metabolites can interact with other chemicals and in a combination become toxic. The mechanism of action (MoA) of a chemical is used to classify chemicals into different toxicological groups to understand the mechanism behind their toxicity. The genotoxic effects are commonly classified into two groups, aneugenic and clastogenic compounds.

1.5.2 Aneugens

Compounds that are classified as aneugens are chemicals that do not interact with the DNA itself but rather cause defects in the mechanisms related to cell division and chromosome separation (Khoury et al., 2016). The separation of chromosomes in mitosis is a complex process involving several proteins. Inhibition or damage to any of these compounds might cause defects in segregation. Aneugenic compounds interact with processes such as mitotic spindle formation or degradation or inhibit mitotic kinases, resulting in improper chromosome segregation or cell cycle arrest. Vinblastine is one well-recognised aneugen, which specifically binds to microtubules in the mitotic spindle and interferes with their function (Chun, Garrett, & Vail, 2007). Likewise, colchicine and paclitaxel are chemicals that interfere with microtubules, colchicine inhibiting their assembly and paclitaxel inhibiting the disassembly (Ganguly, Yang, & Cabral, 2010) (Bharadwaj & Yu, 2004). Both mechanisms inhibit the cells from proceeding with the cell cycle. These compounds, therefore, cause the cells to pause in the M phase, which can be seen by expression of phosphorylated pH3 in the cells (Khoury et al., 2016). In a population, an increase in number of pH3 positive cells, therefore, indicate a mechanism that cause the cells to remain prolonged in the M phase. The improper segregation of chromosomes and errors in division can lead to both chromosome breakage, whole chromosomes being left behind or

transferred to the wrong daughter cell. Aneugenic compounds can also lead to formation of micronuclei, which are fragments of DNA that fail to end up in the main nucleus of the daughter cells. These pieces of DNA form tiny extranuclear bodies which are up to 10-100 times smaller than the main nuclei. (Westerink, Schirris, Horbach, & Schoonen, 2011)

1.5.3 Clastogens

Clastogenic compounds are agents that interact directly with the DNA, thus inducing damage to it (Khoury et al., 2016). There are several ways that a chemical can cause DNA damage and the type of damage caused usually determines the path of DDR. One type of damage is damage to only one strand of the DNA, i.e., modifications to the bases or sugars of the DNA backbone. A more severe type of damage is the DSB which lead to the breakage of both DNA strands. The repair of DSB is usually either via non homologous end joining (NHEJ) or homology-based repair (HRR). As discussed previously, the DSB trigger a pathway that leads to H2AX phosphorylation and is therefore a well-established validated marker for genotoxicity caused by clastogenic compounds. Upon the DDR p53 is in many cases upregulated as a response to the damage (Williams & Schumacher, 2016). Clastogenic damage can arise via several mechanisms. One well-established clastogen is Methyl methanesulfonate (MMS), which is a DNA methylating agent which forms DNA adducts (Takeiri et al., 2019). Other types of clastogens are for example cross-linkers, topoisomerase inhibitors and compounds that form reactive oxygen species (ROS) (Takeiri et al., 2019). Damage caused by clastogens can lead to the formation of micronuclei as unrepaired or incorrectly repaired DSB can cause fragments of DNA to be left behind during mitosis (Westerink et al., 2011).

1.6 Mechanisms for detecting DNA damage

As several mechanisms of DNA damage exist, different methods for genotoxicity testing are required for prediction of these properties. The Organisation for Economic Co-operation and Development (OECD) is an international organisation that provides guidelines for identification and characterisation of potentially hazardous chemicals (*OECD home.*). There are several well-established tests for DNA damage, including the bacterial mutagenesis test, the micronucleus test, the chromosome aberration test and the comet assay test.

The bacterial mutation test, also known as the Ames test, is a method used to detect point mutations in the genome. It is based on a method using a large number of mutated bacteria from different strains, which are exposed to the test chemical. The bacteria are unable to synthesise an essential amino acid as a cause of the mutation, unless the chemical is causing mutations which are able to revert the original mutation. (OECD, 2020)

Whereas the Ames test is only able to detect point mutations, the micronucleus test, the chromosome aberration test and the comet assay test can detect larger damages on the DNA. These are all based on detection of larger DNA fragments that are produced upon DNA damage. The comet assay test is based on detection of DNA fragments on an agarose gel. Cells exposed to test chemicals are lysed and exposed to electrophoresis at a high pH. The stained DNA can then be visualised on the gel as a comet-like structure, where the different-sized DNA fragments have migrated different distances. The intensity and size of the tail represent the amount of DNA damage. (OECD, 2016c) The chromosome aberration test is based on microscopy of cells in metaphase and analyses the structure of the chromatin. The cells are treated with a metaphase arresting substance and stained, after which the chromatin from cells in metaphase are analysed microscopically. (OECD, 2016a) The micronucleus test is similar to the comet assay by means of detecting DNA fragments from the cells. In contrast to the comet assay, the micronucleus test can be performed in several ways where the fragments of nuclei can be visualised by different methods. One approach is to use flow cytometry which involves two-step staining for detection of micronuclei. Cells are stained with one dye prior to lysis, followed by another dye after lysis. This allows for elimination of dying cells which have an exposed plasma membrane, as the first dye penetrates only into dying cells. Upon analysis, when cells are lysed and

stained, only cells that have an intact membrane are stained only with the second dye. The micronucleus test can, therefore, more accurately detect damage which is not a cause of cytotoxicity. (OECD, 2016b) (Westerink et al., 2011) Even though these tests are able to predict potential genotoxic properties of compounds, one drawback is their inability to determine the mechanism of action the genotoxicity. To be able to characterise and assess the true risk of the compound the understanding of its mechanism of action is an important aspect. (Smart, Daniel J. et al., 2020)

In addition to the novel genotoxicity analyses, new methods using different types of biomarkers involved in DNA damage are rapidly evolving. As discussed previously, the DDR involves many types of molecules which become activated upon different types of damage. The Poly (ADP-ribose) polymerase (PARP) protein family is involved in the recognition and repair of single-stranded DNA breaks. Upon a break, PARP binds to the DNA and generates a Poly ADP-ribose chain which serves as a docking site for DNA repair proteins. (Luo & Kraus, 2012) This accumulation of proteins on damaged DNA is used as a source to determine DNA damage. Another biomarker for other types of stress is, for example, the 8-hydroxu-2'-deoxyguanosine which is a major product of DNA oxidation. The presence of this marker, thus, indicates damage through oxidation. (Valavanidis, Vlachogianni, & Fiotakis, 2009) The use of different biomarkers for the determination of the mechanism of action has been of growing interest in the past few years (Corvi & Madia, 2017). This has resulted in commercial availability of a growing number of antibodies and small molecules for detection of several different pathway proteins. Therefore, a combination of novel genotoxicity tests with different biomarkers could provide insight into not only the genotoxicity but, in addition, to the biological mechanisms behind the damage.

1.7 Technologies for genotoxicity screening

For detection of markers indicating genotoxicity several methods have been implied. One of the most used methods in high throughput screening is based on labelling of markers of interest with fluorescent dyes and measurement with flow cytometry. Another method is based on high content imaging where cells are labelled with antibodies or probes and imaged by automated imaging.

1.7.1 Fluorescent labelling allows for detection of several markers

Fluorescent labelling is a method that uses different types of fluorescent dyes, molecules, proteins, or antibodies to detect a specific marker. Several different types of fluorophores that are able to be excited and emit light at known wavelengths are commercially available. These fluorophores can be attached to a variety of motifs that can bind to a specific part of the marker of interest. Immunofluorescence is a technique which allows for detection of a target of interest by the use of fluorescently labelled antibodies. The method can be used either by direct or indirect labelling (figure 5). In the direct labelling the detectable fluorophore is attached directly to the primary antibody. In indirect labelling the primary antibody binds to its target and a secondary antibody carrying the fluorophore is used to detect the primary antibody. The heavy chains of the antibodies are species-specific which allows for secondary antibodies to be targeted against the species of animal where the primary antibody was produced. A wide range of antibodies are commercially available. The combination of primary antibodies from several species allows for the use of several secondary antibodies with different fluorophores at the same time and detecting these by flow cytometry or microscopy.

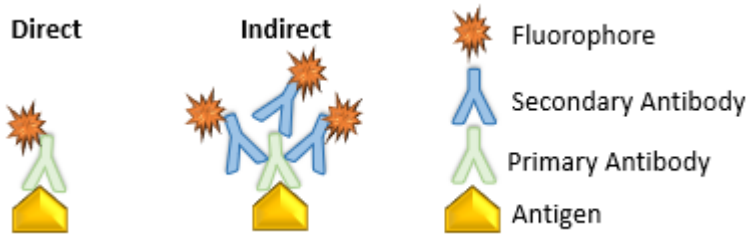

Figure 5, Direct and indirect immunolabelling. Direct labelling uses fluorescent primary antibodies which bind to their target. Indirect labelling uses a primary antibody from a host animal which binds to its target followed by staining with a fluorescent secondary antibody that targets the primary antibody. The indirect labelling allows for amplification of the signal since several secondary fluorescent antibodies can bind to the same primary antibody (Odell & Cook, 2013).

1.7.2 Flow cytometry can be used for detection of fluorophores

To be able to identify the fluorescently labelled markers of interest a machine capable of exciting and detecting the fluorophore is required. To understand how these markers are identified and how data is acquired a short introduction to the basics of flow cytometry is described in this section.

1.7.2.1 Basics of flow cytometry

Flow cytometry is a technology that allows for analysis of single particles using light. The method is dependent on a flow cytometer. The principle of the technology is based on a system that acquires a liquid sample through a thin needle and allows particles, commonly the size of a cell, to pass one by one through a laser beam in the flow cytometer. The light that hits the particle is scattered and detected by different detectors of the flow cytometer. Some detect the scatter of the light which hits the particles while others detect fluorescence from dyes that are used to stain the samples. The signals that the instrument captures are transferred to a computer which interprets them to visible data (figure 6). (Wiederschain, 2011)

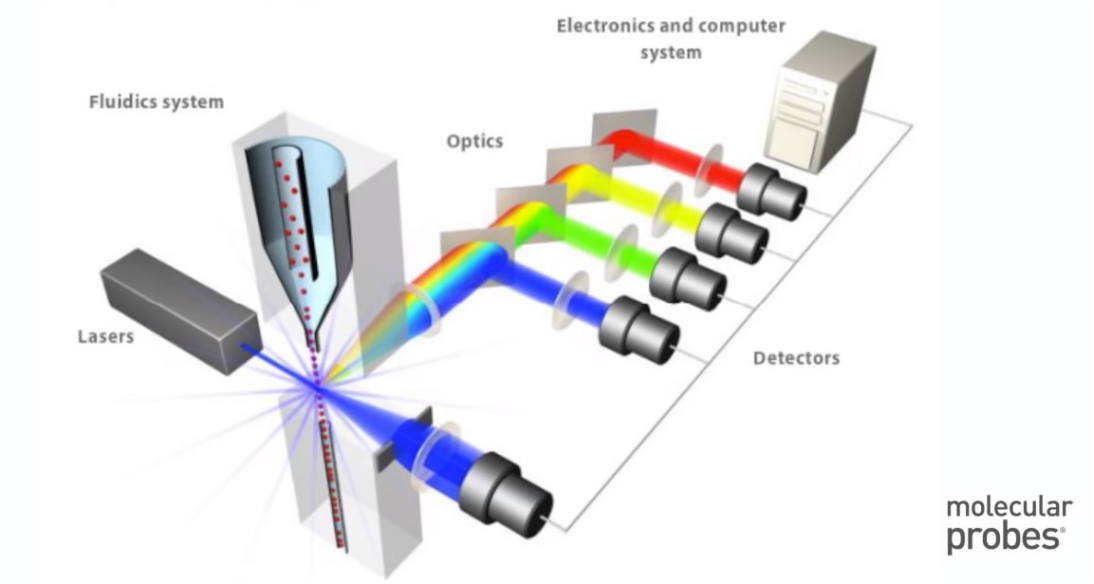

Figure 6, The principles of flow cytometry. Simplified view of flow cytometry. The sample is pumped through the fluidics system of the flow cytometer and passes through a laser beam. The light scatters from the particle and is detected by detectors located in different angles of the light source. The optics of the machine consists of filters that allow different wavelengths of light to pass while reflecting others. The data collected by the detectors is transferred to a computer for further analysis. (Wiederschain, 2011) Image from Molecular Probes (Thermo Fisher Scientific)

1.7.2.2 Detection of light

When a particle passes through the laser beam of the flow cytometer it refracts and scatters light in many directions. The light that hits the particle is detected in form of voltage pulses by the detectors. This scatter can be measured by forward scatter (FSC) and side scatter (SSC). The FSC is detected in front of the laser and consists of light that is scattered in the forward direction which is proportional to the size of the particle. The SSC is detected usually 90° from the particle and indicates the light that is reflected in larger angles from the particle. This light is proportional to the complexity of the particle.

The emitted light of excited fluorescent probes is captured by other detectors in the instrument. Different commercially available probes have a wide range of excitation and emission spectra which allows for simultaneous detection of probes with different emission spectra using specific filters. The filters either reflect or bypass the light of a specific wavelength allowing for the wavelengths emitted by a single particle to be detected.

The signals that arise from the scattered light are detected in forms of voltage pulses, which can be defined by height (H), width (W) and area (A). The width of the pulse is the time that it takes for the particle to pass through the laser beam and is, thus, proportional to the particle size. The height of the pulse is defined as the intensity of the signal and is proportional to the amount of light scattered. The height of the signal can be variable depending on the voltage properties of the instrument. The area is defined as height*width and is, thus, less impacted by the voltage settings than height alone.

1.7.2.3 Data from flow cytometric analyses need to be processed

The data gathered from the flow cytometer is analysed using software suitable for flow cytometry data, generally provided together with the hardware. The software commonly allows for analysis of the gathered data in forms of visual plots and histograms, gates and logical analyses. The amount of data produced by flow cytometry can be extensive, and therefore these types of methods are also known as high content screening (HCS).

The plots allow for visualisation of data using different parameters, including FSC, SSC and channels with different emission filters. For example, in figure 7 a, a gate is created around the population that represents the cells. The plot itself is derived from a logical population of all events excluding counting beads (gated in another plot). The parameters used are the intensity of Propidium Iodide (PI) a fluorescent agent used to stain the DNA, versus FSC which detects particle size. From the population of cells, a histogram can be created (figure 7 b) using the intensity of PI versus number of events. Gates can be created from the histogram which represent the normal nuclei, polyploidy, and 2n-polyploidy.

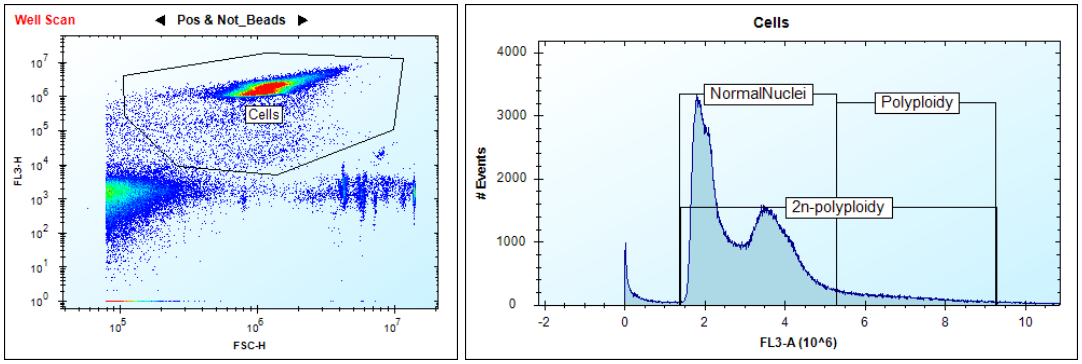

Figure 7, Gating strategies for Flow cytometry data. a) In this dot plot, the parameters fluorescent channel 3 (FL3-H), which represents the intensity of Propidium Iodide (PI), versus forward scatter (FSC-H), which represents the particle size, are used to visualise the cell population in a sample. Each dot in the plot represents one particle. A gate can be created around the population of interest. b) A histogram of the data from the "Cells" gate. The parameters used are FL3-A, representing the intensity of PI, versus number of events to visualise the nuclei. Gates representing the normal nuclei, polyploidy and 2n-polyploidy are created.

1.7.2.4 Commercially available DNA damage screening method - MultiFlow®

The MultiFlow® kit is developed by Litron Laboratories and is validated for the purpose of genotoxic screenings (Kopp, Khoury, & Audebert, 2019b). The kit combines markers for well-established genotoxicity markers. One of the kits uses the markers for γH2AX, pH3 and p53 with a DNA stain and counting beads which allows for an efficient identification of DNA damage in one-step. For the use of MultiFlow® the cell line used needs to have a functional p53 expression to allow for correct

identification of p53. The validation of this MultiFlow®-kit using TK6 cells has been done as an interlaboratory study. The study tested 84 reference compounds with known genotoxic potential. Based on the data from all seven laboratories, cut-off values were used to determine the thresholds for genotoxicity, known as the global evaluation factors (GEFs) for aneugenicity and clastogenicity for TK6 cells. (Bryce et al., 2017) The values are presented as percentage fold increases compared with negative controls on the same plates. The compounds are considered genotoxic if two continuous concentrations exceed two of the GEF criteria. The GEFs for aneugens are, 1.71-fold pH3 at 4h, 1.52-fold 24h pH3, 1.45-fold nuclear p53 at 24h and 5.86-fold 24h polyploidy. The GEFs for clastogens are, 1.51-fold 4h ɣH2AX, 1.40-fold 4h nuclear p53, 2.11-fold 24h ɣH2AX and 1.45-fold 24h nuclear p53. (Bryce et al., 2017) These criteria can be used as a guideline for further genotoxic analysis.

1.7.3 High content analysis provides an imaging-based method for detection of fluorophores

High content imaging (HCI) is a microscopy-based imaging system, based on high throughput automated cellular image acquisition. The method is based on the principle of immunofluorescence and detection of fluorescent probes by different types of light sources in the microscope. The light sources are used to excite the fluorophores and the emitted light is detected by the microscope. In combination with image analysis software, the HCI can produce sensitive, high resolution images on a large scale. The combination of these features enables a High Content Analysis (HCA) (sometimes also known as HCS). (Li & Xia, 2019) Recent studies have suggested that HCA could be preferred over flow cytometry in genotoxic analysis since HCA is considered more sensitive and for instance allows identification of spots within single nuclei or cells and intercellular events (Garcia-Canton, Anadon, & Meredith, 2013). In addition, it does not require cells to be in suspension which allows for samples to be re-analysed if necessary (Garcia-Canton et al., 2013).

III AIMS OF THE STUDY

The aim of this study is to compare *in vitro* genotoxicity screening methods and their predictivity. The comparison is mainly focused on screening by flow cytometry, a method that is validated and currently in use at Orion Pharma, and high content imaging, a method that is set up in this study. To achieve this, 16 reference compounds with known genotoxic properties are screened. First comparison is performed with MultiFlow® method by flow cytometry using two different cell lines, TK6 cells that are validated for this method, and HepG2 cells which are to be used in imaging, to ensure that the same markers can be used in both cell lines. Next, the imaging-based method is set up and tested. For this purpose, suitable antibodies for screening are chosen and tested for concentration and functionality together. The same reference compounds are then screened with the imaging-based method. The results between the methods and cell lines are analysed and improvements to the imaging platform are made if necessary. The goal is to set up an imaging assay that would be able to predict genotoxicity in terms of specificity and sensitivity, more accurately or as accurately as in the flow cytometry-based method currently in use. If a successful imaging system is established, additional compounds and additional markers can be tested to test if false positive results can be reduced with the imaging platform, with the use of for example cytotoxicity markers.

IV EXPERIMENTAL PART

2. Materials and Methods

An overview of the workflow of this project is shown in figure 8. First two cell lines, TK6 and HepG2, are exposed to 16 reference compounds and analysed for DNA damage by MultiFlow®-DNA damage kit in flow cytometry (figure 8 a). Following, an imaging-based assay is set up with HepG2 cells and antibodies for the markers are tested (figure 8 b). Finally, HepG2 cells are exposed to the same reference compounds and the imaging-based method is used to analyse DNA damage (figure 8 c).

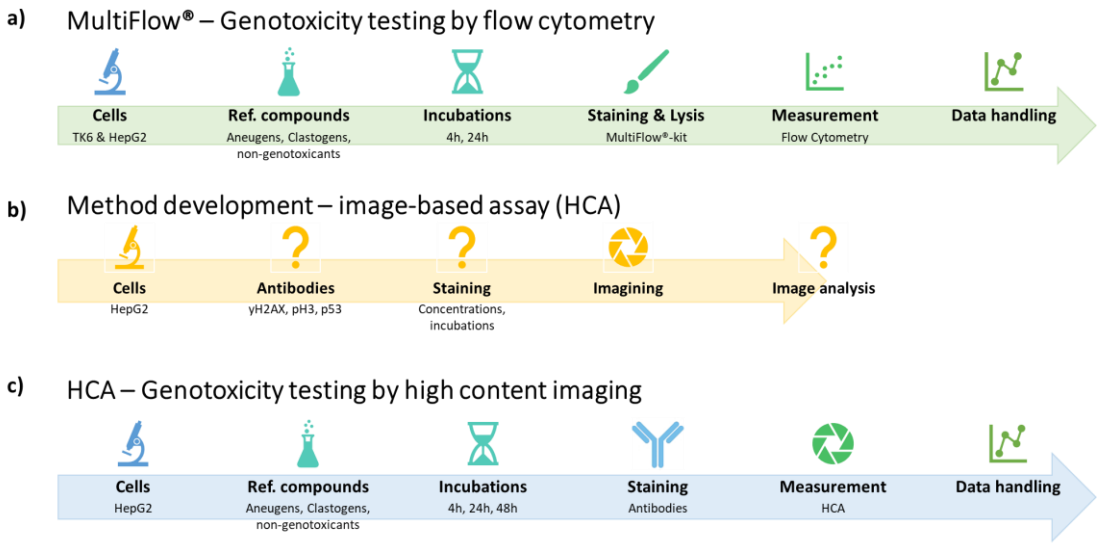

Figure 8, overview of the workflow in this study. a) TK6 cells and HepG2 cells are exposed to 16 reference compounds and analysed for genotoxicity by MultiFlow®-kit and protocol. b) An imaging-based assay is set up with HepG2 cells. c) HepG2 cells are exposed to the same 16 reference compounds and analysed for genotoxicity using the high content analysis (HCA) method.

2.1 Cell lines

One of the two cell lines used in this study was adherent HepG2 cells (C3A [HepG2/C3A, derivate of Hep G2 (ATCC HB-8065)] (ATCC® CRL-10741™) lot 60208249), derived from human liver hepatocellular carcinoma. The other cell line used was the suspension cell line TK6 (ATCC® CRL-8015), human lymphoblasts derived from hereditary spherocytosis from the spleen. TK6 cells were acquired from Gentronix laboratory and HepG2 cells from Lundbeck, Denmark.

2.1.1 Subculturing

Adherent HepG2 cells were grown in TC-Treated 75cm² flasks (Corning®, 430641U) in a growth medium consisting of Dulbecco's Modified Eagle Medium (DMEM), high Glucose (1x) (41965, Gibco Life Technologies) with 1 mM Sodium Pyruvate (11360-039, Gibco Life Technologies), 1x Minimum Essential Medium Non-essential Amino Acids Solution (MEM NEAA) (11140-035, Gibco Life Technologies), 5 mM Hepes (H0887, Sigma), 10% Foetal Bovine Serum (FBS) (Heat Inactivated) (10500-064, Gibco Life Technologies) and 1x Penicillin-Streptomycin (P0781, Sigma). The cells were grown in humified incubators at 37 °C and 5% CO_2. The cells were grown to a 60% confluency and subcultured twice a week. For subculturing, the old medium was aspirated from the cells and the cells were washed twice with 1x Dulbecco's Phosphate buffered saline (DPBS/PBS) (Gibco™, 14190144). Cells were detached with 0.05% Trypsin-EDTA (25300-062, Gibco Life Technologies) for 5 minutes and resuspended in 5 ml growth medium. To minimise the number of aggregated cells the cell-suspension was resuspended five times with a 5 ml pipette tip with a 300 µl tip on its tip. The cells were transferred to 15 ml fresh medium at a concentration of $0.1x10^6$ cells/ml (4-day interval) or $0.2x10^6$ cells/ml (3-day interval).

TK6 cells were grown in uncoated T75-flasks (NUNC™ 156800) in RPMI 1640 Medium (Gibco™ A1049101) with 10% inactivated HI Horse Serum (Gibco™ 26050-088), 97 µg/ml Penicillin-Streptomycin (Gibco™ 15140-122) and 2 mM GlutaMAX™-I Supplement (Gibco™ 35050-061). The cells were grown in a humified incubator at 37 ºC and 5% CO_2. Cells were subcultured twice weekly, by transferring cell suspension from the culture to 50 ml fresh medium at a concentration of $0.004/0.005x10^6$ cells/ml (subculture interval of four days) or $0.015/0.010x10^6$ cells/ml (subculture interval of three days). In order to maintain exponential growth, cells were maintained at a density lower than 1 million cells/ml.

2.1.2 Plating of cells

HepG2 cells were prepared for assay by trypsinization, as described previously, followed by mixing of the cell suspension with a 21g needle and a 5 ml syringe three times. Plating of HepG2 cells was done on Poly-D-lysine coated 96- or 384-well plates. For HCA, Cell Carrier Ultra 384- and 96-well plates (Perkin Elmer) were used and for flow cytometry BioCoat™ 96-well plates (Corning®). On the 96-well plates cells will be plated with the density of 8000 cells/well in 100 µl ($0.08x10^6$ cells/ml) and on the 384-well plates 2800 cells/well in 25 µl ($0.056x10^6$ cells/ml). Cells were counted using a Mammalian Cell Counter (NucleoCounter® NC-100™ from Chemometec) and diluted in growth medium in a concentration depending on the plate type. The cells were plated using a stepper. In HCA, the plates were allowed to warm to room temperature for 1 hour prior to plating and following plating the plates were left for 1 hour in the laminar flow hood before transferring them to the incubator. Plating was performed approximately 24 hours prior to compound administration.

For TK6 cells, the cells were plated on 96-well U-Bottom non-treated microplates (Falcon®) at a concentration of $0.3x10^6$ cells/ml, with 100 µl/well. The culture flask was mixed, and the cells were counted using the NucleoCounter®. The right amount of cell suspension was transferred and diluted to obtain the concentration of $0.3x10^6$ cells/ml. The suspension was plated using a stepper.

2.2 Chemicals

The reference compounds, solvents and their mode of action are listed in Table 1. All chemicals were purchased from Sigma Aldrich. The concentration indicated in the table was the highest concentration studied. All chemicals were diluted to a 100-fold stock solution to obtain a 1% dimethyl sulfoxide (DMSO) concentration on the cells, except for those compounds which were diluted in other solvents. The inconsistency for these compounds was acknowledged but due to the automation of the method could not be adapted. All compounds were tested to a prior known toxic concentration or 1000 µM unless the compounds were insoluble to that extent. In that case, the highest concentration was a 1:100 dilution from the highest soluble concentration. Due to differences in the two cell lines used, the concentrations of some of the compounds were adjusted during the experiment.

Table 1, Reference compounds used in this study. The reference compounds used, the highest tested concentration and the solvent used in this study is listed in this table. The abbreviations, if used, are listed in the "ID used in this study" column. The mode of action (MoA) from previous classifications and the reference are also listed.

ID.	Chemical Name	ID used in this study	Conc. (µM)	Solvent	MoA	Reference
1	Carbonyl cyanide 3-chlorophenylhydrazone	CCCP	100	DMSO	Cytotoxicant - Mitochondrial uncoupler	(Bryce et al., 2017) (Khoury et al., 2016)
2	Paclitaxel	Paclitaxel	0.01	DMSO	Aneugen - Microtubule stabiliser	(Bryce et al., 2017)
3	Methyl methanesulfonate	MMS	1000	H2O	Clastogen - DNA methylator/alkylator	(Kirkland et al., 2016)
4	Mitomycin C	Mitomycin C	15	H2O	Clastogen - DNA cross-linker	(Kirkland et al., 2016) (Bryce et al., 2017)
5	4-Nitroquinoline N-oxide	4NQO	10	DMSO	Clastogen - alkylator, ROS formator	(Kirkland et al., 2016) (Bryce et al., 2017)
6	Cytosine β-D-arabinofuranoside	Cytosine arabinoside	1000	DMSO	Clastogen - antimetabolite/nucleoside analogue	(Kirkland et al., 2016) (Bryce et al., 2017)
7	Benzo[a]pyrene	BAP	1000	DMSO	Clastogen - forms DNA adducts. Requires metabolic activation.	(Khoury, Zalko, & Audebert, 2016b)
8	Colchicine	Colchicine	100	DMSO	Aneugen - Mitotic spindle poison	(Kirkland et al., 2016) (Bryce et al., 2017)
9	Vinblastine Sulphate salt	Vinblastine	0.024	DMSO	Aneugen - Microtubule destabiliser	(Kirkland et al., 2016) (Bryce et al., 2017)
10	Amiodarone hydrochloride	Amiodarone	100	EtOH	Cytotoxicant - Mitochondrial toxin – uncoupler, complex 1 inhibitor, beta oxidation inhibitor	(Waldhauser et al., 2008)

11	2,4-dinitrophenol	2.4-dinitrophenol	1000	DMSO	Cytotoxicant - Mitochondrial toxin – uncoupler	(Grundlingh, Dargan, El-Zanfaly, & Wood, 2011)
12	Nimesulide	Nimesulide	1000	EtOH	Cytotoxicant - Mitochondrial toxin – MPT inducer	(Mingatto et al., 2002)
13	Sodium Chloride	NaCl	1000	DMSO	Non-genotoxicant	(Bryce et al., 2017)
14	Rotenone	Rotenone	1000	DMSO	Cytotoxicant – Mitochondrial toxin – Complex 1 inhibitor	(Heinz et al., 2017a)
15	Sertraline hydrochloride	Sertraline	1000	DMSO	Cytotoxicant	(Davies & Kluwe, 1998)
16	Imipramine hydrochloride	Imipramine	1000	DMSO	Cytotoxicant	(GARRISON & MOFFITT, 1962)

2.3 Compounds to cells

The reference compounds were diluted in DMSO by automated liquid handling equipment (Hamilton Microlab STAR) to obtain a concentration series of the compounds. The compounds were first diluted on a separate dilution plate prior to pipetting on the cells. Addition of compounds to cells was done by the same liquid handling equipment. For flow cytometry a 20-point concentration series was used, starting from the top concentration (TC) and TC*0.75 indicated in table 1. These two concentrations were diluted 1:2 in parallel in 10 steps to obtain the 20-point concentration series. An example using the top concentration 1000 µM is provided in table 2. For HCA the concentration series used was a 10-step dilution with 2 replicates. The compounds were diluted from the same top concentrations in 1:2 for 8 steps and the final 2 steps 1:10. An example using the top concentration 1000 µM is provided in table 3.

Table 2, Concentration series used in flow cytometry in µM. The incubation concentration series for the reference compounds on cells. Here a starting concentration of 1000 µM is used as an example. The values are truncated to one decimal for clarity in the table.

1000	500	250	125	62.5	31.3	15.6	7.8	3.9	2.0
750	375	187.5	93.8	46.9	23.4	11.7	5.9	2.9	1.5

Table 3, Concentration series used in HCA in µM. The incubation concentration series for the reference compounds on cells. Here a starting concentration of 1000 µM is used as an example. The values are truncated to one decimal for clarity in the table.

1000	500	250	125	62.5	31.25	15.62	7.81	0.78	0.08
1000	500	250	125	62.5	31.25	15.62	7.81	0.78	0.08

In addition, 3 controls were used on each plate, CCCP (non genotoxicant), vinblastine (aneugen) and MMS (clastogen) to ensure each experiment was reliable. For flow cytometry the concentrations for the controls (in µM) were as follows: CCCP; 12.5, 6.25, 3.125 and 1,562, vinblastine; 0.012, 0.006, 0.003 and 0.0015 and for MMS; 100, 50, 25 and 12.5. For every 96-well plate there was one series of controls. Due to differences in automation for the different protocols, for HCA no dilution of controls was made, the highest concentration of the compounds mentioned above were used in 10 replicates for every 384-well plate. In addition, for every 96-well plate there were 4 DMSO controls with only 1% DMSO. After compound administration cell plates were transferred to a humified incubator at 37 °C and 5% CO_2 until staining or fixation.

2.4 Measurement of precipitation

From the compound dilution of the reference compounds a separate precipitation plate was made containing only the growth media of the cells and the same concentrations of compounds as on the incubation plates. These plates were measured for precipitation using a Nephelometer (NEPHELOstar® BMG Labtech) which detects insoluble particles in the medium. In addition, the plates were inspected using a light microscope for visible precipitation. The plates were measured at timepoint 0 hours and 24 hours, as well as 4 hours in the flow cytometry assay. The precipitation values acquired by the nephelometer were analysed as fold changes compared to all negative controls for each plate separately. For the compounds where a precipitation fold over

10 was calculated, or visible precipitation was observed, the values above the lowest precipitating concentration were excluded.

2.5 Measurement by flow cytometry

For both cell lines genotoxicity was analysed by the MultiFlow method with the detection of markers for γH2AX, pH3 and p53. These were measured by Flow cytometry using the MultiFlow®-kit developed by Litron laboratories and the protocol used was based on instructions of the manufacturer. The assay was performed similarly on TK6 cells and HepG2 cells with the expectation of detachment of HepG2 cells prior to analysis. The samples were measured with flow cytometer iQue screener (IntelliCyt®). Both cell lines were stained at 4 hours and 24 hours with MultiFlow® complete labelling solution.

2.5.1 Staining of cells

Staining of cells was done using MultiFlow® complete labelling solution, containing Nuclei Release solution with counting beads, DNA stain (Propidium Iodide), RNAse solution, γH2AX-, pH3- and p53 markers. The staining solution was prepared according to table 4. With HepG2 cells FBS was also added to the solution.

Table 4, MultiFlow® kit compounds and volumes. (*MultiFlow(R).*)

Number of wells	Volume of Nuclei Release Solution with Counting Beads	Volume of DNA Stain	Volume of RNase Solution	Volume of γH2AX Antibody Alexa Fluor® 647	Volume of Phospho-Histone H3 Antibody PE	Volume of p53 Antibody FITC	Volume of FBS (attachment cells only)
1	50 µL	1.25 µL	0.25 µL	0.25 µL	0.10 µL	0.25 µL	1.00 µL
96 + 15 % = 110	5.5 mL	137.5 µL	27.5 µL	27.5 µL	11.0 µL	27.5 µL	110.0 µL

With TK6 cells 15 µl of labelling solution was transferred to a 384-well PerkinElmer ProxiPlate and 5 µl cell suspension was added. The solution was thoroughly mixed by resuspension. The ProxiPlate was then transferred onto a shaker for 15 minutes before proceeding with analysis.

With HepG2 cells the medium from the plate was aspirated away and the plate was washed one time with 100 µl PBS. Following, 25 µl cold Accutase® was added to the plate and the plate was incubated for 10 minutes at room temperature prior to adding 50 µl of complete labelling solution on the cells. The suspension was mixed thoroughly by resuspension 15 times and then transferred to Falcon® 96-well U-Bottom non-treated microplates. The plates were then transferred onto a shaker for 15 minutes before proceeding with analysis.

2.5.2 Plate analysis

Intellicyt iQue Screener from IntelliCyt® Corporation was used as hardware for flow cytometry analysis. The software used, Forecyt® was provided by the same company. GLP was followed with the instrument and washes and QC were performed as suggested by the manufacturer. The emission filters of iQue hardware are listed in table 5. For TK6 cells a 6 second sip time/well was used and for HepG2 cells 10 seconds. All plates were shaken 1800 RPM every 6th well.

Table 5, Fluorescent channels and corresponding filters of iQue and the fluorophores these channels were used to detect. (iQue hardware manual.)

Channel position	**Filter**	**Fluorophore used**
FL1	533/30	FITC (p53)
FL2	585/40	PE (pH3)
FL3	670LP	PI (DNA stain)
FL4	675/25	Alexa Fluor® 647 (γH2AX)

2.6 Measurement by high content analysis

For the imaging analysis the same principals as in flow cytometry was adapted. The markers detected were γH2AX, pH3 and p53 at 4-, 24- and 48-hour timepoints. The plates were fixed at these timepoints, stained by fluorescent labelled antibodies and analysed with Operetta High-Content Imaging System from PerkinElmer. Prior to this, the antibodies for the markers were tested with the method. Concentrations for the antibodies and their functionality together were tested with reference compounds and negative controls.

2.6.1 Setting up the HCA assay

For the HCA assay the HepG2 cells were plated as previously described in the first stage on 96-well and later on 384-well plates. In the first stage the staining protocol was set up and the primary and secondary antibodies were tested, both to determine optimal concentrations and functionality in co-incubations. The 96-well plates were divided into sections, one section treated with the aneugen vinblastine, 12 nM with 1% DMSO, one with the clastogen MMS 20 mM, one with Nutlin-3 10 µM with 1% DMSO and the last serving as the control with only 1% DMSO. Plates were fixed at

24-hour timepoint. The antibodies used were selected based on previous in house-tests and literature reviews. The highest concentration of the primary antibodies tested was the concentration recommended by the manufacturer. The primary antibodies used were Phospho-Histone H2A.X (Ser139) Rabbit mAb (#9718 from Cell Signalling technology), Phospho-Histone H3 (Ser10) Mouse mAb (#9706 from Cell Signalling technology), which had both been tested in-house previously. For p53 two alternatives were used, one from Biorbyt (orb153342) and one from Novus (AF 1355), both Goat polyclonal antibodies. The secondary antibodies used were Goat anti-Mouse IgG (H+L) Alexa Fluor® 488, Goat anti-Rabbit IgG (H+L) DyLight 550 and Rabbit anti-Goat IgG (H+L) Alexa Fluor® 647.

2.6.1.1 Staining protocol for HCA

After incubation with compounds the medium was aspirated away, and the plates were washed once with 37ºC PBS. For 96-well plates a 100 µl/well volume was used and for 384-well plates a 50 µl/well volume, unless otherwise stated. The cells were fixed with a 4% paraformaldehyde in PBS solution for 15 minutes. The fixation was aspirated away and 37ºC PBS was added for 5 minutes. Washing procedures were repeated three times with PBS left on the plate. The plates were either stained immediately or stored at +4ºC.

Prior to staining the plates were washed with a permeabilization buffer, containing 0.2% Triton X-100 in PBS (PBST) for 5 minutes. The permeabilization buffer was aspirated away and cells were blocked with a 5% Bovine Serum Albumin (BSA) in PBS (BSA-PBST) solution for 30 minutes at room temperature. BSA-PBST was aspirated away and the primary antibodies in 5% BSA-PBST solution were added. The plates were then incubated either for 2 hours in RT or overnight at +4ºC at a mild shake. The primary antibodies were washed away with 3x PBS for 5 minutes as described previously and the secondary antibody in 5% BSA-PBS was added to the plates. The plates were incubated for 1 hour at room temperature and then washed 3x with PBS for 5 minutes with the last wash containing 0.001 mg/ml Hoechst and incubated for 10 minutes. The plates were washed one last time for 5 minutes with PBS and finally PBS was left on the plates prior to imaging.

2.6.1.2 Antibody concentration determination for HCA

Appropriate antibody concentration determination was performed on 96-well plates with three reference compounds: Vinblastine, MMS, nutlin-3 and a DMSO control. Each concentration was tested as duplicates for all four well types in order to ensure correct binding to target. The concentration ranges tested are stated in table 6. The values provided are stated as dilutions, 1:100 means 1 µl antibody to 99 µl solvent. All the secondary antibodies were diluted 1:500. Following the same protocol, the antibodies were multiplexed to ensure that they were able to both bind to their correct targets and not interfere with each other. For this purpose, a scheme combining all possible combinations with both primary and secondary antibodies were created and tested.

Table 6, Concentration ranges of primary antibodies tested. The highest concentration tested was the concentration provided by the manufacturer. B = Biorbyt, N=Novus.

γH2AX	pH3	p53 (B)	p53 (N)
1:100	1:100	1:200	1:10
1:200	1:200	1:250	1:20
1:400	1:400	1:300	1:25
1:600	1:600	1:400	1:40
1:700	1:700		1:50
1:800	1:800		1:100
1:1000	1:1000		1:150

2.6.1.3 Plate imaging

The software used in combination with Operetta was Harmony High-Content Imaging and Analysis Software from PerkinElmer. The plates were imaged using a 20x water immersion objective. The channels used were determined by the secondary antibodies and Hoechst. The channels used were configured from a database provided with the software. The channels were Hoechst33342 (excitation 355-385, emission 430-500), Alexa Fluor® 488 (excitation 460-490, emission 500-550), DyLight 550 (excitation 530-560, emission 570-650) and Alexa Fluor 647 (excitation 615-645, emission 655-760).

2.7 Data Analysis

2.7.1 Data acquired by flow cytometry

All data acquired by flow cytometry was processed in the ForeCyt® software provided by Intellicyt. Data processing was done based on MultiFlow® instruction manual with some adaptions dependent on the flow cytometer in use. The fluorescent channels and their corresponding fluorophore are listed in table 7.

Table 7, List of the fluorescent channels and filters of iQue and the corresponding fluorophores and markers they detect in this experiment.

Channel position	Filter	Fluorophore	Marker
FL1	533/30	FITC	p53
FL2	585/40	PE	pH3
FL3	670LP	PI	DNA
FL4	675/25	Alexa Fluor® 647	γH2AX

2.7.2 Data acquired by high content analysis

All data acquired by HCA imaging with Operetta was processed with Columbus image analysis software developed by Perkin Elmer.

2.7.3 Statistical analysis

Data from both flow cytometry and HCA methods were exported to be further processed in excel. To acquire data for analysis, the following calculations were made for each plate separately and for all wells:

$$RNC = \frac{Nuclei\ count\ (well)}{Nuclei\ count\ (Average\ of\ DMSO\ contols)}$$

$$pH3\% = \frac{pH3\ count\ (well)}{Nuclei\ count\ (well)}$$

$$pH3\%\ fold\ = \frac{pH3\%\ (well)}{pH3\%\ (Average\ of\ DMSO\ controls)}$$

$$yH2AX\ fold\ = \frac{yH2AX\ intensity\ (well)}{yH2AX\ intensity\ (Average\ of\ DMSO\ controls)}$$

$$p53\ fold\ = \frac{p53\ intensity\ (well)}{p53\ intensity\ (Average\ of\ DMSO\ controls)}$$

For each concentration of each compound the median from the replicated experiments was used for analysis. In addition to this, the median absolute deviation (MAD) was counted. It is defined as the median of the median of all data points minus each data value. The MAD was counted using the formula:

$$MAD = M((M(v1 \dots n) - v1), M((M(v1 \dots n) - v2) \dots (M((v1 \dots n) - vn)$$

Where M = Median, v= value of each data point, n = number of values (Leys, Ley, Klein, Bernard, & Licata, 2013)

For simplicity, for 6 values the MAD is counted as follows:

MEDIAN (ABS(value1-(MEDIAN(all values))), ABS(value3-(MEDIAN(all values))), ABS(value5-(MEDIAN(all values))), ABS(value2-(MEDIAN(all values))), ABS(value4-(MEDIAN(all values))), ABS(value6-(MEDIAN(all values))))

3. Results

3.1. Results from measurements by flow cytometry

The evaluation of genotoxicity of the 16 reference compounds with TK6 cells and HepG2 cells were measured by the MultiFlow® DNA damage kit by flow cytometry. The results for the two cell lines with this method is presented in this section.

3.1.1 Handling of raw data from flow cytometric analyses

All data from the flow cytometric analyses with both TK6 and HepG2 were handled separately for each plate. Each plate corresponded to one experiment with all concentrations for all 16 references, 16 negative controls and 3 x 16 positive controls. From all data gathered the counting beads were gated in a dot plot using the intensity of FITC versus size of the particles (figure 9 a). The beads were used as quality control to ensure even sample uptake from each well (figure 9 b). A logical population consisting of all events excluding beads was created, and from this population the cells were gated using intensity of DNA stain PI versus particle size (figure 9 c). From the population of cells, a histogram was created with number of events versus PI intensity. In this histogram three populations were gated, one representing normal nuclei (or cycling nuclei as stated in figure 10, the other polyploidy, and the third a gate representing both, 2n-polyploidy (figure 9 d). From the 2n-polyploidy population a new dot plot was created with the intensity of PE on the y-axis and PI on the x- axis. From this plot the pH3-positive mitotic cells were visualised and gated (figure 9 e). Due to some spectral overlap between the DNA-associated fluorescence and PE fluorescence, compensation between the channels were adjusted if necessary, in a way that the pH3-positive cells were distinguished from the main population, as indicated by the MultiFlow® instructions. For the two final populations, γH2AX and nuclear p53, the logical population used was normal nuclei (from figure 9 d) excluding pH3-positive events (from figure 9 e). From this population, the intensity of AlexaFluor®647 and PI was used for visualisation and gating of γH2AX (figure 9 f). Likewise, for p53 the intensities of FITC and PI were used for gating nuclear p53 (figure 9 g). The summarised gating logic is presented in figure 10. The data inside the gates represent the data that was exported in each specific category.

The data collected was exported to Excel, with each well represented as one sample in one row. The data exported for each well was Count of Beads, Count of Cells, Count

of 2n-polyploidy, Count of Normal Nuclei, Count of pH3-positive, Median FL1-A of Nuclear p53 and Median FL4-A of γH2AX. The “Count” represents all particles that localise inside the gated area of the specific parameter. The “Median” was the median intensity of the signal from the area of the specified channel from all particles that were localised inside the gate of the specific parameter.

From the exported data, the metrics for the parameters Count of Cells, Count of pH3-positive, Median FL1-A of Nuclear p53 and Median FL4-A of γH2AX were presented as folds over negative controls for each plate. The formulas used are presented in section 2.7.3. To ensure that the experiments were successful the positive controls were checked to meet the GEFs for aneugen (vinblastine) and clastogen (MMS), as well as that the negative controls did not show any marked increases in genotoxicity markers.

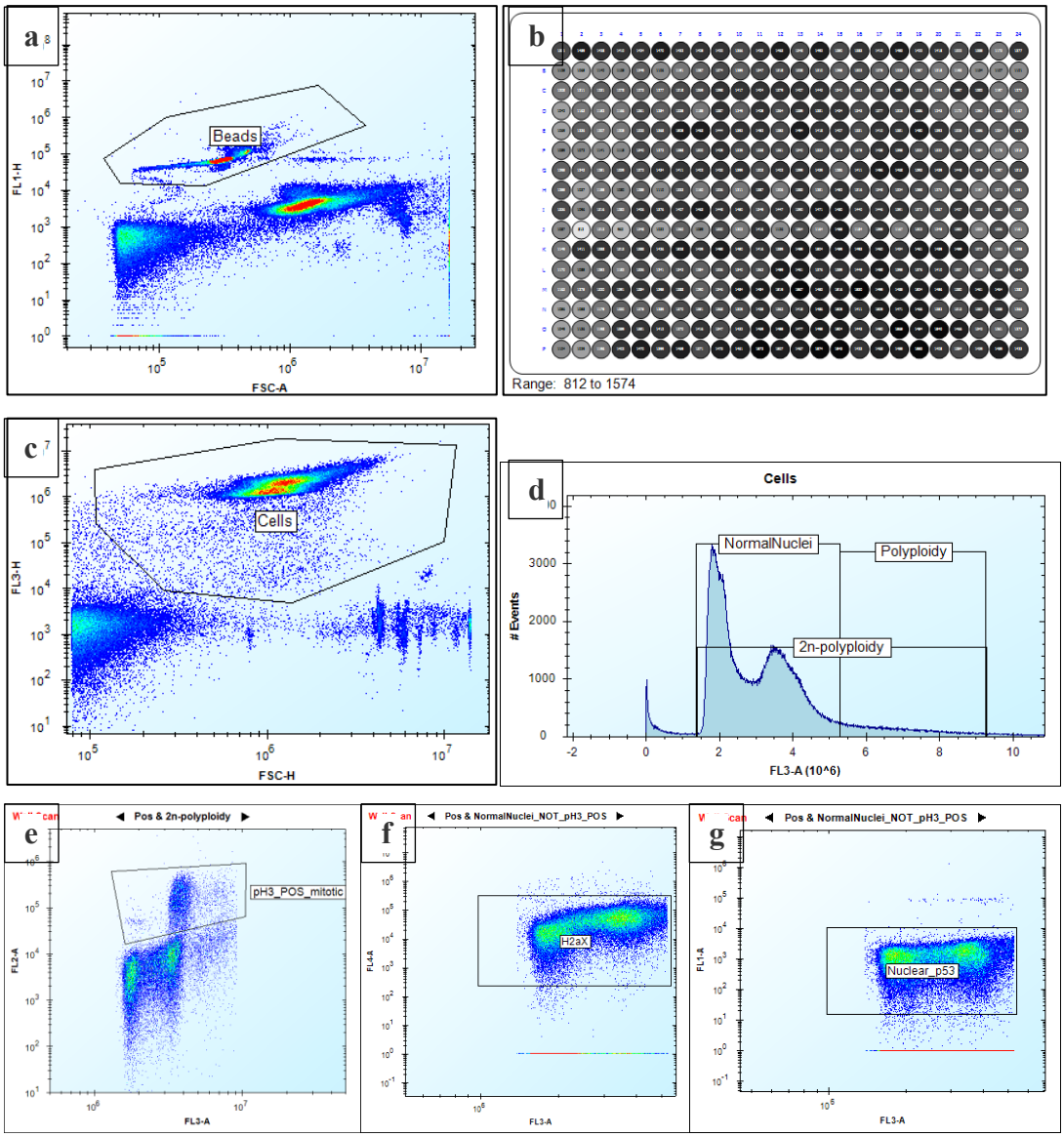

Figure 9, Gating of MultiFlow events in ForeCyt® software. The fluorophores used and their corresponding parameters in the software are FITC (p53) – FL1, PE (pH3) – FL2, PI (DNA stain) – FL3, AlexaFluor® 647 (γH2AX) – FL4. FSC = Forward scatter, A = Area, H = Height. Gating was done based on instructions by the manufacturer. **a)** Counting beads were gated in a dot plot representing all captured events with FL1-H on the y-axis and FSC-A on the x-axis. The size and fluorescence of the beads are provided by the manufacturer which allows for identification based on these parameters. This population was named "Beads" **b)** A heat map was created based on the "Beads" gate, which represents the number of beads for each well. This ensured even uptake of samples from each well in the experiment. **c)** A logical population with all events excluding the beads from a) was created, and with FL3-H on the y-axis and FSC-H on the x-axis the cells were identified. A gate was created around this population and named "Cells". **d)** Based on the "Cells"-gate a histogram with the number of events on the y-axis and FL3 on the x-axis the nuclei were visualised. The gates for "Normal

Nuclei" and 2n-polyploidy were created to exclude all events but the nuclei. **e)** From the 2n-polyploidy population the pH3-positive cells were identified with FL2-A on the y-axis and FL3-A on the x-axis. The gate for pH3 positive cells was named "pH3_POS" f) A logical gate of "Normal Nuclei" excluding the "pH3_POS" cells were used to identify the nuclei that express γH2AX. These events were gated using FL4-A on the y-axis and FL3-A on the x-axis. g) Similarly, from the same logical population the nuclei expressing p53 were identified with FL1-A on the y-axis and FL3-A on the x-axis.

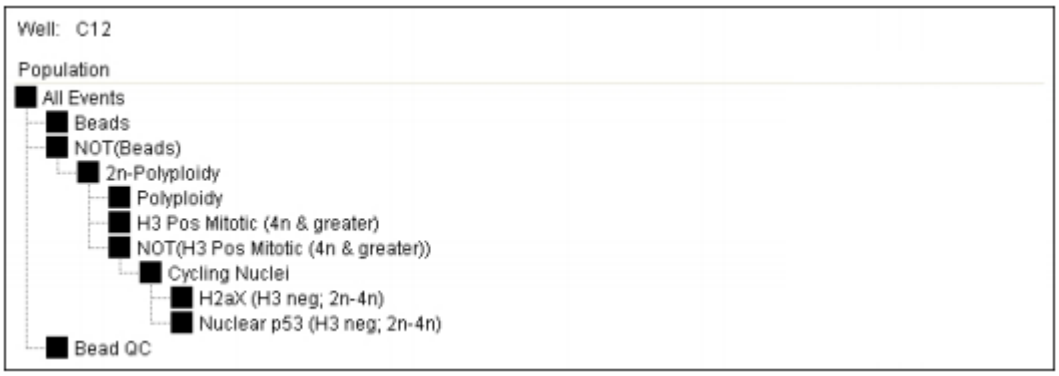

Figure 10, Summarised gating logic of MultiFlow. (*MultiFlow(R).*)

3.1.2 Analysing genotoxicity in TK6 cells using flow cytometry

Results for genotoxic prediction of flow cytometric analyses with TK6 cells are presented in table 8. The lowest effective concentration (LEC) and lowest precipitating concentration (LPC) are presented. For each concentration of each compound, the relative nuclei count (RNC, fold of pH3, γH2AX and p53 were counted as a fold increase compared to the average of negative controls. For a compound to be classified as genotoxic, the GEF introduced by Bryce et al. (2017), described in chapter 1.7.2.4, was used (Bryce et al., 2017). In addition, if RNC dropped below 0.2, the concentration was considered cytotoxic, and these values were excluded. Precipitating concentrations were taken into consideration as described in chapter 2.4. In addition to the results presented in the table, for mitomycin C and amiodarone the highest concentration tested was dependent of solubility properties, for cytosine arabinoside the lowest tested concentration gave a genotoxic result and CCCP and imipramine were cytotoxic at 75 µM and 250 µM correspondingly. Rotenone gave a false positive result.

Table 8, Results of MultiFlow® with TK6 cells. The table indicates the compounds studied, highest concentration of each compound and the classification according to the GEFs. Bolded text represents an effect that does not correspond with the prior classification (as indicated in table 1). The lowest effective concentration (LEC) and lowest precipitating concentration (LPC) are indicated for each compound.

Nr.	Compound	Max conc. (µM)	Classification	LEC (µM)	LPC (µM)
1	CCCP	100	Non genotoxic	-	-
2	Paclitaxel	0.01	Aneugen	0.000625	-
3	MMS	200	Clastogen	37.5	-
4	Mitomycin C	15	Clastogen	0.021973	-
5	4NQO	10	Clastogen	0.3125	-
6	Cytosine arabinoside	1	Clastogen	0.001465	-
7	BAP	1000	Non genotoxic	-	15.625
8	Colchicine	0.25	Aneugen	0.011719	-
9	Vinblastine	0.024	Aneugen	0.006	-
10	Amiodarone	100	Non genotoxic	-	-
11	2.4-dinitrophenol	1000	Non genotoxic	-	-
12	Nimesulide	1000	Non genotoxic	-	-
13	NaCl	1000	Non genotoxic	-	-
14	Rotenone	10	**Aneugen**	1.875	-
15	Sertraline	1000	Non genotoxic	-	93.75
16	Imipramine	1000	Non genotoxic	-	375

3.1.3 Analysing genotoxicity in HepG2 cells using flow cytometry

Flow cytometric data with HepG2 cells were analysed using the same criteria as for TK6 cells except for that RNC having a value less than 0.5 being excluded (discussed in detail in section 4.3). Issues with sample acquisition by flow cytometry occurred with HepG2 cells which resulted in largely variable cell numbers and, therefore, exclusion of several concentrations. Inconsistent wells where cell or bead counts differed from the normal distribution were excluded. The LECs where not calculated due to several concentration ranges being excluded from analysis. The classification of compounds using GEFs with HepG2 cells are stated in table 9. Carryover between samples was also considered and the results are, therefore, not considered accurate. Further comparison between TK6 cells and HepG2 cells with flow cytometry was not made.

Table 9, Results of flow cytometric analyses with HepG2 cells. Compounds and the maximal concentration tested. The observed effect is listed under "Classification", bolded values represent effects that do not correspond with the prior classification, "*" represents a correct classification of genotoxicant but with the wrong mode of action. Inconclusive result is indicated if more than half of the concentrations of the compound were excluded.

Nr.	Compound	Max conc. (µM)	Classification
1	CCCP	100	Non genotoxic
2	Paclitaxel	0.01	Aneugen
3	MMS	200	**Non genotoxic**
4	Mitomycin C	15	**Non genotoxic**
5	4NQO	10	Clastogen
6	Cytosine arabinoside	1	**Non genotoxic**
7	BAP	1000	Non genotoxic
8	Colchicine	0.25	**Clastogen***
9	Vinblastine	0.024	Aneugen
10	Amiodarone	100	**Aneugen**
11	2.4-dinitrophenol	1000	Non genotoxic
12	Nimesulide	1000	Non genotoxic
13	NaCl	1000	Inconclusive
14	Rotenone	10	Inconclusive
15	Sertraline	1000	Inconclusive
16	Imipramine	1000	Inconclusive

3.2 Using high content analysis to measure genotoxicity

Before the high content analysis method was used to measure genotoxicity in HepG2 cells the steps of the method were determined. The results for antibody concentrations and co-incubations (multiplex) for the markers γH2AX, pH3 and p53 are presented. Following, the image analysis for the markers and the raw data is presented before proceeding to the genotoxicity results for the 16 reference compounds in HepG2 cells.

3.2.1 HCA assay setup

To analyse the markers γH2AX, pH3 and p53 by imaging, antibody concentrations for each marker were determined by analysing the fluorescence intensities from images stained with different concentrations of antibodies. The control treatments used for antibody determinations were 200 µM MMS, 12 nM vinblastine and 10 µM nutlin-3. The antibodies were diluted in a way that the detection intensity of Operetta was not exceeded and could be clearly distinguished from the background. The dilution of Hoechst 33342 was not tested separately, since the 1 µg/ml was found to be a suitable concentration based on another in-house assay. The concentrations chosen and the intensity histograms are shown for all channels in figure 11 a-h. The final concentrations chosen for each primary antibody was 1:1000 for γH2AX and pH3, and 1:300 for p53 (Novus). All secondary antibodies were diluted 1:500.

First multiplexes were done with primary antibodies γH2AX and pH3 and the secondary anti-rabbit and anti-mouse antibodies, respectively. All wells showed results as expected, wells stained with γH2AX and anti-mouse secondary antibody, pH3 and anti-rabbit secondary antibody or only secondary antibodies showed no signal. Wells stained with all of the antibodies at the same time showed increases in total signals as predicted, vinblastine treated wells showed an increase in pH3 and MMS treated wells an increase in γH2AX (figure 12). The staining patterns for both markers were also identical to the examples shown in figure 11 c and e. Based on these results the multiplex of these four antibodies was considered successful.

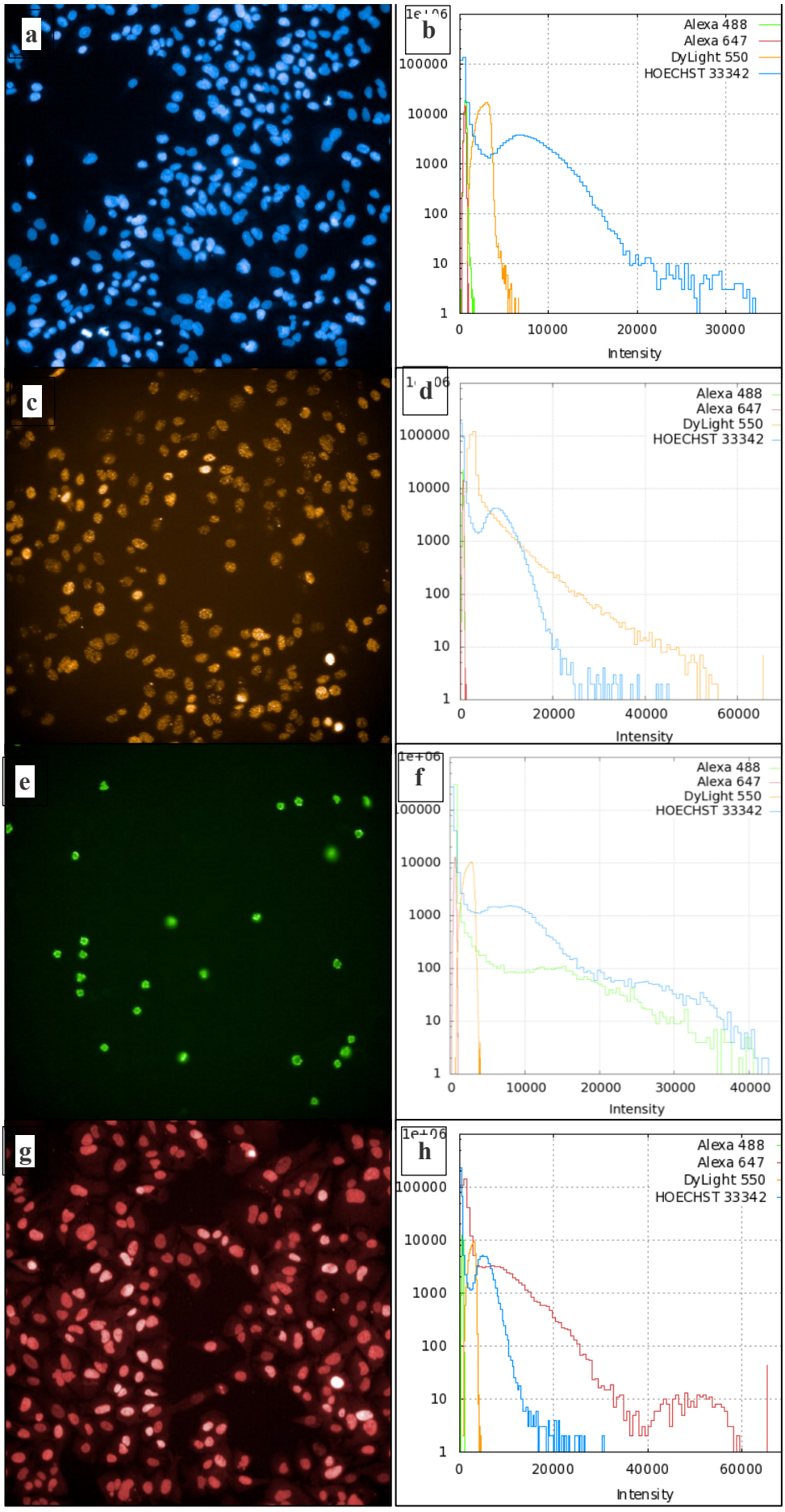
a
b
Alexa 488
Alexa 647
DyLight 550
HOECHST 33342
Intensity
c
d
Alexa 488
Alexa 647
DyLight 550
HOECHST 33342
Intensity
e
f
Alexa 488
Alexa 647
DyLight 550
HOECHST 33342
Intensity
g
h
Alexa 488
Alexa 647
DyLight 550
HOECHST 33342
Intensity

Figure 11, Antibody concentration determination based on fluorescent intensities. All pictures in the left panel were acquired with Operetta 20x water immersion objective. In the right panel histograms for each channel are presented with the number of pixels on the y-axis and the intensity of the fluorescence on the x-axis. For better visualisation of the markers the Hoechst dye is excluded in images c, e and g even if it is present in the histograms. a) Image from a negative control well (vehicle, 1% DMSO treatment), where nuclei were imaged by Hoechst 33342 staining b) The blue curve on the histogram represents the fluorescence intensity of Hoechst dye. c) Image from a well treated with 200 µM MMS, stained with γH2AX primary antibody diluted 1:1000 and anti-rabbit secondary antibody diluted 1:500, imaged with DyLight550 channel. Each spot seen on the picture represents a DSB on the DNA. d) Intensity of DyLight550 represented by the orange curve. e) Image from a well treated with 12 nM vinblastine, stained with pH3 primary antibody diluted to 1:1000 and anti-mouse secondary antibody diluted 1:500, imaged with Alexa488 channel. Each stained nucleus represents a cell in mitosis. f) Intensity of Alexa488 represented by the green curve. g) Image from a well treated with 10 µM Nutlin-3, stained with Novus p53 primary antibody diluted to 1:300 and anti-Goat secondary antibody diluted 1:500, imaged with Alexa647 channel. Nutlin-3 promotes the localisation of p53 to the nucleus where the highest intensities can be visualised. Presence of p53 in the cytoplasm can be detected with a weaker intensity. h) Intensity of Alexa 647 represented by the red curve.

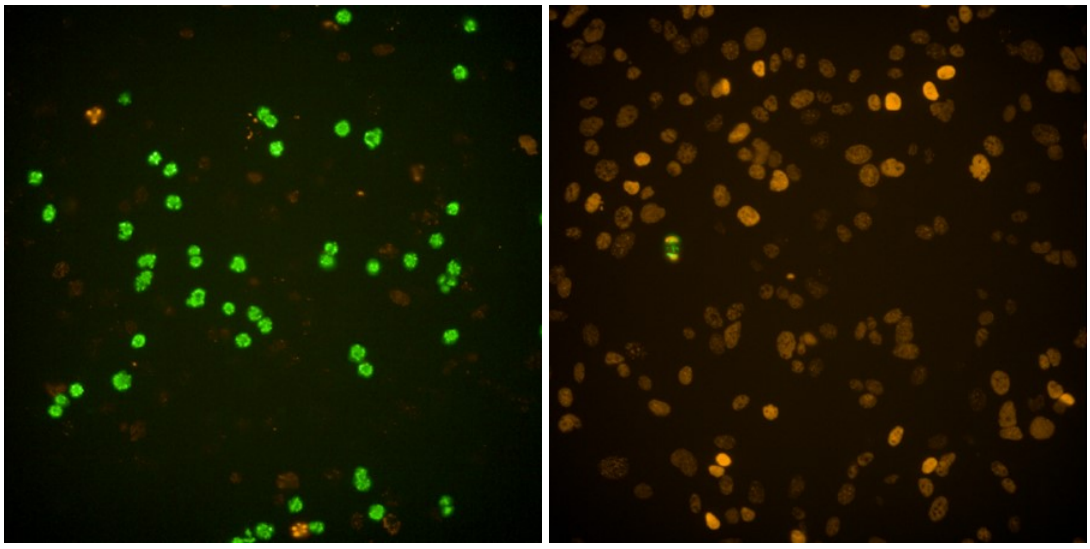

Figure 12, Multiplex of primary antibodies γH2AX and pH3 and the secondary antibodies anti-mouse Alexa488 and anti-rabbit DyLight550. a) Wells treated with 12 µM vinblastine shows an increase in pH3 cells (green). Some cells also express γH2AX as a result from the treatment. b) Wells treated with 20 µM MMS show an increased number of cells with γH2AX expression.

Adding the primary p53 antibody and anti-goat secondary antibody to the multiplexing scheme resulted in that unspecific binding was observed. It was noticed that the secondary antibodies anti-rabbit and anti-mouse were produced in goat, which resulted in binding of the anti-Goat secondary antibody to both of the other secondary antibodies. This resulted in the decision to stain p53 on another plate. The plates where therefore done in duplicates, with one plate stained with Hoechst, γH2AX and pH3 and the other one with Hoechst and p53.

3.2.2 Image analysis for HCA

In order to obtain the raw data from the images an image analysis template was created in Columbus image analysis software from Perkin Elmer. The analysis was made based on the same criteria as used for flow cytometry. First, using Hoechst 33342 channel the nuclei were identified by the algorithm "Find Nuclei". The parameters used were "Diameter" 30 μm^2, "Splitting sensitivity" and "Threshold 0.3" (figure 13 a). From the "Nuclei" population a new population with removed border objects were created, excluding all items that were located partly outside the frames. This "Nuclei Selected" population was used for all further analyses (figure 13 b). To identify pH3-positive nuclei, the intensity properties of Alexa 488 were calculated from the nuclei. Based on these intensities in positive and negative controls, all nuclei with a mean Alexa 488 intensity >1000 were marked pH3 positive nuclei. Similarly, a population with mean Alexa 488 <1000 was created and marked "pH3 negative" (Figure 14). From the "pH3 negative" population of nuclei the mean intensity of DyLight550 was calculated and named γH2AX intensity. For p53 which was tested on a separate plate, the same steps for "Nuclei selected" population were made. From this population the mean intensity for Alexa 647 was calculated. The image analysis was performed on all images and data for each well was exported to be further processed in Excel.

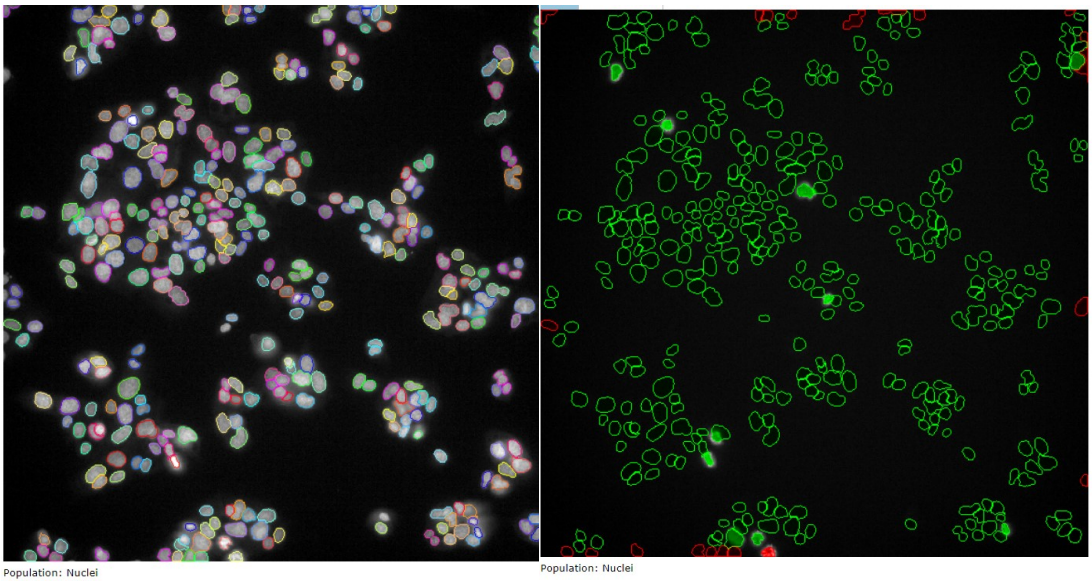

Figure 13, Identifying nuclei from acquired image. a) The nuclei can be visualised using Hoechst 33343 channel. The algorithms of the software are able to identify and "gate" each nucleus. The parameters were adjusted to obtain best resolution based on negative controls. b) Nuclei on the edges of the frames were excluded from analysis.

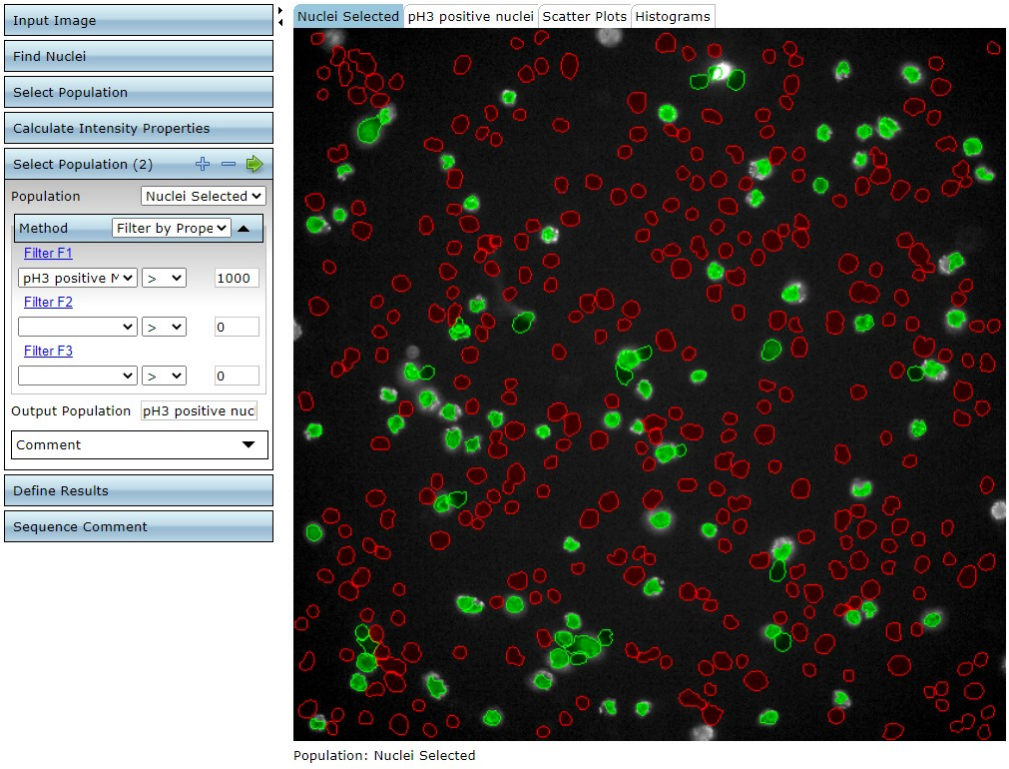

Figure 14, Visualisation and identification of pH3-positive nuclei. The intensity properties of Alexa 488 were analysed and all nuclei showing a mean intensity >1000 were considered pH3-positive (marked green).

3.2.3 Raw data handling for genotoxicity determination in HCA

Each 384-well plate measured by HCA contained the selected 16 reference compounds studied at duplicates for every concentration. All plates were stained for Hoechst and either for γH2AX and pH3 or p53. The 4- and 24-hour timepoint plates for γH2AX and pH3 were replicated in three experiments. The p53-stained plates were done in one replicate for 4 hours and two replicates for 24 hours. In addition, one plate with a 48-hour incubation was measured after noticing that a 24-hour incubation was in several cases not sufficient for γH2AX expression. For all plates, 16 wells with only DMSO treatment served as the negative controls. The calculations described in chapter 2.7.3 were adapted for all wells. The amount of data points for each compound at each concentration for every marker is presented in table 10. This applied for all other compounds, excluding those compounds which had an adjusted concentration. For these the data points may vary from two to four. The median used for analysis, as well as the MAD were counted from these data points. The MAD for each value presented as error bars in the graphs in appendix B. Two separate RNC values are also counted for each concentration, one from the plate stained for γH2AX and pH3 and one from the plate stained for p53. It was also noted that the p53 intensities were counted from all nuclei in HCA, as an exception from MultiFlow, where the pH3-positive nuclei were excluded.

Table 10, the amount of data points for each compound at each concentration for all the marker used for analysis in HepG2 cells in HCA. In the upper column are the three timepoints analysed in this study and on the right-hand side the three calculated marker folds. For example, with the 4-hour incubations there were three plates stained with γH2AX and pH3, and as all concentrations were found in duplicates there are 6 data points for both γH2AX- and pH3-folds for each compound at each concentration. The 48-hour incubations on the other hand were done without replicates and, therefore, there are only 2 datapoints for each marker.

	4 hours	24 hours	48 hours
γH2AX-fold	6	6	2
pH3%-fold	6	6	2
p53-fold	2	4	2

For the γH2AX- and pH3-stained plates, the positive controls for vinblastine and MMS were also analysed to verify that the controls and thereby the whole experiment was successful. The p53-stained plates were handled in the same experiments and assumed to be identical in terms of compound handling and fixation performed by automation. The staining steps were performed manually and as the p53 marker could be seen in the images these plates were also considered successful. It was, however, noted that one of the 24-hour plates had a decrease in γH2AX shift for MMS control but since the results for the reference compounds were in line with the other plates this plate was not discarded. Variation may have been caused by a pipetting error as the MMS control had a different liquid class than the other control compounds (MMS was diluted in H_2O and the other compounds in DMSO) or the control stock used could have been more diluted due to a pipetting error.

The first plate measured was incubated for 24 hours and it was noticed that concentrations of some compounds needed to be adjusted, for example vinblastine did not cause an increase in pH3 signal at the same concentrations as in TK6 cells and was increased for the next test. As the suggested RNC value for HepG2 cells in genotoxicity testing is higher than for TK6 cells (discussed more in detail in section 4.3), some concentrations resulted in a cytotoxic effect earlier and the starting concentration was reduced. It was also observed that some compounds were precipitating at lower concentrations possibly as a cause of repeated freeze and thaw cycles. Fresh samples were made for precipitating samples and the precipitation was determined for each plate separately. These adjustments can be observed in the results as some of the compounds have more or less concentration-data points than others. As the RNC values were counted separately for each plate, the values for the markers presented later are provided only if the RNC is above threshold for the plate in question for that concentration.

3.2.4 Results with HepG2 cells in HCA

For HepG2 cells the results from genotoxicity testing by HCA were plotted in graphs to visualise the markers in relation to the concentrations for each compound. As an example, the non-genotoxicant NaCl is shown here as baseline (figure 15). The values for γH2AX and pH3 and the RNC from these plates were plotted in one graph and the values for p53 and RNC from those plates on another. The folds for γH2AX are represented by orange lines, the fold of pH3 as green lines and the fold of p53 as red lines. Each line represents a different time-point, the lightest for 4 hours and darkest for 48 hours. The scale for the genotoxicity markers is presented on the y-axis to the left and is represented as a fold to the negative control. The RNC is represented as grey lines and the scale is on the y-axis on the right side of the graph. The concentrations are presented on the x-axis in a logarithmic scale. The scale on the graphs showing the results for the same compounds are the same for clarity. Results for all compounds can be found in appendix A. Precipitated concentrations are not shown in the graphs. Further, some of the data from HCA is shown in section 3.3, in comparison with results from TK6 cells in MultiFlow.

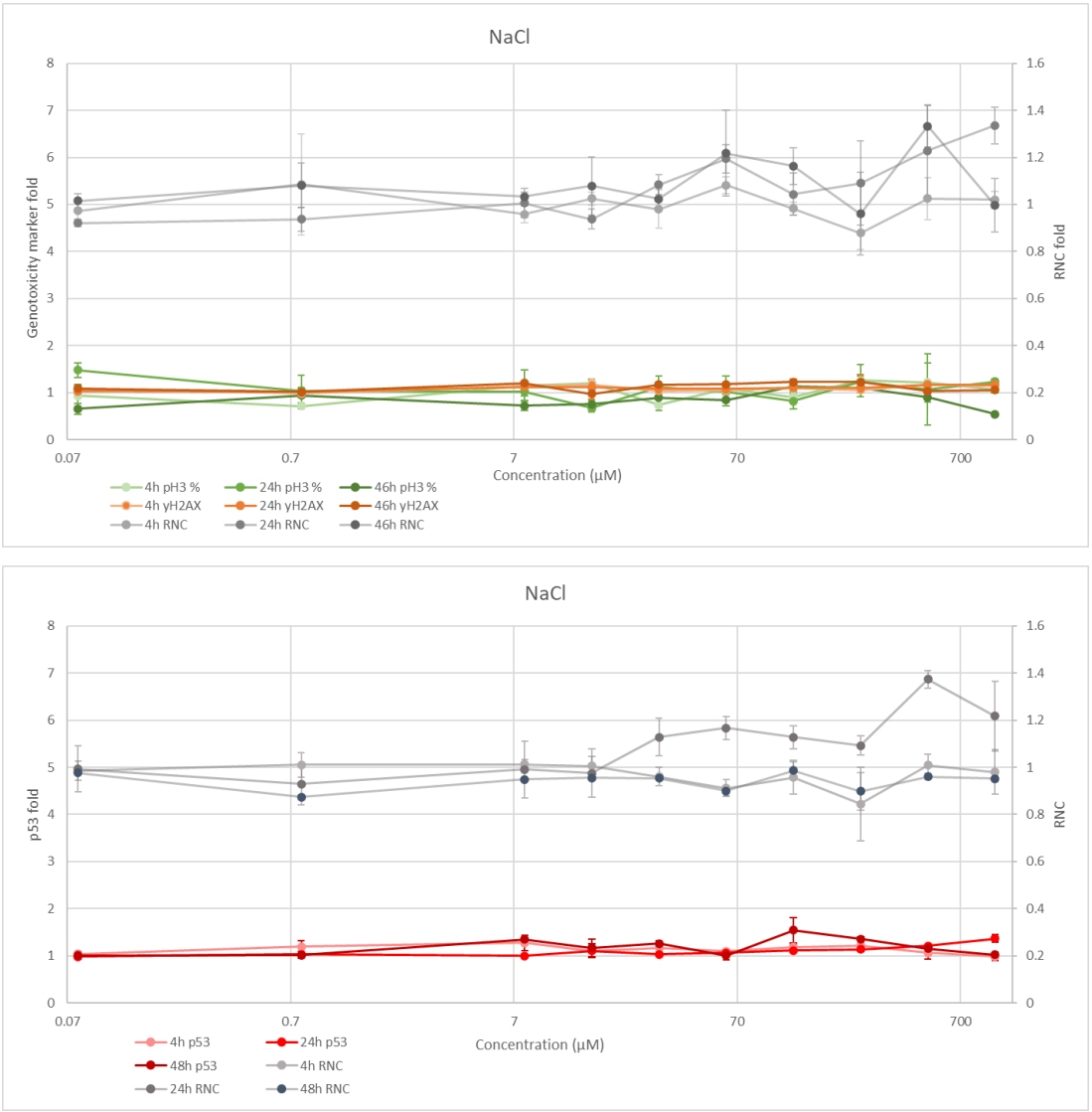

Figure 15, Results for HCA measurement of HepG2 cells treated with NaCl. Coloured lines indicate the genotoxicity markers γH2AX (orange), pH3(green) (upper graph) and p53 (red) (lower graph). Grey lines represent the RNC. The MAD is shown as y-error bars for each data point. The baseline for the markers lies around 1 (scale on the left-hand side) and no significant fold increases or decreases can be seen for any of the markers as is expected for a non-genotoxicant. RNC baseline also lies around 1 but is set higher for clarity (scale on the right-hand side).

3.2.4 Determination of thresholds for genotoxicity

From the medians of the 4-hour and 24-hour data a range of different criteria and thresholds were tested to see which could predict the genotoxicity of the compounds most precisely. The different combinations of thresholds were based on criteria used for MultiFlow and previous studies of genotoxicity testing using HepG2 cells (Khoury, Zalko, & Audebert, 2016c). The comparisons were performed in Excel by a system where different criteria were tested on all compounds at the same time. In the same way as with the GEFs, for a compound to be considered as an aneugen or a clastogen, two of the criteria needed to be met at two continuous concentrations. The criteria tested are presented in table 11. For each set of criteria, the prediction was counted as a score. Each compound predicted correctly, according to previous classifications described in the literature (as indicated in table 1), gave a score of 1, resulting in a maximum score of 16. Using these reference compounds, the prediction of endpoints at rows 5 and 8 in table 11 gave the best predictivity with 15/16 compounds determined correctly. In both cases the one compound with an inaccurate prediction was BAP which did not elevate the γH2AX response sufficiently at these timepoints as seen in the previous section. Both of these models did not include p53 as a marker which in the case for example CCCP indicated a false positive response using criteria 1 and 2.

As previously mentioned, it was seen that the 4-hour incubation plate did not increase the γH2AX response in several clastogens in HepG2 in the same way as in TK6 cells, and therefore, the 4-hour timepoint was suspected to be too short for γH2AX expression in HepG2 cells. Therefore, the 48-hour incubation plate was also incorporated in the analysis and data was analysed from these three timepoints in parallel. With 3 timepoints a strategy where at least 2 out of 3 criteria were met gave the best results. For aneugens, thresholds based on MultiFlow was used, a pH3 increase 1.71-fold at 4 hours, 1.52-fold at 24 hours and, in addition, 1.52-fold at 48 hours. For clastogens, the thresholds for γH2AX increase at 4 hours and 24 hours was 1.3-fold and for 48 hours 2.11-fold, as in MultiFlow. The RNC threshold for 4 hours was kept at 0.5 and decreased to 0.2 for 24 and 48 hours. By this strategy, all compounds could be identified correctly, even BAP.

Table 11, Different criteria tested for genotoxicity predictions. In the table below is listed all the genotoxicity endpoints tested on the data from HCA with HepG2 cells. In the first column a number is given to the criteria at that row (1-8) which is used in the text as an identifier for the criteria in question. In the "RNC" column the RNC threshold used for the criteria on that row. In the columns below "Aneugen" is the fold increases for the different markers at different timepoints for aneugens, and likewise in the column "Clastogen" the markers for clastogens at different timepoints. In the "Score" column is the number of compounds predicted correctly by using that set of criteria.

		Aneugen			Clastogen				
Row	**RNC**	**pH3-fold at 4h**	**pH3-fold at 24 h**	**p53-fold at 24h**	**γH2AX-fold at 4h**	**p53-fold at 4h**	**γH2AX-fold at 24h**	**p53-fold at 24h**	**Score (/16)**
1	0.2	1.71	1.52	1.45	1.51	1.4	2.11	1.45	**12**
2	0.5	1.71	1.52	1.45	1.51	1.4	2.11	1.45	**13**
3	0.2	1.71	1.52		1.51		2.11		**13**
4	0.5	1.71	1.52		1.51		2.11		**12**
5	0.2	1.3	1.3		1.3		1.3		**15**
6	0.5	1.3	1.3		1.3		1.3		**14**
7	0.2	1.3	1.3		1.3		1.3	0.7	**14**
8	0.5	1.3	1.3		1.3		1.3	0.7	**15**

3.3 Comparison of MultiFlow with TK6 cells and HCA with HepG2 cells

For a more detailed comparison between the cell lines, the results from MultiFlow with TK6 cells were plotted in graphs. The same plotting logic was used in these graphs as described previously with HepG2 cells in HCA. The same reference compound NaCl, which is a non-genotoxicant, is shown in figure 16 as baseline. Values for γH2AX and pH3 are represented in one graph together with RNC for those plates (represented as lines for the 4-hour and 24-hour incubations separately) and p53 values with RNC for those plates separately in another graph. Genotoxicity markers (γH2AX, pH3 and p53) are presented as fold increase relatively to negative controls as described previously and are plotted on the y axis to the left. RNC are plotted on the y-axis on the right-hand side and the concentration series on the x-axis as a logarithmic scale. All data for the studied compounds can be found in appendix A for TK6 cells and appendix B for HepG2 cells.

For a better overview, the genotoxicity markers γH2AX, pH3 and p53 for all timepoints studied were visualised in spider plots to allow for a comparison of all compounds using the two different methods (figure 17). For simplicity, RNC values and the distribution of data are not shown in these graphs. The same compound in the two different methods is presented next to each other, with the data from MultiFlow with HepG2 cells on the right-hand side and the data from HCA with HepG2 cells on the left-hand side. In the plots the concentration series is presented as lines, with the darkest line representing the highest concentration (as indicated at the bottom of the graphs).

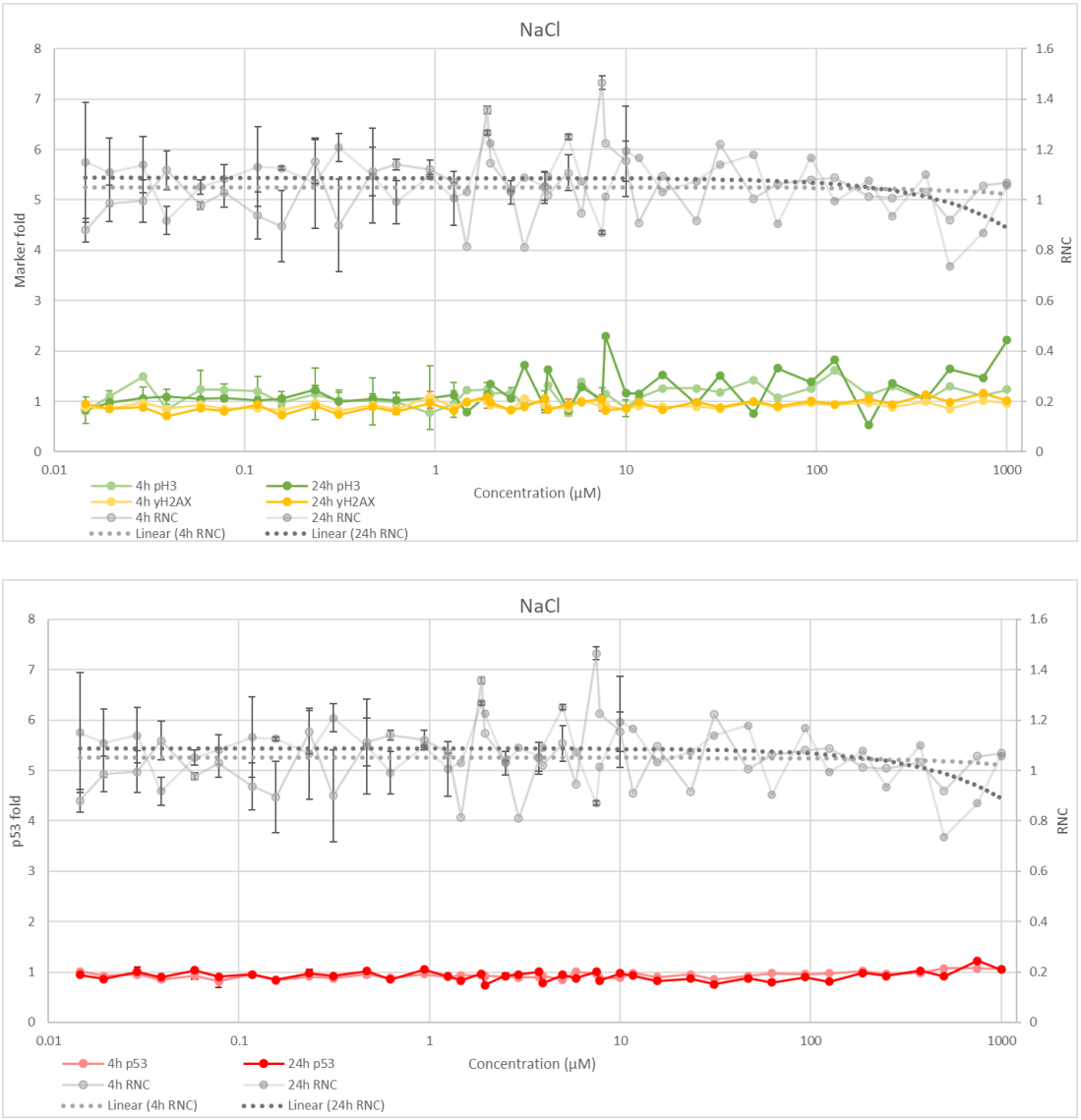

Figure 16, Results for MultiFlow measurement of TK6 cells treated with NaCl. Coloured lines indicate the genotoxicity markers γH2AX (yellow), pH3(green) (upper graph) and p53 (red) (lower graph). Grey lines represent the RNC which are the same both plots. The MAD is shown as y-error bars for each data point. The baseline for the markers lies around 1 (scale on the left-hand side) and no significant fold increases or decreases can be seen for any of the markers as is expected for a non-genotoxicant. RNC baseline lies around 1 but is set higher for clarity (scale on the right-hand side).

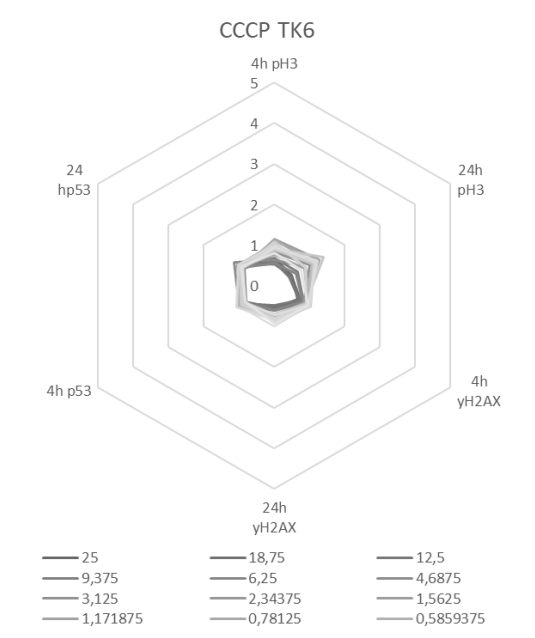
CCCP TK6
4h pH3
24h pH3
4h yH2AX
24h yH2AX
4h p53
24 hp53
25
18,75
12,5
9,375
6,25
4,6875
3,125
2,34375
1,5625
1,171875
0,78125
0,5859375

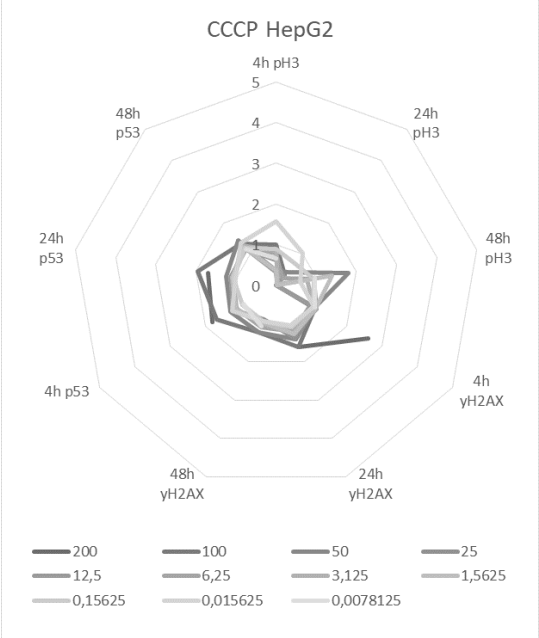
CCCP HepG2
4h pH3
24h pH3
48h pH3
4h yH2AX
24h yH2AX
48h yH2AX
4h p53
24h p53
48h p53
200
100
50
25
12,5
6,25
3,125
1,5625
0,15625
0,015625
0,0078125

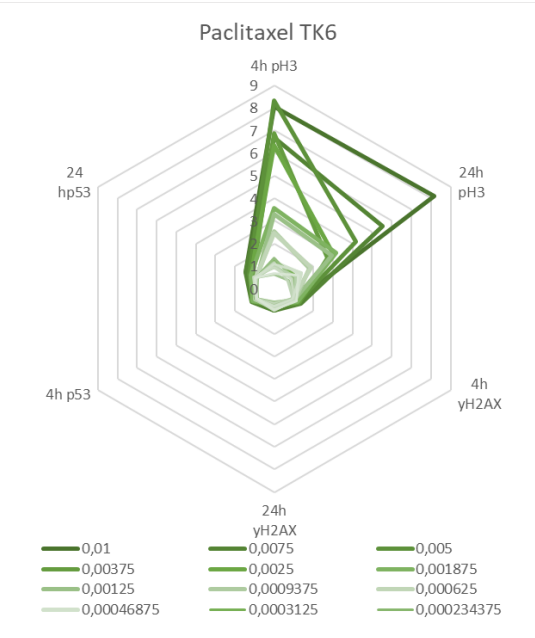
Paclitaxel TK6
4h pH3
24h pH3
4h yH2AX
24h yH2AX
4h p53
24 hp53
0,01
0,0075
0,005
0,00375
0,0025
0,001875
0,00125
0,0009375
0,000625
0,00046875
0,0003125
0,000234375

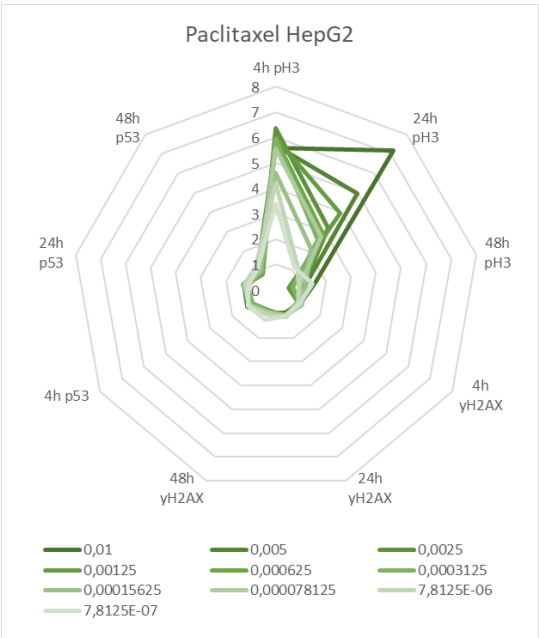
Paclitaxel HepG2
4h pH3
24h pH3
48h pH3
4h yH2AX
24h yH2AX
48h yH2AX
4h p53
24h p53
48h p53
0,01
0,005
0,0025
0,00125
0,000625
0,0003125
0,00015625
0,000078125
7,8125E-06
7,8125E-07

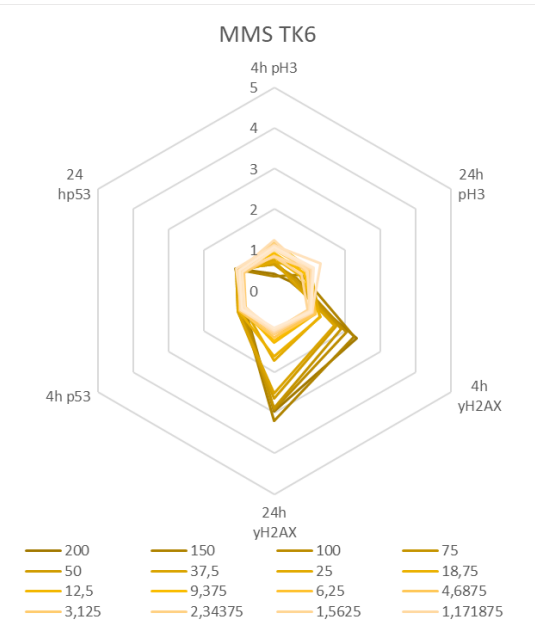
MMS TK6
4h pH3
24h pH3
4h yH2AX
24h yH2AX
4h p53
24 hp53
200
150
100
75
50
37,5
25
18,75
12,5
9,375
6,25
4,6875
3,125
2,34375
1,5625
1,171875

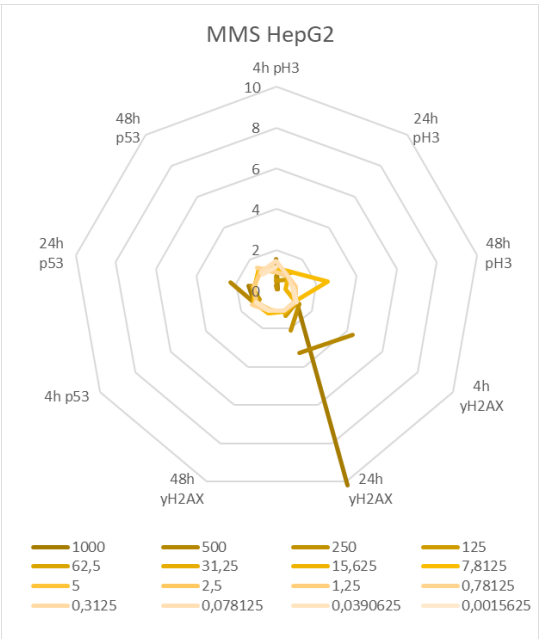
MMS HepG2
4h pH3
24h pH3
48h pH3
4h yH2AX
24h yH2AX
48h yH2AX
4h p53
24h p53
48h p53
1000
500
250
125
62,5
31,25
15,625
7,8125
5
2,5
1,25
0,78125
0,3125
0,078125
0,0390625
0,0015625

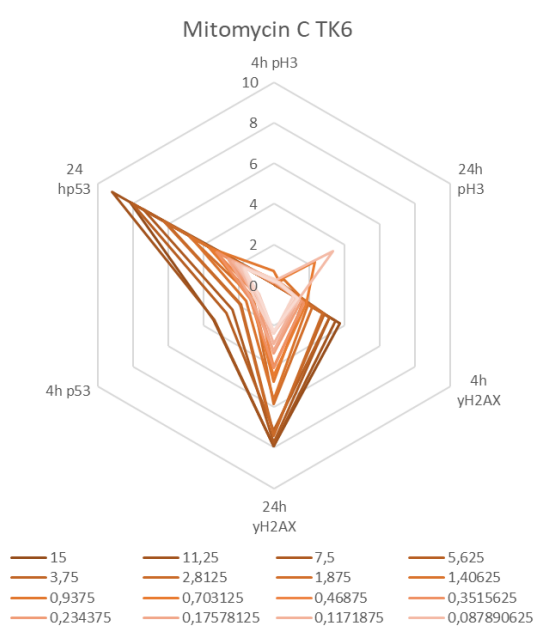
Mitomycin C TK6
4h pH3
24h pH3
4h yH2AX
24h yH2AX
4h p53
24 hp53
15
11,25
7,5
5,625
3,75
2,8125
1,875
1,40625
0,9375
0,703125
0,46875
0,3515625
0,234375
0,17578125
0,1171875
0,087890625

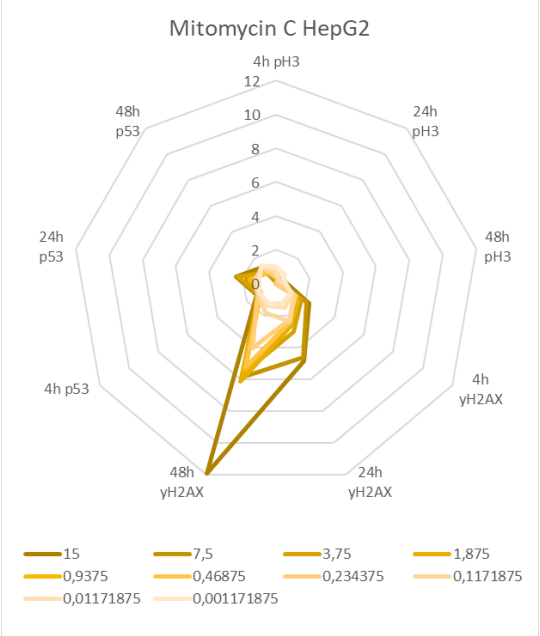
Mitomycin C HepG2
4h pH3
24h pH3
48h pH3
4h yH2AX
24h yH2AX
48h yH2AX
4h p53
24h p53
48h p53
15
7,5
3,75
1,875
0,9375
0,46875
0,234375
0,1171875
0,01171875
0,001171875

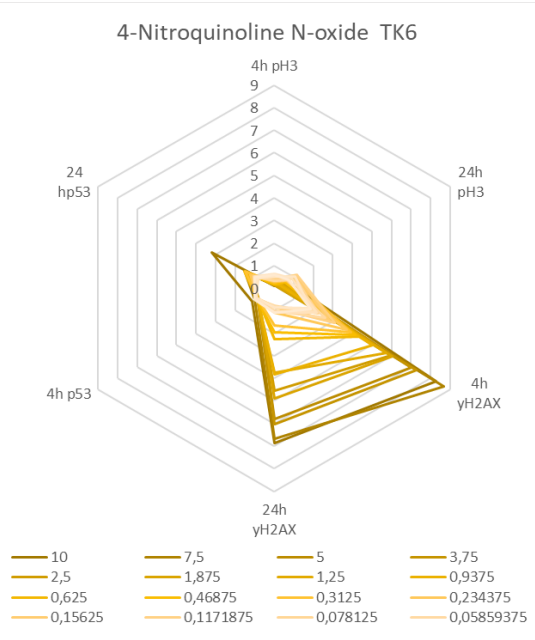
4-Nitroquinoline N-oxide TK6
4h pH3
24h pH3
4h yH2AX
24h yH2AX
4h p53
24 hp53
10
7,5
5
3,75
2,5
1,875
1,25
0,9375
0,625
0,46875
0,3125
0,234375
0,15625
0,1171875
0,078125
0,05859375

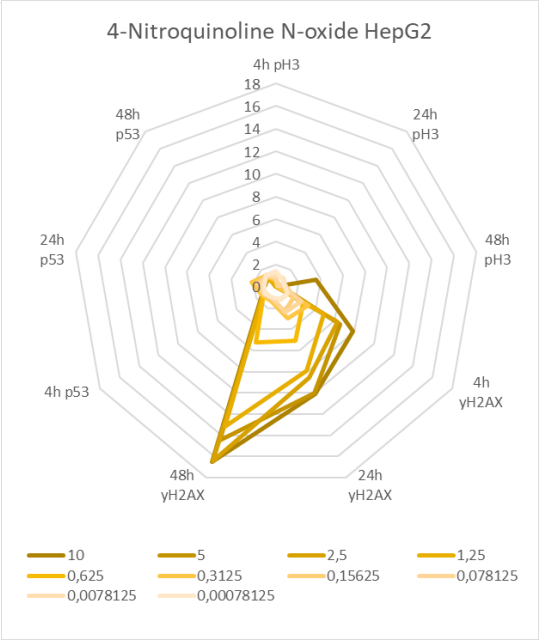
4-Nitroquinoline N-oxide HepG2
4h pH3
24h pH3
48h pH3
4h yH2AX
24h yH2AX
48h yH2AX
4h p53
24h p53
48h p53
10
5
2,5
1,25
0,625
0,3125
0,15625
0,078125
0,0078125
0,00078125

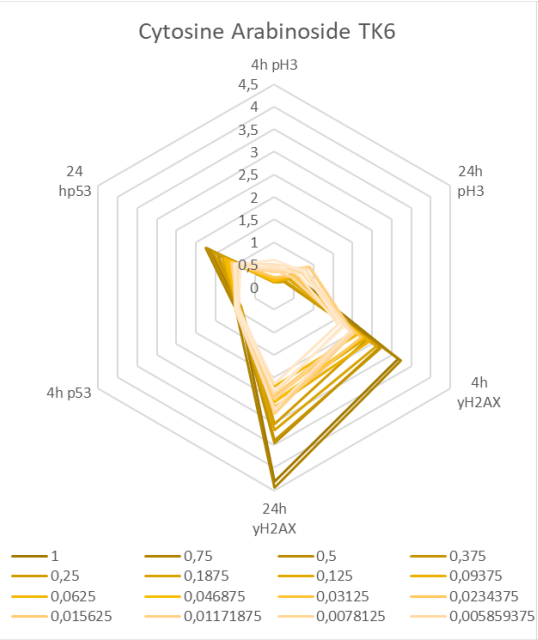
Cytosine Arabinoside TK6
4h pH3
24h pH3
4h yH2AX
24h yH2AX
4h p53
24 hp53
1
0,75
0,5
0,375
0,25
0,1875
0,125
0,09375
0,0625
0,046875
0,03125
0,0234375
0,015625
0,01171875
0,0078125
0,005859375

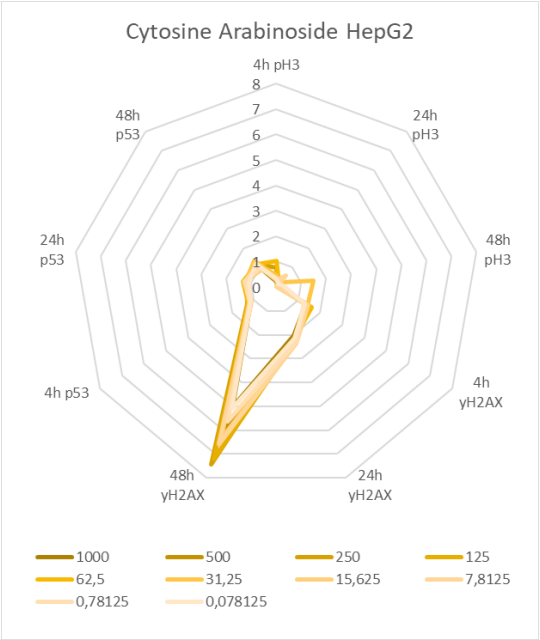
Cytosine Arabinoside HepG2
4h pH3
24h pH3
48h pH3
4h yH2AX
24h yH2AX
48h yH2AX
4h p53
24h p53
48h p53
1000
500
250
125
62,5
31,25
15,625
7,8125
0,78125
0,078125

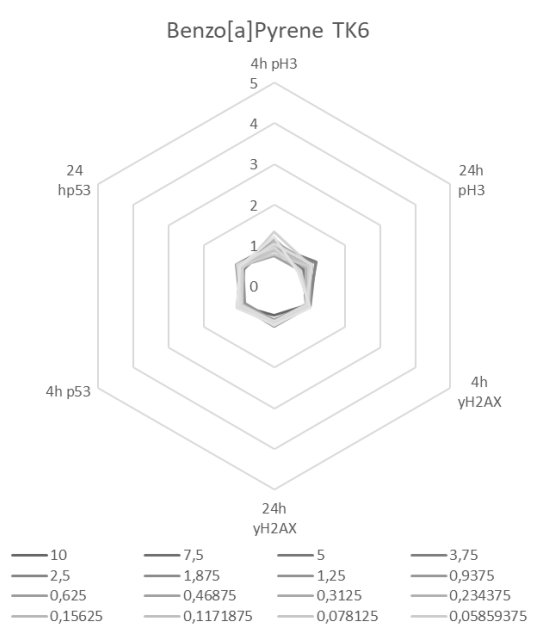
Benzo[a]Pyrene TK6
4h pH3
24h pH3
4h yH2AX
24h yH2AX
4h p53
24 hp53
10
7,5
5
3,75
2,5
1,875
1,25
0,9375
0,625
0,46875
0,3125
0,234375
0,15625
0,1171875
0,078125
0,05859375

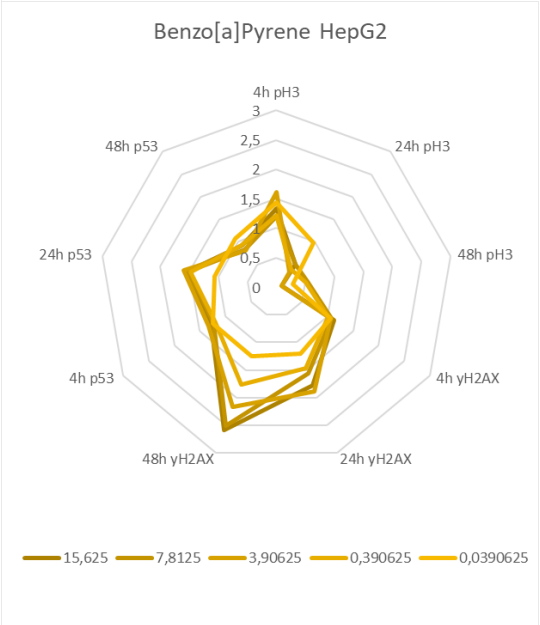
Benzo[a]Pyrene HepG2
4h pH3
24h pH3
48h pH3
4h yH2AX
24h yH2AX
48h yH2AX
4h p53
24h p53
48h p53
15,625
7,8125
3,90625
0,390625
0,0390625

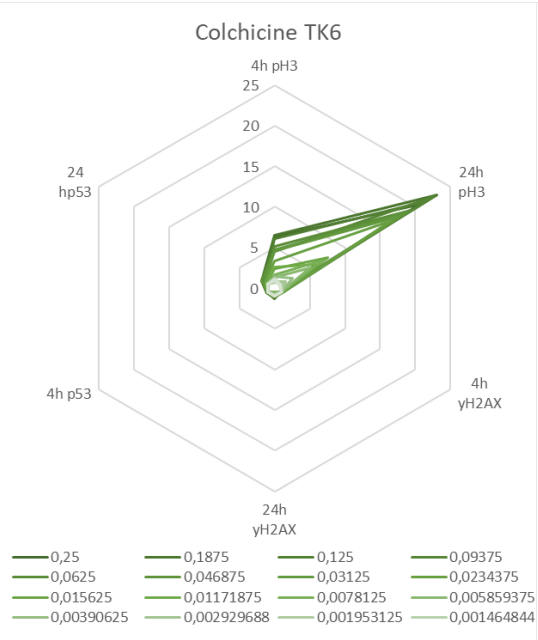
Colchicine TK6
4h pH3
24h pH3
4h yH2AX
24h yH2AX
4h p53
24 hp53
0,25
0,1875
0,125
0,09375
0,0625
0,046875
0,03125
0,0234375
0,015625
0,01171875
0,0078125
0,005859375
0,00390625
0,002929688
0,001953125
0,001464844

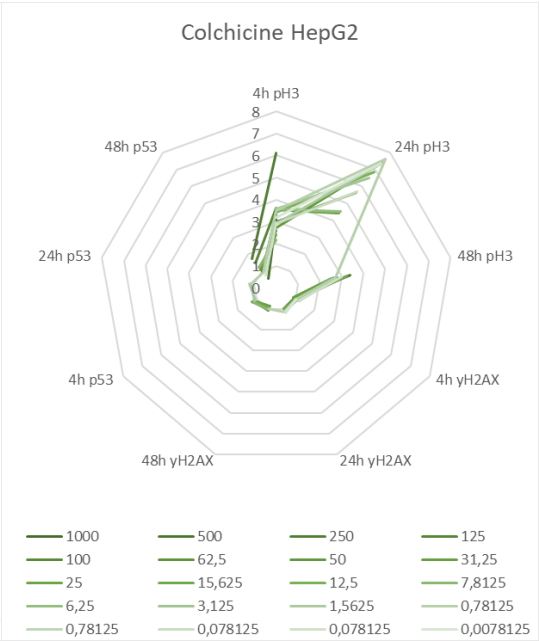
Colchicine HepG2
4h pH3
24h pH3
48h pH3
4h yH2AX
24h yH2AX
48h yH2AX
4h p53
24h p53
48h p53
1000
500
250
125
100
62,5
50
31,25
25
15,625
12,5
7,8125
6,25
3,125
1,5625
0,78125
0,78125
0,078125
0,078125
0,0078125

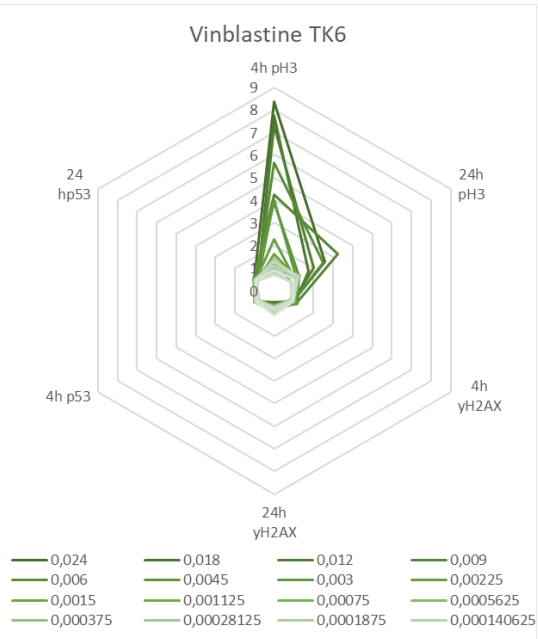
Vinblastine TK6
4h pH3
24h pH3
4h yH2AX
24h yH2AX
4h p53
24 hp53
0,024
0,018
0,012
0,009
0,006
0,0045
0,003
0,00225
0,0015
0,001125
0,00075
0,0005625
0,000375
0,00028125
0,0001875
0,000140625

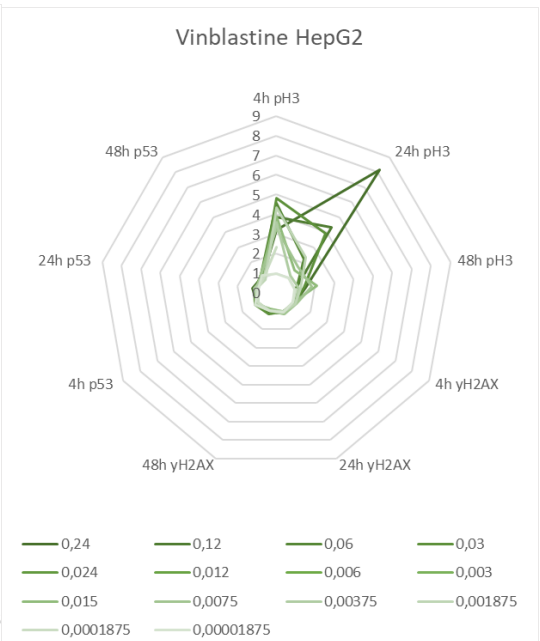
Vinblastine HepG2
4h pH3
24h pH3
48h pH3
4h yH2AX
24h yH2AX
48h yH2AX
4h p53
24h p53
48h p53
0,24
0,12
0,06
0,03
0,024
0,012
0,006
0,003
0,015
0,0075
0,00375
0,001875
0,0001875
0,00001875

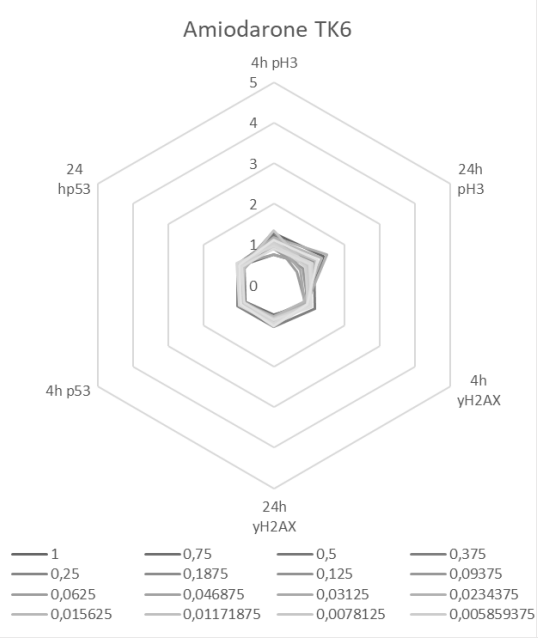
Amiodarone TK6
4h pH3
24h pH3
4h yH2AX
24h yH2AX
4h p53
24 hp53
1
0,75
0,5
0,375
0,25
0,1875
0,125
0,09375
0,0625
0,046875
0,03125
0,0234375
0,015625
0,01171875
0,0078125
0,005859375

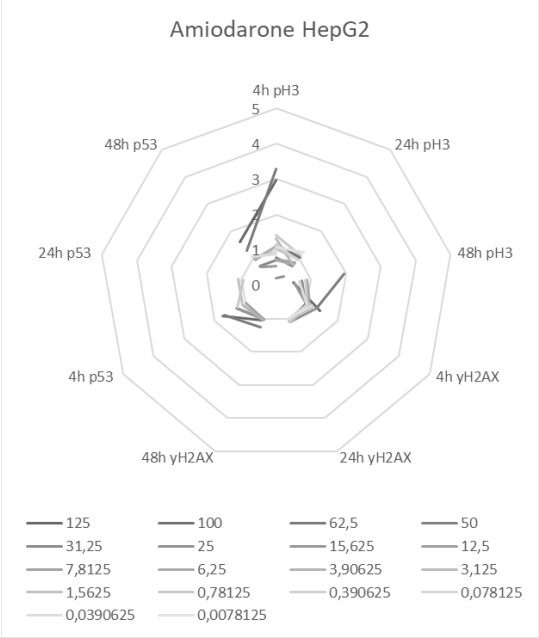
Amiodarone HepG2
4h pH3
24h pH3
48h pH3
4h yH2AX
24h yH2AX
48h yH2AX
4h p53
24h p53
48h p53
125
100
62,5
50
31,25
25
15,625
12,5
7,8125
6,25
3,90625
3,125
1,5625
0,78125
0,390625
0,078125
0,0390625
0,0078125

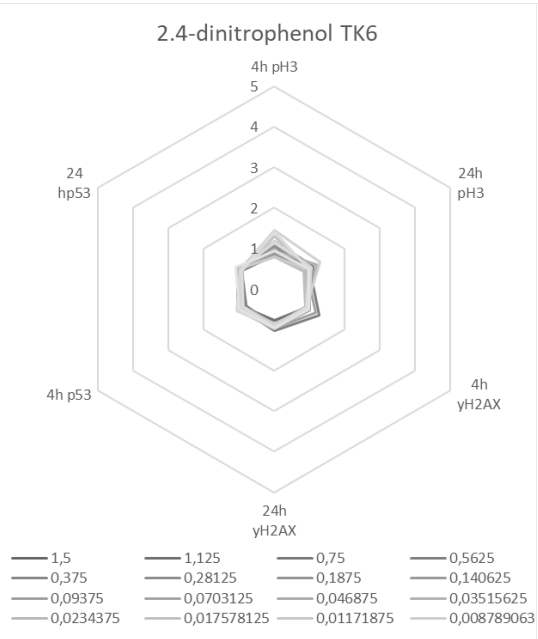
2.4-dinitrophenol TK6
4h pH3
24h pH3
4h yH2AX
24h yH2AX
4h p53
24 hp53
1,5
1,125
0,75
0,5625
0,375
0,28125
0,1875
0,140625
0,09375
0,0703125
0,046875
0,03515625
0,0234375
0,017578125
0,01171875
0,008789063

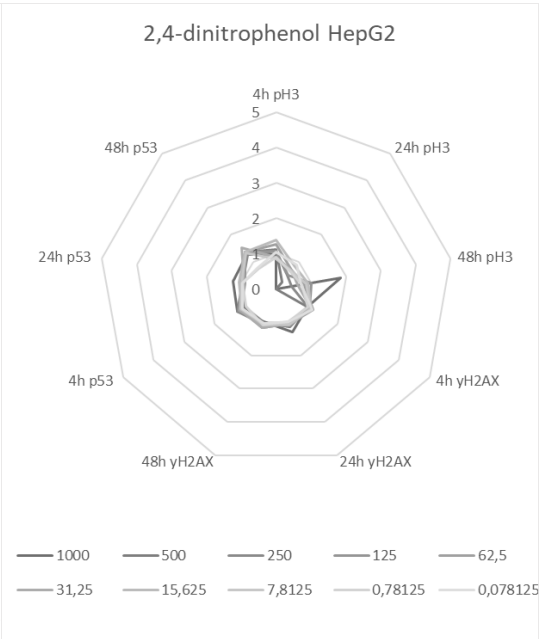
2,4-dinitrophenol HepG2
4h pH3
24h pH3
48h pH3
4h yH2AX
24h yH2AX
48h yH2AX
4h p53
24h p53
48h p53
1000
500
250
125
62,5
31,25
15,625
7,8125
0,78125
0,078125

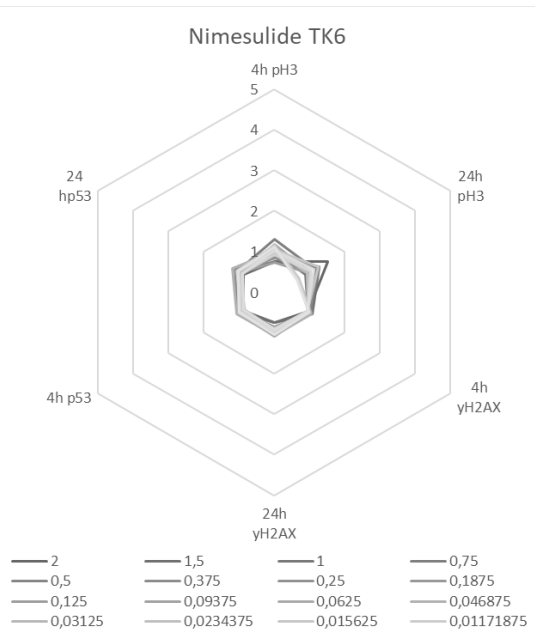
Nimesulide TK6
4h pH3
24h pH3
4h yH2AX
24h yH2AX
4h p53
24 hp53
2
1,5
1
0,75
0,5
0,375
0,25
0,1875
0,125
0,09375
0,0625
0,046875
0,03125
0,0234375
0,015625
0,01171875

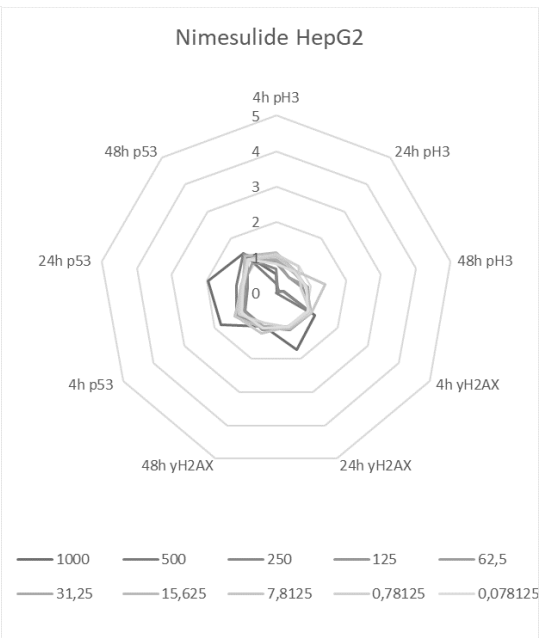
Nimesulide HepG2
4h pH3
24h pH3
48h pH3
4h yH2AX
24h yH2AX
48h yH2AX
4h p53
24h p53
48h p53
1000
500
250
125
62,5
31,25
15,625
7,8125
0,78125
0,078125

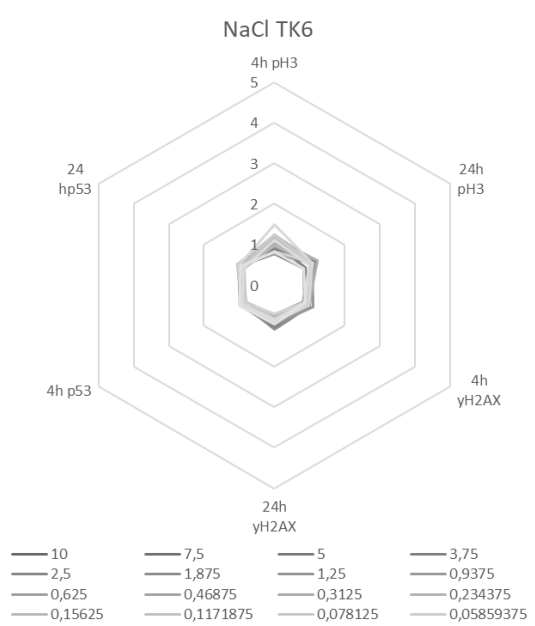
NaCl TK6
4h pH3
24h pH3
4h yH2AX
24h yH2AX
4h p53
24 hp53
10
7,5
5
3,75
2,5
1,875
1,25
0,9375
0,625
0,46875
0,3125
0,234375
0,15625
0,1171875
0,078125
0,05859375

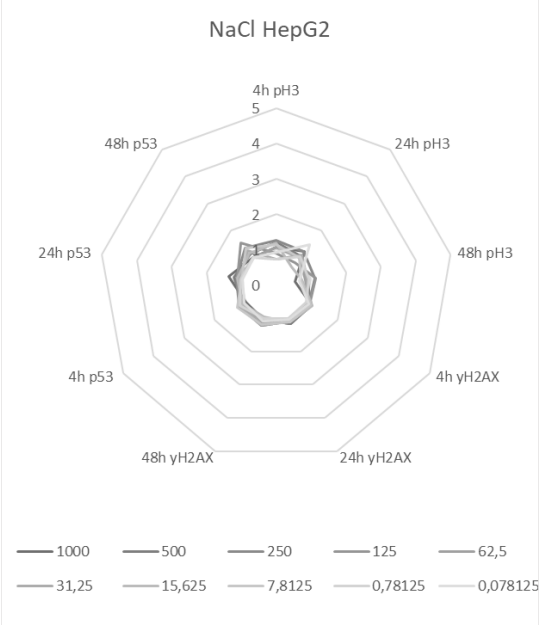
NaCl HepG2
4h pH3
24h pH3
48h pH3
4h yH2AX
24h yH2AX
48h yH2AX
4h p53
24h p53
48h p53
1000
500
250
125
62,5
31,25
15,625
7,8125
0,78125
0,078125

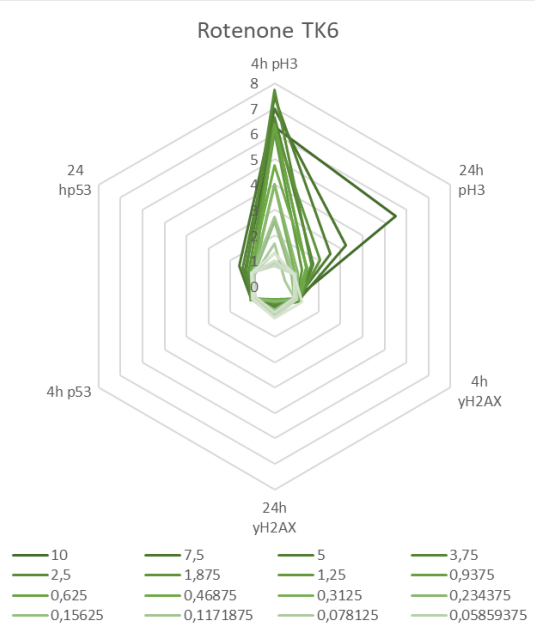
Rotenone TK6
4h pH3
24h pH3
4h yH2AX
24h yH2AX
4h p53
24 hp53
10
7,5
5
3,75
2,5
1,875
1,25
0,9375
0,625
0,46875
0,3125
0,234375
0,15625
0,1171875
0,078125
0,05859375

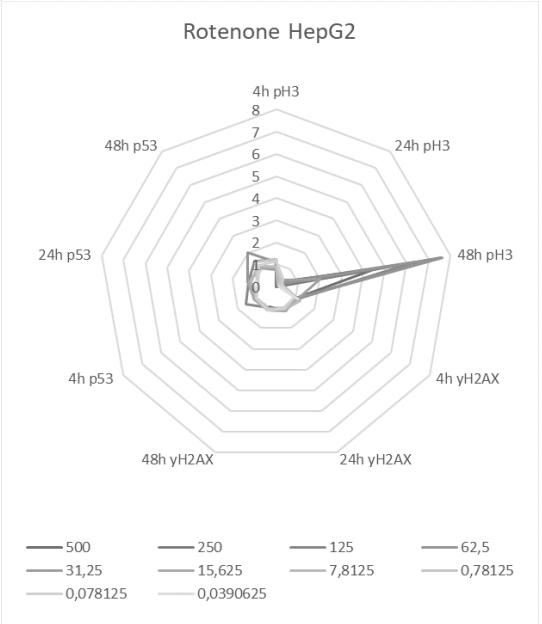
Rotenone HepG2
4h pH3
24h pH3
48h pH3
4h yH2AX
24h yH2AX
48h yH2AX
4h p53
24h p53
48h p53
500
250
125
62,5
31,25
15,625
7,8125
0,78125
0,078125
0,0390625

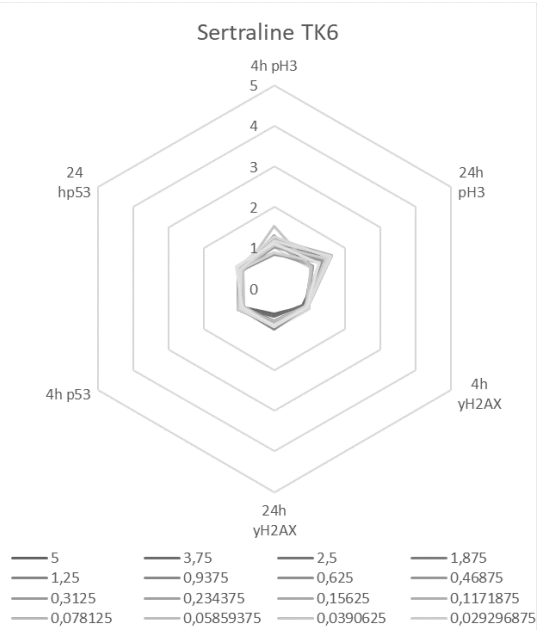
Sertraline TK6
4h pH3
24h pH3
4h yH2AX
24h yH2AX
4h p53
24 hp53
5
3,75
2,5
1,875
1,25
0,9375
0,625
0,46875
0,3125
0,234375
0,15625
0,1171875
0,078125
0,05859375
0,0390625
0,029296875

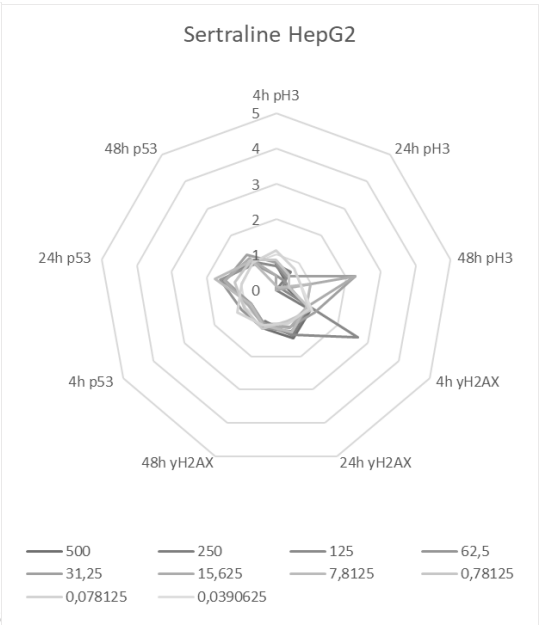
Sertraline HepG2
4h pH3
24h pH3
48h pH3
4h yH2AX
24h yH2AX
48h yH2AX
4h p53
24h p53
48h p53
500
250
125
62,5
31,25
15,625
7,8125
0,78125
0,078125
0,0390625

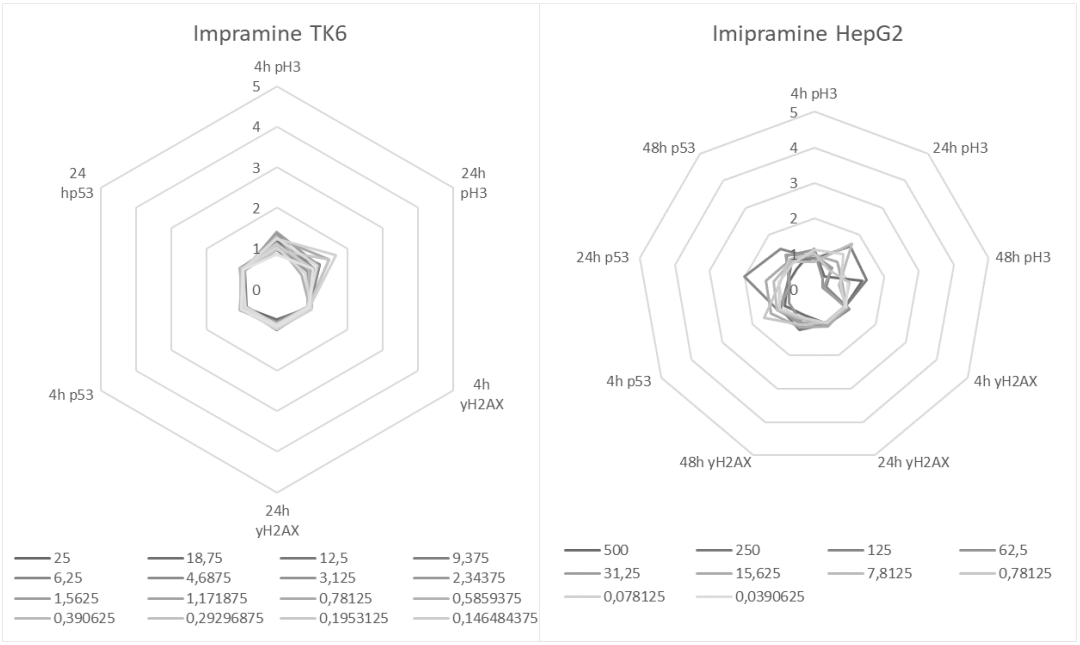

Figure 17, Comparison of expression of genotoxicity markers at different time points in TK6 cells by flow cytometry and HepG2 cells by HCA. Spider plots are used to visualise the expression of the markers γH2AX, pH3 and p53 (as fold changes related to negative controls) in TK6 cells and HepG2 cells. The plots for TK6 cells are on the left-hand side and for HepG2 cells on the right-hand side, to allow for easier comparison of the same compound. In the upper right are the fold changes of pH3 at all studied timepoints, at the bottom the fold changes of γH2AX and in the upper left the fold changes of p53. The plots are not completely identical since one additional timepoint is included for HepG2 cells. The concentration series are the lines plotted on the graph and the values are presented at the bottom. The darkest lines represent the highest concentrations. The colour of the lines represents the prediction for the compound for the cell line in question (green = aneugen, orange = clastogen, grey = non genotoxicant. In addition, mitomycin C in TK6 cells is shaded in a deeper colour to note the difference in p53 expression.) As some compounds had differing concentrations at different timepoints and tests, the lines of some plots have gaps. The corresponding data can be found in another format in Appendix A and B.

For all aneugens, paclitaxel, vinblastine, and colchicine, a correspondence in pH3-folds at both 4-hour and 24-hour timepoints was seen. As one example, in cells treated with paclitaxel increases in pH3 were present in both cell lines at 4 hours and 24 hours, but some difference could be seen in the sensitivity. In HepG2 cells, the signal at the 4-hour timepoint increased at a lower concentration, which also could be seen with the other aneugens, while the response at the 24-hour timepoint was seen first at a higher concentration. On the contrary, in TK6 cells the pH3-folds increased at the same concentration at both time points. At the 48-hour timepoint the pH3 marker was no longer seen for vinblastine and paclitaxel but persisted in colchicine. The p53-folds in the aneugens also showed a good correspondence, except for paclitaxel, where the p53-fold increased over threshold at 0.04 µM in TK6 cells at the 24-hour timepoint, but no similar effect was seen in HepG2 cells.

For the clastogens, the increase in γH2AX-fold at 4 hours was significantly lower in HepG2 cells for all compounds. The 24-hour γH2AX-folds from HepG2 cells were more comparable with the 4-hour folds from TK6 cells and the 48-hour folds from HepG2 with the 24-hour folds from TK6. This can be seen for most of the clastogens in figure 17 as the peaks of γH2AX at 4 hours in TK6 cells corresponds better with the peaks at 24 hours in HepG2 cells, and correspondingly the peaks at 24 hours in TK6 cells corresponds with the peaks at 48 hours in HepG2 cells. The effective concentration was also in many cases higher in HepG2 cells than TK6 cells, for example with MMS. In addition, for MMS an interesting phenomenon could be noticed. A steady rise of γH2AX expression in correspondence to the concentration could be seen in TK6 cells, while the increase in HepG2 peaked at higher concentrations. In the TK6 cells the increase in γH2AX expression was measured around 30 µM while in HepG2 the corresponding concentration was around 200 µM. For the 48-hour timepoint, a subthreshold concentration was mostly likely the reason for a lack of response. Apart from this difference in concentrations, the response detected in the markers correspond well. As the γH2AX markers increased, a decrease in the fold change of pH3 could also be seen in both cell lines for all timepoints. For p53 there was no evident change in either cell line. A difference in the HepG2 cells could also be seen for BAP which showed an increase in γH2AX-folds at 24 and 48 hours. The pH3-decrease and a slight increase in nuclear p53 could also be seen at

these same concentrations. In TK6 cells no similar expression was seen for any of the markers.

The p53-folds for all compounds, except for mitomycin C showed no significant increases affecting the classification of the compounds. With mitomycin C the different expression of p53 was evident as seen in figure 17. The increase was much more evident in TK6 cells than in HepG2 cells. A small increase could be seen at 24 hours in HepG2 cells but at 48 hours the signal was no longer detected. This did, however, not affect the classification since the γH2AX response could be seen in both cell lines. A p53-shift could in many cases be witnessed in correspondence with a decrease in RNC, as in CCCP, colchicine and 4QNO. In TK6 cells the p53-folds at 24 hours increased for these compounds in a manner not seen in HepG2 cells, although a slight elevation could be seen for the marker.

The only false positive in TK6 cells, rotenone, showed a difference in the expression of pH3 markers at all timepoints. For TK6 cells the increases in pH3-fold were evident at both 4 hours and 24 hours and labelled the compound as an aneugen. In HepG2 cells no similar pH3-fold increase could be seen at these timepoints but in contrast, at 24 hours a decrease in pH3 is seen at all concentrations studied. The same phenomenon was seen at 48 hours, with the drastic change at 30 μM when the pH3-fold increased considerably. This increase was, however, coupled with a drop in RNC below 0.2 and therefore the exceptionally high values were not taken into consideration in genotoxicity analysis. A fold increase in p53 could also be seen especially at the cytotoxic concentrations.

Overall, the RNC for TK6 cells decreased for most of the compounds at a lower concentration than for HepG2 cells and a corresponding p53-increase could be seen for several compounds, for example in sertraline, imipramine, rotenone, Nimesulide and 2,4-dinitrophenol.

In the spider plots, differences in marker expression between various classes of genotoxins can also be seen. For the aneugens for example, in paclitaxel the highest increase in pH3 is seen after 4 hours, while with colchicine the increase is more evident after 24 hours. For vinblastine, the increase is also higher after 4 hours, but the expression decreases more rapidly after 24 hours than for paclitaxel. For the clastogens similar differences can be seen, for example for 4NQO in TK6 cells, the γH2AX

expression is higher after 4 hours than the corresponding concentration after 24 hours, in contrast to cytosine arabinoside in TK6 cells, where the response after 24 hours is higher than that detected after 4 hours.

For most of the compounds the patterns of studied markers for genotoxicity were similar between the two cell lines studied (with the assumption, that for the γH2AX marker, the 48-hour timepoint in HepG2 cells corresponds with the 24-hour timepoint in TK6 cells and likewise the 24-hour timepoint in HepG2 with the 4-hour timepoint in TK6). Differences in marker expression can be clearly seen for mitomycin C, BAP and rotenone. Some deviation can also be seen for vinblastine, 4NQO and cytosine arabinoside, mainly at the different timepoints when markers are expressed.

A concluding prediction for the two studied cell lines using two different methods is presented in table 12. For TK6 cells the only criteria used were the GEFs, which resulted in a predictivity of 87.5% (with a specificity of 87.5% and sensitivity of 87.5%). The one false negative was BAP, which, as seen from figure 17, did not cause expression of any of the genotoxicity markers. The false positive rotenone in contrary showed increases in pH3 as described previously and was predicted as an aneugen. For the HCA method a 100% predictivity could be established using the 3-timepoint criteria as discussed previously. With the GEFs as comparison the sensitivity was only 62.5%, with MMS, cytosine arabinoside and BAP predicted as false negatives. As seen from figure 17 the γH2AX response for all of these compounds was not evident at 4 hours. With these criteria CCCP was also classified as a false positive leading to a specificity of 87.5% and an overall predictivity of 75%.

Table 12, Prediction of genotoxicity using different criteria for TK6 cells in flow cytometry and HepG2 cells in HCA. The genotoxic compounds are grouped on the top of the table and the sensitivity is counted based on the prediction of genotoxic properties of these. Likewise, the specificity is counted based on the prediction of non-genotoxic compounds. For TK6 cells, the only criteria used for the evaluation was the GEFs. For HepG2 cells, the same GEFs are used as a comparison and, in addition, the criteria provided by Khoury et al. (column 8 in table 10) and criteria based on three timepoints. The overall predictivity is evaluated based on the combination of sensitivity and specificity.

	Compound	TK6			HepG2						
			GEFs			GEFs		Khoury et al.		3 timepoints	
		Max conc.	Genotoxic (µM)	MoA	Max conc.	Genotoxic (µM)	MoA	Genotoxic (µM)	MoA	Genotoxic (µM)	MoA
Aneugens	Paclitaxel	0.01	0.000625	1	0.01	0.000078125	1	0.000078125	1	0.000078125	1
	Vinblastine	0.024	0.006	1	0.24	0.0075	1	0.0001875	1	0.0075	1
	Colchicine	0.25	0.01171875	1	1000	0.078125	1	1.5625	1	0.078125	1
Clastogens	Methyl methanesulphonate	200	37.5	1	1000	-	0	125	1	250	1
	Mitomycin C	15	0.021972656	1	15	0.9375	1	0.1171875	1	0.234375	1
	4-Nitroquinoline N-oxide	10	0.3125	1	10	0.078125	1	0.078125	1	0.078125	1
	Cytosine arabinoside	1	0.001464844	1	1000	-	0	0.078125	1	0.078125	1
	Benzo[a]pyrene	1000	-	0	1000	-	0	-	0	3.90625	1
Sensitivity (%)				**87.5**			**62.5**		**87.5**		**100**
Non-genotoxicants	CCCP	100	-	1	200	100	0	-	1	-	1
	Amiodarone	100	-	1	100	-	1	-	1	-	1
	2.4-dinitrophenol	1000	-	1	1000	-	1	-	1	-	1
	Nimesulide	1000	-	1	1000	-	1	-	1	-	1
	NaCl	1000	-	1	1000	-	1	-	1	-	1
	Rotenone	10	1.875	0	1000	-	1	-	1	-	1
	Sertraline	1000	-	1	1000	-	1	-	1	-	1
	Imipramine	1000	-	1	1000	-	1	-	1	-	1
Specificity (%)				**87.5**			**87.5**		**100**		**100**
Predictivity (%)				**87.5**			**75**		**93.75**		**100**

4. Discussion

4.1 Comparison between cell lines based on flow cytometry

One of the major issues in this study was the inconclusive results with HepG2 cells in MultiFlow, which did not allow for a proper comparison between the cell lines using the same method. This was an unexpected drawback, since the protocol of the MultiFlow®-kit suggests the use of HepG2 cells in case adherent cells are used. Based on the first attempts to measure HepG2 cells with the flow cytometer it seemed that the cells were not properly detaching from the plate. Change of solution to the same trypsin used in subculturing did not improve the result. A prolonged incubation with Accutase® and proper flushing of the wells resulted in lower variation in cell number between wells. When analysing multiple wells, issues with well identification occurred, most likely due to clogging of the sampler and carryover between samples. The issue was attempted to be resolved by adding several washes between sample acquisition but despite that, some clogging and carryover was seen in each run. Since one experiment was run on four plates and the clogging occurred towards the end of the run, some of the samples could be analysed to a certain extent. For the most potent genotoxins, as indicated in TK6 cells, a correspondence between TK6 and HepG2 cells was seen and the cell line was considered eligible for genotoxicity testing, as indicated in literature (Kopp, Zalko, & Audebert, 2018) (Ando, Yoshikawa, Iwase, & Ishiura, 2014). Based on the results from MultiFlow with HepG2 cells, it seemed that the concentration range used was not sufficient for γH2AX expression with some of the clastogens, such as MMS and mitomycin C and the concentration of those compounds were therefore elevated, if allowed by solubility properties. Similarly, some compounds, if not precipitating or expressing genotoxic or cytotoxic properties, were retested in TK6 cells up to 1 mM (or the highest solubility), as indicated by ICH guidelines (Food and Drug Administration, HHS, 2012). Further comparison between TK6 cells and HepG2 cells using flow cytometry was not performed.

4.2 The role of p53 as a genotoxicity marker

When analysing the HCA data of HepG2 cells the meaningfulness of p53 as a genotoxicity marker was questioned. Genotoxicity criteria for HepG2 cells in literature were in most cases limited to fold increases in phosphorylation of pH3 and

γH2AX (Khoury et al., 2016) (Kopp et al., 2018) (Khoury et al., 2016) (Smart, D. J., Ahmedi, Harvey, & Lynch, 2011). Despite its role in inducing apoptosis as a consequence of DNA damage, p53 is believed to also be involved in responses triggered by several other types of cellular stress (Reaves et al., 2000) (Brooks & Gu, 2010). For the compounds used in this experiment, p53 was not a critical marker but increases in p53-folds could be seen mostly for cytotoxic concentrations in HepG2 cells. For example, if using GEFs in HepG2 cells the p53 increase at 4 and 24 hours falsely predicted for example CCCP to be genotoxic. Some variation was also seen between plates, as indicated by the error bars in the p53 graphs. It is evident from the images that the translocation of p53 was more pronounced on some plates than others. In addition, for some reason, one of the plates had a much larger number of cells in the wells used as negative controls, resulting in a lower RNC count for the 4-hour plates and a large variation between samples. Based on the two first experiments, as the p53 did not seem to have an effect in the outcome with these compounds, the experiments were not replicated in triplicates. The plate incubated for 48 hours was studied at the end of this project as an additional timepoint but there was some precipitation, most likely from the p53 antibody itself, seen in the images. As there was not enough antibody left to retest the p53 expression after a 48-hour incubation to confirm the result, it was not included in this study. Importance of p53 as an indicator of genotoxicity remained inconclusive for these compounds. Generally, on one hand, some atypical genotoxic compounds, such as the clastogen 5-Fluorouracil which is a typical reference compound, do not cause a significant γH2AX increase (*MultiFlow(R).*). 5-Fluorouracil does instead cause an increase in p53 and, therefore, would possibly go undetected as a false negative without the use of p53 (Bryce, Bernacki, Bemis, & Dertinger, 2016). On the other hand, some compounds, such as Nutlin-3, which is not classified as a genotoxicant, cause increases in p53 and would therefore be classified as a clastogen based on the GEF criteria. In HepG2 cells, it also seemed that the cytotoxic compounds induced a p53 increase prior to cell death (measured as RNC) and, therefore, could also induce false positive results for cytotoxicants. To be able to determine if p53 brings a value to an imaging-based analysis a larger number of compounds and a more detailed image analysis should be considered.

Another aspect that could be considered is the replacement of p53 in the imaging analysis. The advantage of an image-based analysis is the ability to analyse the images for several markers and endpoints at intracellular levels. In this way, the relevance of the p53 marker could decrease if a combination of other markers would provide a better prediction. For clastogenic compounds, other proteins involved in the DDR response have also been suggested. In one study, Kopp et al. used a variety of proteins involved in the DDR as markers in order to study if a combination of markers could provide insight into the mode of action of clastogens (Kopp, Dario, Zalko, & Audebert, 2018). In their study, they reported that the phosphorylated form of p53 at Serine15 corresponded better with γH2AX response than nuclear p53 (Kopp et al., 2018). This suggests that the phosphorylated form at this residue of p53 would potentially be a better marker. However, from the compounds they tested, the γH2AX response was present with all compounds at 24- or 48-hour timepoints, including 5-Fluorouracil. Therefore, the value of p53 as an indicator for clastogenicity in HepG2 cells was not seen based on their data either.

4.3 Genotoxicity criteria in different cell lines

As discussed previously, the GEFs for TK6 cells have been established by an interlaboratory study with a large number of reference compounds and data from several laboratories (Bryce et al., 2017). A similar comprehensive validation has not been performed for HepG2 cells and, therefore, the genotoxicity criteria for these cells needed to be adapted. As mentioned previously, the nuclear p53-fold marker has not been as widely used in HepG2 cells and, therefore, a similar set of criteria as the GEFs in TK6 cells was difficult to establish. The endpoint was, therefore, to find criteria that could predict the genotoxicity of the compounds, as described in the literature, as accurately as possible. The first endpoint in the criteria was the cytotoxicity threshold. Although many of the criteria described previously used a cytotoxicity of 50% measured as RNC in HepG2 cells, it was noted that other thresholds could change the outcome of the results. Based on the cytotoxicity levels of TK6 and HepG2 cells it seemed that the HepG2 cells were more tolerable to toxic compounds seen by a higher survival (measured as RNC), at least by these methods. It could also be beneficial to use a relative population doubling (RPD) count, in addition to the RNC count, to be able to determine cytotoxicity correctly. The RPD could potentially have provided

better information on the doubling time of the HepG2 cells, which was not separately tested here. The combination of a longer doubling time and the tolerance of the HepG2 cells could have been the reason for the delay in the γH2AX response and, therefore, the longer 48-hour incubation might be necessary to determine genotoxic properties of compounds. At the 48-hour timepoint, however, the RNC of 50% as threshold led to an exclusion of a large number of samples. The lowering of the threshold to 20% at this timepoint led to a better prediction and was therefore considered. To assess an optimal incubation time and the cytotoxicity limit a wider range of timepoints between 24 and 48 hours should be further evaluated.

For the other markers used, the thresholds of the criteria should be considered critically. The 1.3-fold increase used by Khoury et al. is significantly lower than that of the GEFs in TK6 cells, which can lead to false positive results. On the other hand, a threshold set too high can lead to genotoxicity remaining undetected for less potent compounds, or compounds which have an atypical genotoxic response. The decrease in pH3 was also one aspect considered. As seen from the data, the γH2AX response was coupled to a decrease of pH3 for most of the compounds. This decrease is most likely coupled to the DDR response of the damage where the cell cycle progression is inhibited, and the cells are not able to enter mitosis. However, a decrease in pH3 could also be a cause of an aneugen. As previously discussed, many aneugens disturb the mitotic kinases. A compound that inhibits the Aurora kinase, which is responsible for pH3 phosphorylation, would lead to a depletion of pH3. In this case, a combination of pH3 decrease and γH2AX increase would indicate a clastogenic action, while a steeper decrease would indicate an aneugenic action. The mechanisms behind the genotoxic effects would, therefore, also be an interesting and important subject of study in order to be able to better classify the compounds based on the thresholds. A combination of several markers could enhance the sensitivity and specificity of testing, both by more accurate predictions and by excluding false positives and negatives.

Overall, the aim of the criteria is to be able to predict the genotoxic properties of compounds as accurately as possible. For example, if a compound expresses cytotoxic properties of more than 50% *in vitro*, does its genotoxic potential at these concentrations have any meaning *in vivo*? Most of the guidelines of genotoxicity testing are based on the OECD guidelines, mainly of the micronucleus assay and previous classification of compounds. Therefore, whichever criteria are used should

be consistent with both guidelines and an accurate prediction of previously classified compounds.

4.4 Improvements to HCA platform

Based on the experiments done in this study, the imaging platform would provide a promising alternative for genotoxicity testing, but the method and models need to be further developed. The concentration series used in HCA was chosen based on automation of the method but could be more optimal if a 20-point dilution series with a dilution factor of e.g. 1.4 would be implicated, especially if the same criteria of two continuous concentrations are used. An optimisation of incubation times could provide an alternative to using two instead of three different plates with three timepoints. HepG2 cells have been used successively in several earlier genotoxicity testing studies and were therefore chosen to be used here (Khoury et al., 2016) (Garcia-Canton et al., 2013). However, the cell line used for HCA could also be re-considered. The longer doubling time of HepG2 cells most likely was one of the reasons for a delayed γH2AX response and the need of a third, longer incubation time. The metabolic activity of HepG2 cells was also not as evident as expected. The assumption was that the cells expressed enzymes capable of phase-I and phase-II metabolism and, therefore, also could predict genotoxicity of compounds requiring metabolic activation (Westerink et al., 2011). This was seen to some extent with BAP, although the increase in γH2AX-fold was seen only slightly and mostly after a 48-hour incubation. No similar increase in the TK6 cells was seen, so this would indicate that there is some metabolic activity in the HepG2 cells used. The metabolic activity in the cell line used is an advantage since it could predict the genotoxicity of metabolites of compounds which also would be formed in the liver *in vivo*. The HepG2 cells also have a competent p53 which is dysfunctional in many other malignant cell lines. The functional p53 is a presumption if the p53 marker is used but it also has an important function in the DDR and, therefore, is an important factor in genotoxicity screening (Westerink et al., 2011). A cell line considered for further testing would therefore preferably be a metabolically active human cell line with a functional p53, form micronuclei upon DNA damage, be an adherent cell line suitable for imaging and preferably have a more rapid doubling time, as with TK6 cells.

One additional endpoint that could be considered in image analysis would be the formation of micronuclei. As the micronucleus test is still one of the main studies in

determination of genotoxic properties, the formation of micronuclei could most likely conveniently be detected in HCA (Westerink et al., 2011). This was one endpoint that was considered for the image analysis but the micronucleus formation in HepG2 cells was not as evident and the resolution of the images or the amount of cells imaged was most likely not adequate for this purpose. With some compounds the formation of micronuclei could, however, be seen in the images. For example, with vinblastine and mitomycin C, which are micronucleus positive compounds, the formation of micronuclei could be seen (figure 18) (Kirkland et al., 2016). The micronuclei can be identified as small fragments of DNA in close proximity to the main nucleus and could, therefore, also be considered to be included in the image analysis. The micronuclei are also in many cases shown to express γH2AX phosphorylation, regardless of the mechanism which causes the formation (Watters, Smart, Harvey, & Austin, 2009). In other words, the γH2AX response in micronuclei can be seen also for aneugens, which are otherwise detected by pH3. Since the micronuclei do not require any additional marker than the Hoechst dye and possibly γH2AX in assisting the identification, the addition of micronucleus identification to HCA analysis could provide further insight into the genotoxic potential of the compounds.

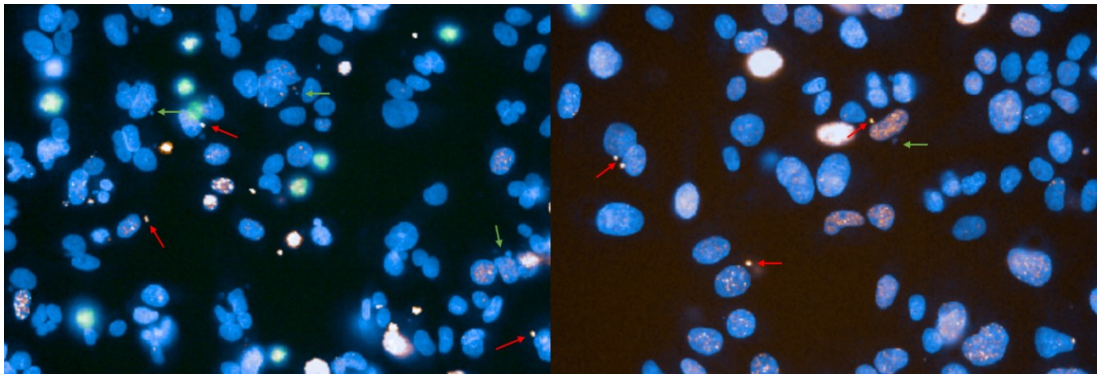

Figure 18, Micronucleus formation in HepG2 cells, visualised by HCA. HepG2 cells stained for nuclei (Hoechst, blue), pH3 (green) and γH2AX (orange) and imaged by HCA after a 48-hour incubation with compounds. To the left the cells are treated with 0.015 µM vinblastine and to the right with 0.011 µM mitomycin C. The red arrows indicate micronuclei that also express γH2AX and the green arrows micronuclei without the expression of γH2AX.

4.5 Advantages of HepG2 cells in genotoxicity screenings

The 16 reference compounds studied showed a good prediction of genotoxic properties by imaging of HepG2 cells, even though some of the compounds were chosen on a basis of a possibly false positive result. One of these was rotenone, which was predicted as an aneugen in flow cytometry with TK6 cells. Rotenone is known to act as mitochondrial toxin by inhibiting complex 1 in the respiratory chain and, therefore, leads to cytotoxicity by energy deprivation (Heinz et al., 2017b). Some mitochondrial toxins are of particular interest in genotoxicity testing, since the energy deprivation might also cause dysfunctions in DDR and cell cycle progression, thereby leading to a misleading positive genotoxicity result (Tsai et al., 2020). The mitochondrial toxins Nimesulide, amiodarone and 2,4-dinitrophenol were therefore of particular interest. Surprisingly, none of the mitochondrial toxins showed genotoxicity using the HCA method with HepG2 cells. This could possibly be explained by the growth medium of HepG2 cells which was high in glucose and could provide an alternative mechanism for energy production, based on glycolysis (Kamalian et al., 2015). This could also partially explain the effect of rotenone seen after a 48-hour incubation. As long as the cells have glucose to utilise for their energy needs the defects in mitochondria do not affect the cells, but as soon as the glucose is consumed the same effect that could be seen in TK6 cells at 4 hours is seen in HepG2 cells. The glycolytic properties of HepG2 cells could therefore be seen as an advantage for genotoxicity testing as the cells might not be as sensitive to mitochondrial toxins and lead to a false positive genotoxic prediction as a consequence of this. Another compound of interest was BAP, which becomes genotoxic upon metabolic activation. For the longer incubation times an increase in γH2AX was seen, which would indicate an expression of the metabolic enzymes CYP1A1, 1B1 and1A2, involved in BAP metabolism (Shah et al., 2016). For improved determination, the metabolic capabilities and enzymes involved should be measured for the cell line. An optimal cell line would express all the relevant CYP enzymes involved in metabolism of compounds.

4.6 Further perspectives

For further perspectives, the method used here would need to be adjusted and a significantly larger number of compounds would need to be tested to be able to predict if an imaging-based platform could be used for a more accurate prediction. Several authorities, including the EURL ECVAM (EU Reference Laboratory for alternatives to animal testing), provide a comprehensive recommended list of genotoxic and non-genotoxic chemicals suitable for validation of genotoxicity tests (Kirkland et al., 2016). Based on data from a larger validation test set, more powerful image analysis platforms and mathematical models could be used to analyse a larger amount of data form the samples and possibly even provide insight into the mechanisms behind the damage. As seen in the spider plots, different types of mechanisms behind the damage cause different types of responses in the cells. These changes in pattern can be seen by both flow cytometry and HCA and for the MultiFlow®-kit there has, in fact, been suggested machine learning approaches for determination of the molecular targets behind the damage (Dertinger et al., 2019) (Bernacki, Bryce, Bemis, & Dertinger, 2019). Especially for the aneugens, an approach where the assembly or disassembly of the mitotic spindles or kinase inhibition mechanisms could be predicted by the use of three markers (Bernacki et al., 2019). An imaging-based assay could be of advantage for these types of analyses in the future, as the image analysis could possibly provide even more insight into the state of the cell compared to flow cytometry. For example, without any addition of markers, the properties of the nuclei, such as the size, roundness and intensity, can provide insight into the health of the cell. Using these properties, even the state of the cell cycle could possibly be determined. In addition to this, the imaging-based assay could also provide insight into the intracellular events, which is not always possible to the same extent by flow cytometry. For example, markers for mitochondrial membrane potentials could be included to measure the health of mitochondria. This could further reduce the misleading positives which might be caused by energy deprivation rather than straight damage to the DNA. Additional studies of the DNA damage pathways could reveal promising markers involved in a response to genotoxins. For these, further studies are needed but an imaging-based assay would provide a good platform for this type of studies. In addition, a large number of commercially available fluorophores and the possibility to image several markers on the same plate provide the opportunity to analyse several

endpoints and mechanisms. This, in combination with machine learning could provide new information, opportunities and insights into the field of genotoxicity testing and classification of compounds.

V CONCLUSIONS

The aim of this project was to compare the predictivity of high content *in vitro* methods for genotoxicity in drug discovery. For this purpose, an imaging-based HCA assay was successfully set up and tested using 16 reference compounds with known genotoxic- or non-genotoxic properties. The results from the HCA assay with HepG2 cells were compared with the results from a flow cytometry-based assay with TK6 cells. A comparison between HepG2 cells and TK6 cells in the flow cytometry data could not be done due to low quality data with HepG2 cells caused most likely by aggregation of the cells during the protocol.

As a comparison between the cell lines using the same methods could not be established and previous genotoxicity criteria for HepG2 cells was not validated, a range of genotoxicity criteria was adapted based on literature and the known genotoxic potential of the reference compounds used. Using two timepoints the criteria could predict 15 out of 16 reference compounds correctly. For γH2AX expression a 4-hour incubation did not seem sufficient, therefore, a 48-hour incubation was included. By studying 3 timepoints all 16 compounds could be predicted correctly using the following criteria: For aneugens, the criteria used were a pH3 increase over 1.71-fold at 4 hours, 1.52-fold at 24 hours or 1.52-fold at 48 hours. For clastogens, the criteria used were γH2AX increase over 1.3-fold at 4 hours, 1.3-fold at 24 hours or 2.11-fold at 48 hours. Genotoxicity was indicated if at least two out of three of these were met at two continuous concentrations, as well as the RNC was above 50% at 4 hours and above 80% at 24 hours and 48 hours. With TK6 cells the criteria used were from a previously validated study which predicted 14 out of 16 compounds correctly. The genotoxicity endpoints in HepG2 cells did not include p53, which in some cases instead gave a false positive result if included in the criteria.

In conclusion, based on the reference compounds tested, the HCA method seems to provide a promising alternative for flow cytometry-based screening. The genotoxicity markers γH2AX and pH3 were able to distinguish between aneugens and clastogens in HepG2 cells. Genotoxic effects could even be detected for the compound BAP requiring metabolic activity. However, to be able to determine more specific criteria and the correct prediction for additional compounds a significantly larger validation

set is still necessary in order to confirm these results. The criteria for genotoxicity should also be determined based on a larger validation set and better mathematical models. In addition, some improvements and adjustments for the imaging assay should be considered. Even though HepG2 cells showed promising results, some other cell line with better properties should be considered for this assay.

To improve predictivity, the imaging platform provides some advantages over flow cytometry. One of these is visualisation of intracellular events, such as mitochondrial membrane potentials, which could allow for reduction of false positive interpretations caused by energy deprivation. Another endpoint could be to study other molecules involved in DNA damage responses and consider them as markers for genotoxicity. In addition, the image analysis tools could allow for analysis of other genotoxicity endpoints, such as micronuclei in the same test without addition of additional markers. False negative results could also be excluded by using a metabolically active cell line. The adaptation of machine learning, and additional markers could also provide insight into the biological mechanisms of actions behind the damage. In conclusion, an imaging-based genotoxicity screening method provides great promise in the field, but further studies and development and still needed to take full advantage of all of the potential of the method.

VI SUMMARY IN SWEDISH – Svensk sammanfattning

Jämförelse av screeningmetoder för genotoxicitet *in vitro* inom läkemedelsindustrin

Toxikologisk testning är viktigt inom alla branscher som hanterar kemikalier av något slag. Alla kemikalier som är avsedda att användas av människor eller djur är strikt reglerade av myndigheterna. Inom läkemedelsindustrin testas alla potentiella läkemedel för toxicitet av olika slag. Ett av dessa är genotoxicitet, studien om ämnen som förorsakar skada på genomet, d.v.s. det ärftliga materialet DNA. Det finns flera metoder som används för att detektera skador på DNA *in vitro* men nya, mer effektiva metoder är ständigt eftertraktade. Ett av de största problemen med de nuvarande metoderna är förekomsten av falska positiva resultat *in vitro*, vilket kan leda till onödiga *in vivo* djurförsök, vilka är både dyra och etiskt ifrågasatta. Målsättningarna för detta projekt var att sätta upp en metod baserad på visualisering genom högeffektiv automatiserad mikroskopi (high content analysis, HCA) och att jämföra resultatet från denna med metoder som används för tillfället.

Som jämförelse fungerade en metod baserad på flödescytometri, en metod där enskilda celler i vätska passerar i ett flöde genom en laserstråle. På basis av ljuset som reflekteras från cellerna, emissionen från fluorescerande antikroppar eller molekyler som cellkomponenter färgats med, kan dessa detekteras genom en dator kopplad till flödecytometern. De cellkomponenter som användes i denna studie var γH2AX, pH3 och p53. H2AX och H3 är båda histoner, molekyler som är tätt kopplade till DNA och därmed även involverade i signalräckor som styr processer relaterade till DNA såsom translation, replikation och reparation av skador. Då DNA:t utsätts för en skada aktiveras en process som kollektivt kallas för DNA skaderespons (DNA damage response, DDR). En molekyl som genomgår förändringar då DNA bryts på mitten är H2AX som i detta fall fosforyleras och bildar γH2AX. Ifall ett ämne ger upphov till skador på dubbelsträngen kan en ökning av halten γH2AX iakttas i cellerna. I motsats till detta utgör fosforyleringen av H3 till pH3 en del av den normala cellcykeln. Denna reaktion är kopplad till mitos, då DNA kondenseras inför celldelning fosforyleras H3 till pH3. Genast då cellen delat sig och DNA återvänder till ett mindre kondenserade tillstånd defosforyleras även pH3. Genotoxicitet kan även bero på störningar i fördelningen av DNA vid mitos, vilket kan leda till en ojämn distribution av

kromosomerna. Detta resulterar ofta i att cellerna blir kvar i mitos. Ett ämne som förorsakar denna typ av skada ger därigenom upphov till en förlängd mitos som kan iakttas som en ökning i pH3 expresserande celler. Utöver dessa två histonproteiner är p53 ett protein som är involverat i DDR-responsen. Då en viss typ av skada sker förflyttas p53 till cellkärnan där den aktiverar gener som är involverade i DNA:s reparationsmekanismer. Förflyttningen av p53 från cytoplasman till kärnan kan på grund av detta i vissa fall vara kopplad till genotoxicitet.

I denna studie användes 16 referensämnen antingen med kända genotoxiska egenskaper, eller ämnen som inte uppvisar genotoxicitet. Dessa ämnen testades med två olika cellinjer, TK6 och HepG2-celler. TK6-celler är humana lymfocyter som använts mycket i flödescytometri och HepG2 är humana leverceller som används mycket inom HCA. Cellerna utsattes för ämnena under 4 och 24 timmar varefter de färgades för att detektera möjliga förändringar i markörerna för genotoxicitet. I studierna med flödescytometri användes ett kommersiellt tillgängligt och validerat kit, MultiFlow®. För HCA testades och lades ett immunfärgningsprotokoll upp som färgade markörerna med hjälp av antikroppar. Flödescytometri användes för att testa båda celltyperna. Det visade sig att HepG2-cellerna inte lämpade sig väl för denna metod och en jämförelse mellan de båda cellinjerna kunde därför inte göras. För att få jämförbara resultat från HCA metoden tolkades markörerna i bilderna genom bildanalys och jämfördes med de negativa kontrollerna. På basis av den respons som kunde iakttas med referensämnena och publicerade resultat från den vetenskapliga litteraturen föreslogs kriterier för genotoxicitet vid användning av HepG2-celler. Genotoxiciska egenskaper kunde förutsägas korrekt för 14 av 16 referens-ämnen genom flödescytometrisk analys med TK6-celler. Av de två ämnen som gav inkorrekt resultat var den ena en falsk positiv och den andra falska negativa skulle ha krävt metabolisk aktivitet för att ge ett positivt resultat. Med HCA metoden med HepG2-celler kunde samtliga 16 ämnen förutsägas korrekt med de kriterier som föreslogs. Dessa var dock upplagda på basis av resultaten av endast 16 ämnen. För att ytterligare bekräfta resultaten borde ett betydligt större antal referensämnen testas.

En intressant aspekt som framkom var betydelsen av p53 som markör. I HepG2-cellerna kunde genotoxiciteten för de analyserade ämnena förutsägas utan användning av denna markör, vilket även kunde möjliggöra användning av andra markörer i stället. Fördelen med en bildbaserad analysmetod är möjligheten att även analysera händelser

i cytoplasman. Exempelvis kan mitokondriella toxiner leda till falska positiva genotoxiska resultat. Markörer som detekterar mitokondriernas tillstånd kunde därför möjligen användas för att minska antalet falska resultat. Fördelar med en bildbaserad analys är även mångfalden av det som kan avläsas med olika metoder i själva analysen. Till exempel är analys av uppkomsten av mikrokärnor, d.v.s. små DNA fragment som skapas vid skador på DNA, en mycket använd metod i genotoxiska studier. Dessa små DNA element kunde möjligtvis även direkt detekteras i bildanalys utan tillsatts av ytterligare markörer. Eftersom en stor del data kan analyseras utgående från bildmaterialet kunde skillnader i genotoxitetsmarkörernas uttrycksprofiler även indikera mekanismerna bakom de skador som uppstår. På basis av denna studie visade en bildbaserad analys för genotoxicitet ha en stor potential. För att kunna bekräfta detta krävs dock fortsatta studier och bekräftelse genom användning av ett större antal referensämnen. Om metoden påvisar sig mer prediktiv kunde den även tillämpas med maskinlärning för en större förståelse av biologin bakom skadorna.

VII REFERENCES

Ando, M., Yoshikawa, K., Iwase, Y., & Ishiura, S. (2014). Usefulness of monitoring gamma-H2AX and cell cycle arrest in HepG2 cells for estimating genotoxicity using a high-content analysis system. *Journal of Biomolecular Screening, 19*(9), 1246-1254. doi:10.1177/1087057114541147 [doi]

Banerjee, T., & Chakravarti, D. (2011). A peek into the complex realm of histone phosphorylation. *Molecular and Cellular Biology, 31*(24), 4858-4873. doi:10.1128/MCB.05631-11 [doi]

Bartova, E., Krejci, J., Harnicarova, A., Galiova, G., & Kozubek, S. (2008). Histone modifications and nuclear architecture: A review. *The Journal of Histochemistry and Cytochemistry : Official Journal of the Histochemistry Society, 56*(8), 711-721. doi:10.1369/jhc.2008.951251 [doi]

Bernacki, D. T., Bryce, S. M., Bemis, J. C., & Dertinger, S. D. (2019). Aneugen molecular mechanism assay: Proof-of-concept with 27 reference chemicals. *Toxicological Sciences : An Official Journal of the Society of Toxicology, 170*(2), 382-393. doi:10.1093/toxsci/kfz123 [doi]

Bharadwaj, R., & Yu, H. (2004). The spindle checkpoint, aneuploidy and cancer. *Oncogene, 23*(11), 2016-2027. doi:10.1038/sj.onc.1207374 [doi]

Brooks, C. L., & Gu, W. (2010). New insights into p53 activation. *Cell Research, 20*(6), 614-621. doi:10.1038/cr.2010.53 [doi]

Bryce, S. M., Bernacki, D. T., Bemis, J. C., & Dertinger, S. D. (2016). Genotoxic mode of action predictions from a multiplexed flow cytometric assay and a

machine learning approach. *Environmental and Molecular Mutagenesis, 57*(3), 171-189. doi:10.1002/em.21996 [doi]

Bryce, S. M., Bernacki, D. T., Bemis, J. C., Spellman, R. A., Engel, M. E., Schuler, M., et al. (2017). Interlaboratory evaluation of a multiplexed high information content in vitro genotoxicity assay. *Environmental and Molecular Mutagenesis, 58*(3), 146-161. doi:10.1002/em.22083 [doi]

Chatterjee, N., & Walker, G. C. (2017). Mechanisms of DNA damage, repair and mutagenesis. *Environmental and Molecular Mutagenesis, 58*(5), 235-263. doi:10.1002/em.22087 [doi]

Chen, R., Kang, R., Fan, X. G., & Tang, D. (2014). Release and activity of histone in diseases. *Cell Death & Disease, 5*, e1370. doi:10.1038/cddis.2014.337 [doi]

Chun, R., Garrett, L. D., & Vail, D. M. (2007). Chapter 11 - cancer chemotherapy. In S. J. Withrow, & D. M. Vail (Eds.), *Withrow & MacEwen's small animal clinical oncology (fourth edition)* (pp. 163-192). Saint Louis: W.B. Saunders. doi:https://doi.org/10.1016/B978-072160558-6.50014-9

Corvi, R., & Madia, F. (2017). In vitro genotoxicity testing-can the performance be enhanced? *Food and Chemical Toxicology : An International Journal Published for the British Industrial Biological Research Association, 106*(Pt B), 600-608. doi:S0278-6915(16)30290-3 [pii]

Custer, L. L., & Sweder, K. S. (2008). The role of genetic toxicology in drug discovery and optimization. *Current Drug Metabolism, 9*(9), 978-985. doi:10.2174/138920008786485191 [doi]

Davies, T. S., & Kluwe, W. M. (1998). Preclinical toxicological evaluation of sertraline hydrochloride. *Drug and Chemical Toxicology, 21*(4), 521-537. doi:10.3109/01480549809002220 [doi]

Dertinger, S. D., Kraynak, A. R., Wheeldon, R. P., Bernacki, D. T., Bryce, S. M., Hall, N., et al. (2019). Predictions of genotoxic potential, mode of action, molecular targets and potency via a tiered multiflow(R) assay data analysis strategy. *Environmental and Molecular Mutagenesis, 60*(6), 513-533. doi:10.1002/em.22274 [doi]

Dickey, J. S., Redon, C. E., Nakamura, A. J., Baird, B. J., Sedelnikova, O. A., & Bonner, W. M. (2009). H2AX: Functional roles and potential applications. *Chromosoma, 118*(6), 683-692. doi:10.1007/s00412-009-0234-4 [doi]

European Medicines Agency. (2012). *ICH guideline S2 (R1) on genotoxicity testing and data interpretation for pharmaceuticals intended for human use.*https://www.ema.europa.eu/en/ich-s2-r1-genotoxicity-testing-data-interpretation-pharmaceuticals-intended-human-use

Food and Drug Administration, HHS. (2012). International conference on harmonisation; guidance on S2(R1) genotoxicity testing and data interpretation for pharmaceuticals intended for human use; availability. notice. *Federal Register, 77*(110), 33748-33749.

Ganguly, A., Yang, H., & Cabral, F. (2010). Paclitaxel-dependent cell lines reveal a novel drug activity. *Molecular Cancer Therapeutics, 9*(11), 2914-2923. doi:10.1158/1535-7163.MCT-10-0552 [doi]

Garcia-Canton, C., Anadon, A., & Meredith, C. (2013). Assessment of the in vitro gammaH2AX assay by high content screening as a novel genotoxicity test. *Mutation Research, 757*(2), 158-166. doi:10.1016/j.mrgentox.2013.08.002 [doi]

GARRISON, H. F., & MOFFITT, E. M. (1962). Imipramine hydrochloride intoxication. *Jama, 179*, 456-458. doi:10.1001/jama.1962.03050060066016 [doi]

Grundlingh, J., Dargan, P. I., El-Zanfaly, M., & Wood, D. M. (2011). 2,4-dinitrophenol (DNP): A weight loss agent with significant acute toxicity and risk of death. *Journal of Medical Toxicology : Official Journal of the American College of Medical Toxicology, 7*(3), 205-212. doi:10.1007/s13181-011-0162-6 [doi]

Hans, F., & Dimitrov, S. (2001). Histone H3 phosphorylation and cell division. *Oncogene, 20*(24), 3021-3027. doi:10.1038/sj.onc.1204326 [doi]

Heinz, S., Freyberger, A., Lawrenz, B., Schladt, L., Schmuck, G., & Ellinger-Ziegelbauer, H. (2017a). Mechanistic investigations of the mitochondrial complex I inhibitor rotenone in the context of pharmacological and safety evaluation. *Scientific Reports, 7*, 45465. doi:10.1038/srep45465 [doi]

Heinz, S., Freyberger, A., Lawrenz, B., Schladt, L., Schmuck, G., & Ellinger-Ziegelbauer, H. (2017b). Mechanistic investigations of the mitochondrial complex I inhibitor rotenone in the context of pharmacological and safety evaluation. *Scientific Reports, 7*, 45465. doi:10.1038/srep45465 [doi]

Hustedt, N., & Durocher, D. (2016). The control of DNA repair by the cell cycle. *Nature Cell Biology, 19*(1), 1-9. doi:10.1038/ncb3452 [doi]

iQue hardware manual. Retrieved from https://intellicyt.com/wp-content/uploads/2016/07/iQue-Hardware-Manual.pdf

Jackson, S. P., & Bartek, J. (2009). The DNA-damage response in human biology and disease. *Nature, 461*(7267), 1071-1078. doi:10.1038/nature08467 [doi]

Kamalian L., Chadwick, A. E., Bayliss, M., French, N. S., Monshouwer, M., Snoeys, J., Park, K. (2015) The utility of HepG2 cells to identify direct mitochondrial dysfunction in the absence of cell death. *Toxicology in Vitro* 29(4), 732-740 doi:10.1016/j.tiv.2015.02.011. [doi]

Khoury, L., Zalko, D., & Audebert, M. (2016a). Complementarity of phosphorylated histones H2AX and H3 quantification in different cell lines for genotoxicity screening. *Archives of Toxicology, 90*(8), 1983-1995. doi:10.1007/s00204-015-1599-1 [doi]

Khoury, L., Zalko, D., & Audebert, M. (2016d). Evaluation of four human cell lines with distinct biotransformation properties for genotoxic screening. *Mutagenesis, 31*(1), 83-96. doi:10.1093/mutage/gev058 [doi]

Kirkland, D., Kasper, P., Martus, H. J., Muller, L., van Benthem, J., Madia, F., et al. (2016). Updated recommended lists of genotoxic and non-genotoxic chemicals for assessment of the performance of new or improved genotoxicity tests. *Mutation Research.Genetic Toxicology and Environmental Mutagenesis, 795*, 7-30. doi:10.1016/j.mrgentox.2015.10.006 [doi]

Kopp, B., Dario, M., Zalko, D., & Audebert, M. (2018). Assessment of a panel of cellular biomarkers and the kinetics of their induction in comparing genotoxic

modes of action in HepG2 cells. *Environmental and Molecular Mutagenesis, 59*(6), 516-528. doi:10.1002/em.22197 [doi]

Kopp, B., Khoury, L., & Audebert, M. (2019a). Validation of the gammaH2AX biomarker for genotoxicity assessment: A review. *Archives of Toxicology, 93*(8), 2103-2114. doi:10.1007/s00204-019-02511-9 [doi]

Kopp, B., Khoury, L., & Audebert, M. (2019b). Validation of the gammaH2AX biomarker for genotoxicity assessment: A review. *Archives of Toxicology, 93*(8), 2103-2114. doi:10.1007/s00204-019-02511-9 [doi]

Kopp, B., Zalko, D., & Audebert, M. (2018). Genotoxicity of 11 heavy metals detected as food contaminants in two human cell lines. *Environmental and Molecular Mutagenesis, 59*(3), 202-210. doi:10.1002/em.22157 [doi]

Leys, C., Ley, C., Klein, O., Bernard, P., & Licata, L. (2013). Detecting outliers: Do not use standard deviation around the mean, use absolute deviation around the median. *Journal of Experimental Social Psychology, 49*(4), 764-766.

Li, S., & Xia, M. (2019). Review of high-content screening applications in toxicology. *Archives of Toxicology, 93*(12), 3387-3396. doi:10.1007/s00204-019-02593-5 [doi]

Luo, X., & Kraus, W. L. (2012). On PAR with PARP: Cellular stress signaling through poly(ADP-ribose) and PARP-1. *Genes & Development, 26*(5), 417-432. doi:10.1101/gad.183509.111 [doi]

Menolfi, D., & Zha, S. (2020). ATM, ATR and DNA-PKcs kinases-the lessons from the mouse models: Inhibition not equal deletion. *Cell & Bioscience, 10*, 8-x. eCollection 2020. doi:10.1186/s13578-020-0376-x [doi]

Mingatto, F. E., Rodrigues, T., Pigoso, A. A., Uyemura, S. A., Curti, C., & Santos, A. C. (2002). The critical role of mitochondrial energetic impairment in the toxicity of nimesulide to hepatocytes. *The Journal of Pharmacology and Experimental Therapeutics, 303*(2), 601-607. doi:10.1124/jpet.102.038620 [doi]

*MultiFlow(R).*https://litronlabs.com/getattachment/90ff922b-bd97-4dfd-858a-63cd59e3a2e3/Instruction-Manual-MultiFlow-DNA-Damage-Kit-p5.aspx

Niida, H., & Nakanishi, M. (2006). DNA damage checkpoints in mammals. *Mutagenesis, 21*(1), 3-9. doi:gei063 [pii]

Odell, I. D., & Cook, D. (2013). Immunofluorescence techniques. *The Journal of Investigative Dermatology, 133*(1), e4. doi:10.1038/jid.2012.455 [doi]

OECD. (2016a). *Test no. 473: In vitro mammalian chromosomal aberration test* doi:https://doi.org/https://doi.org/10.1787/9789264264649-en

OECD. (2016b). *Test no. 487: In vitro mammalian cell micronucleus test* doi:https://doi.org/https://doi.org/10.1787/9789264264861-en

OECD. (2016c). *Test no. 489: In vivo mammalian alkaline comet assay* doi:https://doi.org/https://doi.org/10.1787/9789264264885-en

OECD. (2020). *Test no. 471: Bacterial reverse mutation test* doi:https://doi.org/https://doi.org/10.1787/9789264071247-en

*OECD home.*OECD.org

Podhorecka, M., Skladanowski, A., & Bozko, P. (2010). H2AX phosphorylation: Its role in DNA damage response and cancer therapy. *Journal of Nucleic Acids, 2010*, 10.4061/2010/920161. doi:10.4061/2010/920161 [doi]

Ramakrishna, S., Tian, L., Wang, C., Liao, S., & Teo, W. E. (2015). *Medical devices: Regulations, standards and practices* Woodhead Publishing.

Reaves, S. K., Fanzo, J. C., Arima, K., Wu, J. Y., Wang, Y. R., & Lei, K. Y. (2000). Expression of the p53 tumor suppressor gene is up-regulated by depletion of intracellular zinc in HepG2 cells. *The Journal of Nutrition, 130*(7), 1688-1694. doi:10.1093/jn/130.7.1688 [doi]

Shah, U. K., Seager, A. L., Fowler, P., Doak, S. H., Johnson, G. E., Scott, S. J., et al. (2016). A comparison of the genotoxicity of benzo[a]pyrene in four cell lines with differing metabolic capacity. *Mutation Research.Genetic Toxicology and Environmental Mutagenesis, 808*, 8-19. doi:10.1016/j.mrgentox.2016.06.009 [doi]

Smart, D. J., Ahmedi, K. P., Harvey, J. S., & Lynch, A. M. (2011). Genotoxicity screening via the gammaH2AX by flow assay. *Mutation Research, 715*(1-2), 25-31. doi:10.1016/j.mrfmmm.2011.07.001 [doi]

Smart, D. J., Helbling, F. R., Verardo, M., Huber, A., McHugh, D., & Vanscheeuwijck, P. (2020). Development of an integrated assay in human TK6 cells to permit comprehensive genotoxicity analysis in vitro. *Mutation*

Research/Genetic Toxicology and Environmental Mutagenesis, 849, 503129. doi:https://doi.org/10.1016/j.mrgentox.2019.503129

Takeiri, A., Matsuzaki, K., Motoyama, S., Yano, M., Harada, A., Katoh, C., et al. (2019). High-content imaging analyses of gammaH2AX-foci and micronuclei in TK6 cells elucidated genotoxicity of chemicals and their clastogenic/aneugenic mode of action. *Genes and Environment : The Official Journal of the Japanese Environmental Mutagen Society, 41*, 4-8. eCollection 2019. doi:10.1186/s41021-019-0117-8 [doi]

Tsai, P. K., Wu, S. W., Chiang, C. Y., Lee, M. W., Chen, H. Y., Chen, W. Y., et al. (2020). Evaluation of cytotoxicity, apoptosis and genotoxicity induced by indium chloride in macrophages through mitochondrial dysfunction and reactive oxygen species generation. *Ecotoxicology and Environmental Safety, 193*, 110348. doi:S0147-6513(20)30187-1 [pii]

Tu, W. Z., Li, B., Huang, B., Wang, Y., Liu, X. D., Guan, H., et al. (2013). gammaH2AX foci formation in the absence of DNA damage: Mitotic H2AX phosphorylation is mediated by the DNA-PKcs/CHK2 pathway. *FEBS Letters, 587*(21), 3437-3443. doi:10.1016/j.febslet.2013.08.028 [doi]

Valavanidis, A., Vlachogianni, T., & Fiotakis, C. (2009). 8-hydroxy-2' -deoxyguanosine (8-OHdG): A critical biomarker of oxidative stress and carcinogenesis. *Journal of Environmental Science and Health.Part C, Environmental Carcinogenesis & Ecotoxicology Reviews, 27*(2), 120-139. doi:10.1080/10590500902885684 [doi]

Waldhauser, K. M., Brecht, K., Hebeisen, S., Ha, H. R., Konrad, D., Bur, D., et al. (2008). Interaction with the hERG channel and cytotoxicity of amiodarone and amiodarone analogues. *British Journal of Pharmacology, 155*(4), 585-595. doi:10.1038/bjp.2008.287 [doi]

Wan, G., Liu, Y., Han, C., Zhang, X., & Lu, X. (2014). Noncoding RNAs in DNA repair and genome integrity. *Antioxidants & Redox Signaling, 20*(4), 655-677. doi:10.1089/ars.2013.5514 [doi]

Watters, G. P., Smart, D. J., Harvey, J. S., & Austin, C. A. (2009). H2AX phosphorylation as a genotoxicity endpoint. *Mutation Research, 679*(1-2), 50-58. doi:10.1016/j.mrgentox.2009.07.007 [doi]

Westerink, W. M., Schirris, T. J., Horbach, G. J., & Schoonen, W. G. (2011). Development and validation of a high-content screening in vitro micronucleus assay in CHO-k1 and HepG2 cells. *Mutation Research, 724*(1-2), 7-21. doi:10.1016/j.mrgentox.2011.05.007 [doi]

Whitebread, S., Hamon, J., Bojanic, D., & Urban, L. (2005). Keynote review: In vitro safety pharmacology profiling: An essential tool for successful drug development. *Drug Discovery Today, 10*(21), 1421-1433. doi:S1359-6446(05)03632-9 [pii]

Wiederschain, G. Y. (2011). No title. *The Molecular Probes Handbook.A Guide to Fluorescent Probes and Labeling Technologies,*

Williams, A. B., & Schumacher, B. (2016). p53 in the DNA-damage-repair process. *Cold Spring Harbor Perspectives in Medicine, 6*(5), 10.1101/cshperspect.a026070. doi:10.1101/cshperspect.a026070 [doi]

APPENDIX A

Expression of genotoxicity markers yH2AX, pH3 and p53 in TK6 cells presented as folds to negative controls. The markekrs for yH2AX and pH3 are presented together with the RNC in one graph, with the scale for the markers on the y-axis on the left-hand side and the scale for RNC on the right-hand side. The green lines represent pH3-folds, the yellow lines yH2AX-folds and the grey lines the RNC. Likewise, the marker for p53 and the RNC are shown on the other seprate graph with the same logic and p53-folds as red lines. The concnentration series is presented in µM as a logarithmic scale on the x-axis. The two same-coloured lines represent the two different timepoints measured, after a 4-hour incubation and a 24-hour incubation. The values presented are the median of all measured values for the same compound at the same concentration. The error bars represent the median absolute deviation (MAD). Results for each compound used in this study is shown on separate pages.

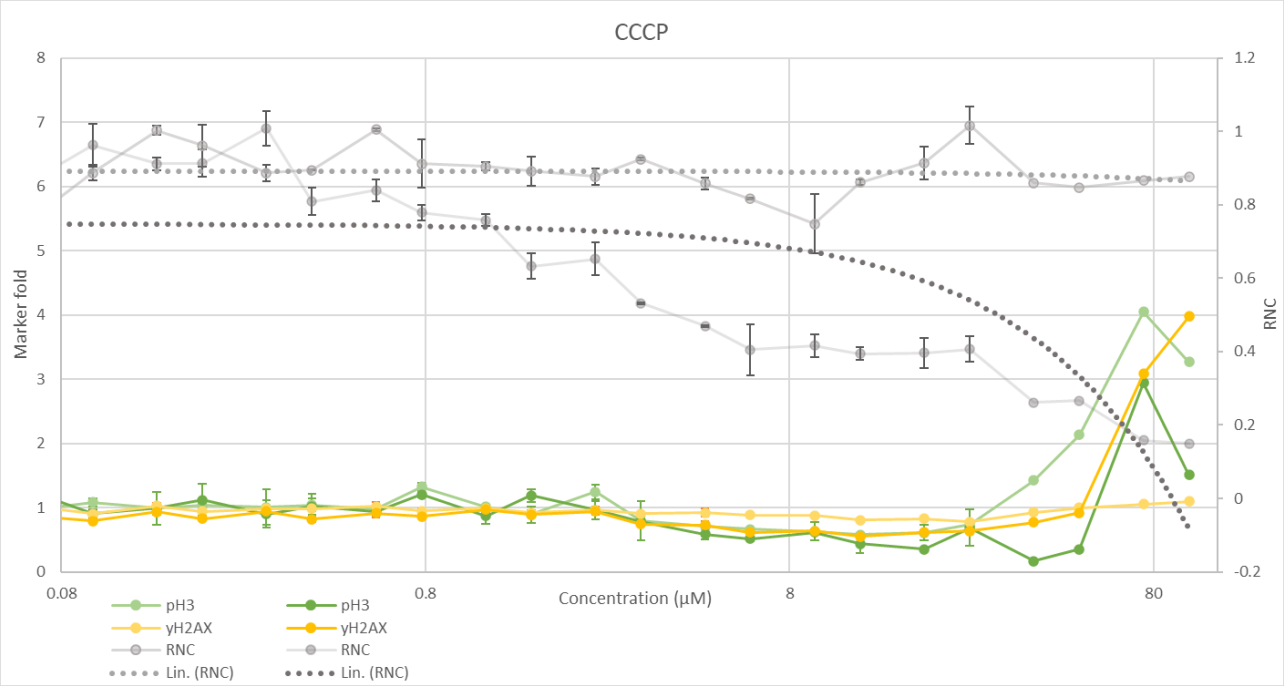
CCCP
Marker fold
RNC
Concentration (µM)
0.08
0.8
8
80
pH3
yH2AX
RNC
Lin. (RNC)
pH3
yH2AX
RNC
Lin. (RNC)

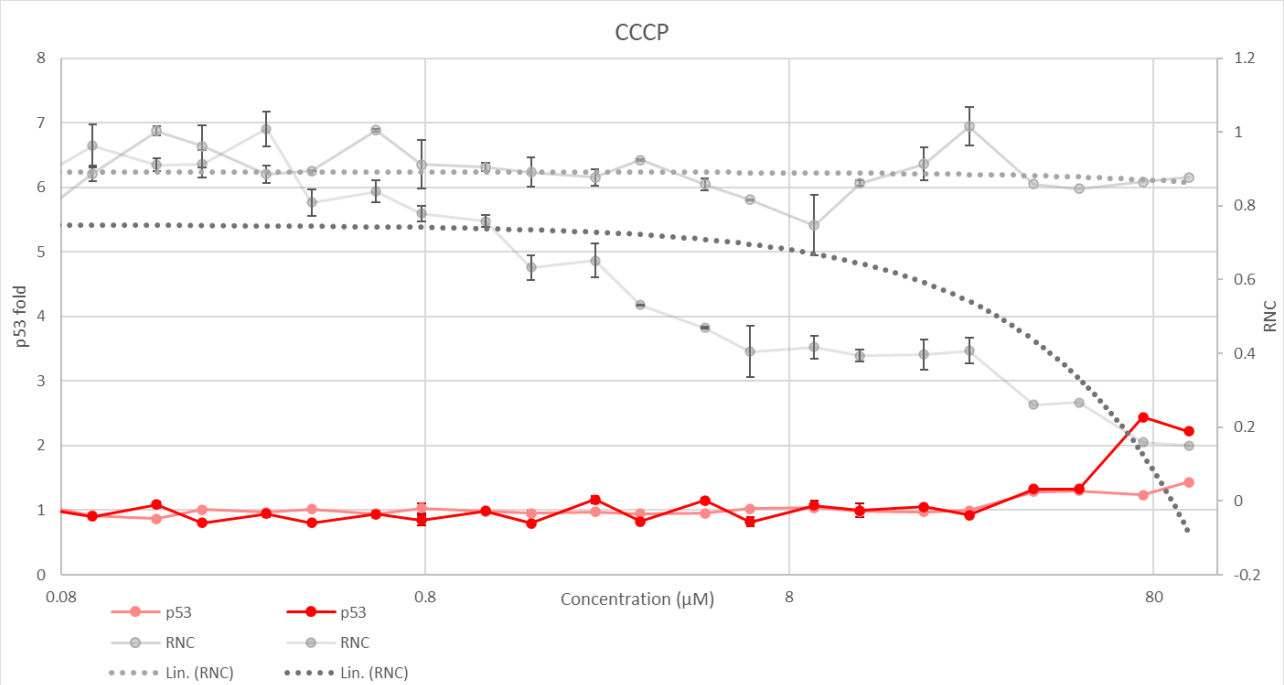
CCCP
p53 fold
RNC
Concentration (µM)
0.08
0.8
8
80
p53
RNC
Lin. (RNC)
p53
RNC
Lin. (RNC)

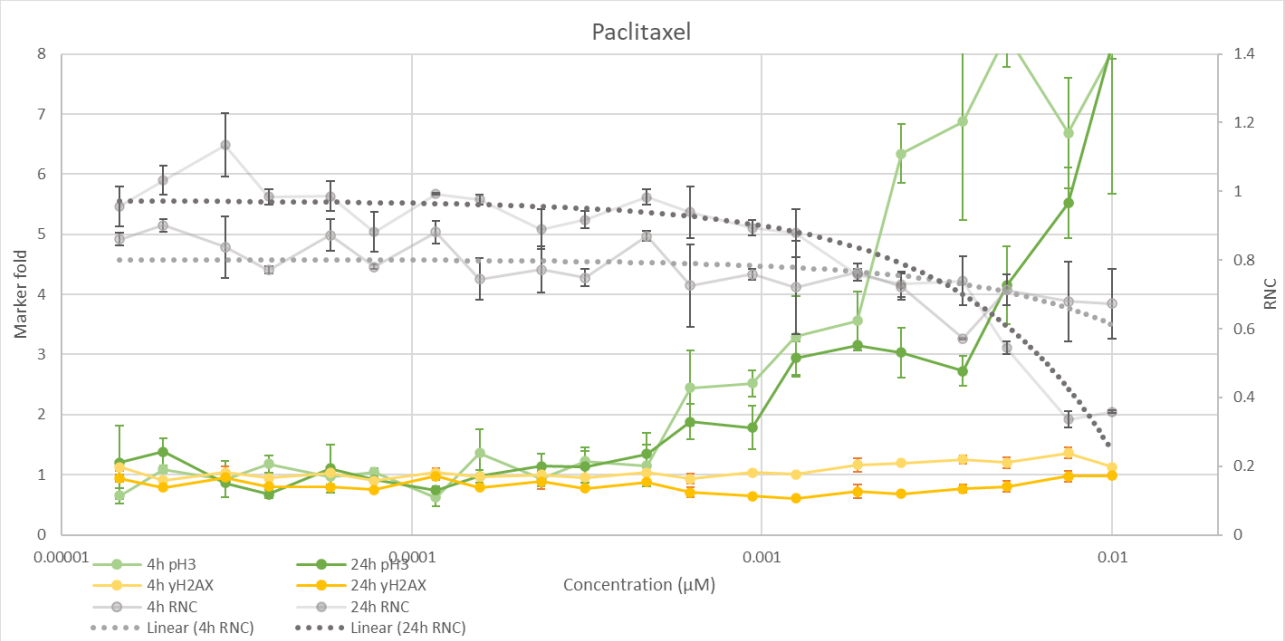
Paclitaxel
Marker fold
RNC
Concentration (µM)
0.00001
0.0001
0.001
0.01
4h pH3
24h pH3
4h γH2AX
24h γH2AX
4h RNC
24h RNC
Linear (4h RNC)
Linear (24h RNC)

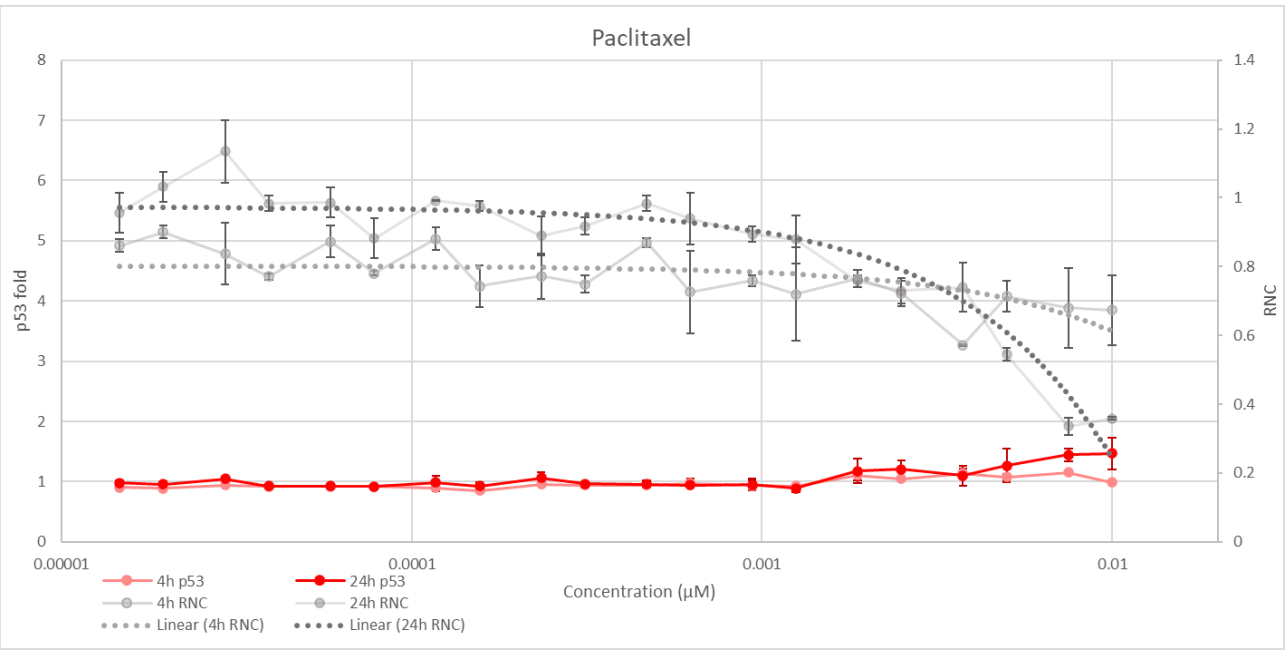
Paclitaxel
p53 fold
RNC
Concentration (µM)
0.00001
0.0001
0.001
0.01
4h p53
24h p53
4h RNC
24h RNC
Linear (4h RNC)
Linear (24h RNC)

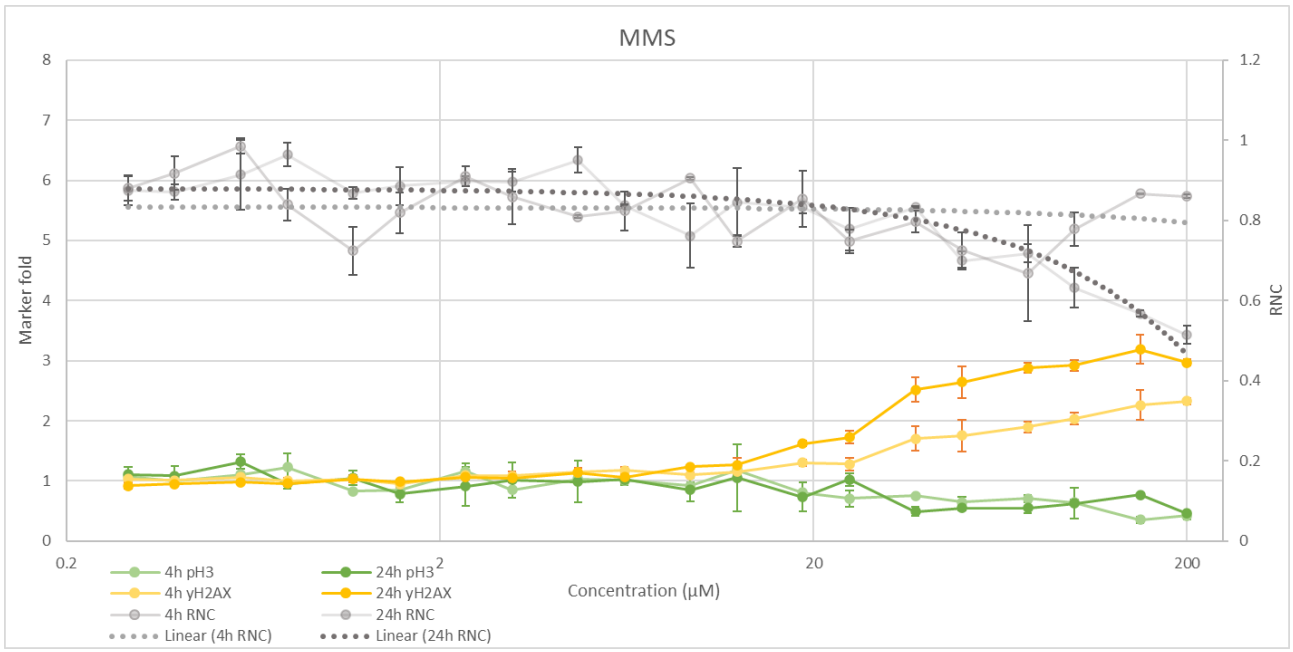
MMS
Marker fold
RNC
Concentration (µM)
0.2
2
20
200
4h pH3
24h pH3
4h γH2AX
24h γH2AX
4h RNC
24h RNC
Linear (4h RNC)
Linear (24h RNC)

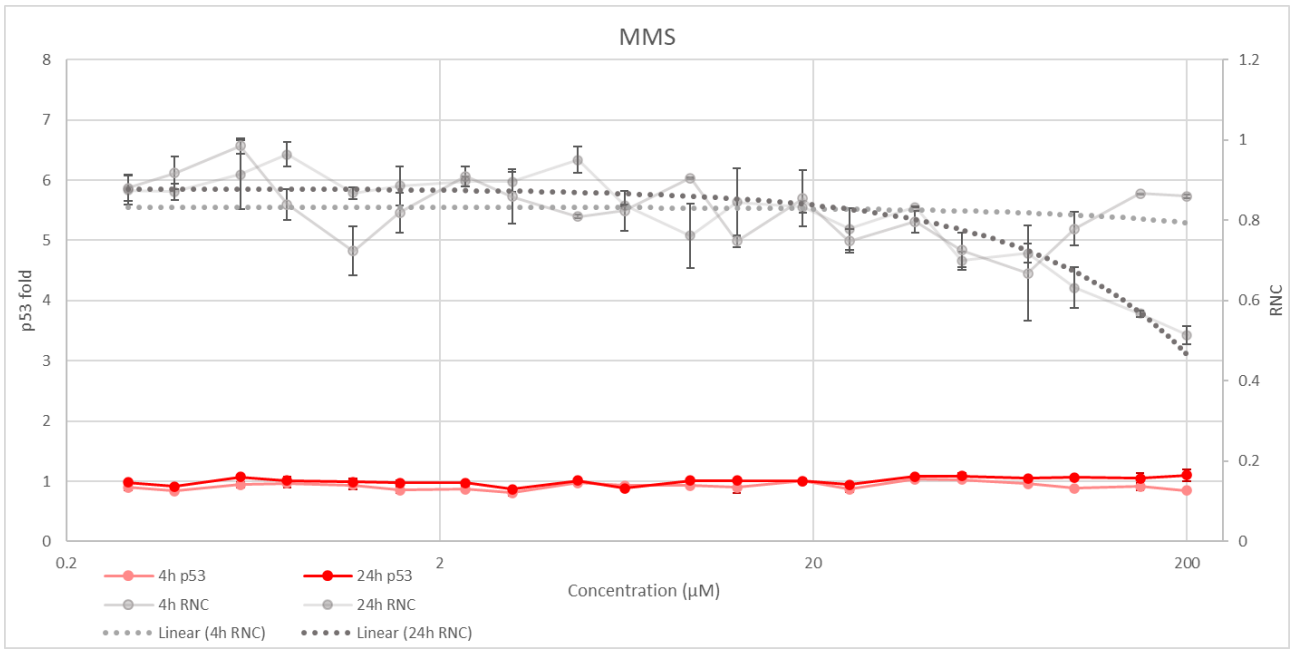
MMS
p53 fold
RNC
Concentration (µM)
0.2
2
20
200
4h p53
24h p53
4h RNC
24h RNC
Linear (4h RNC)
Linear (24h RNC)

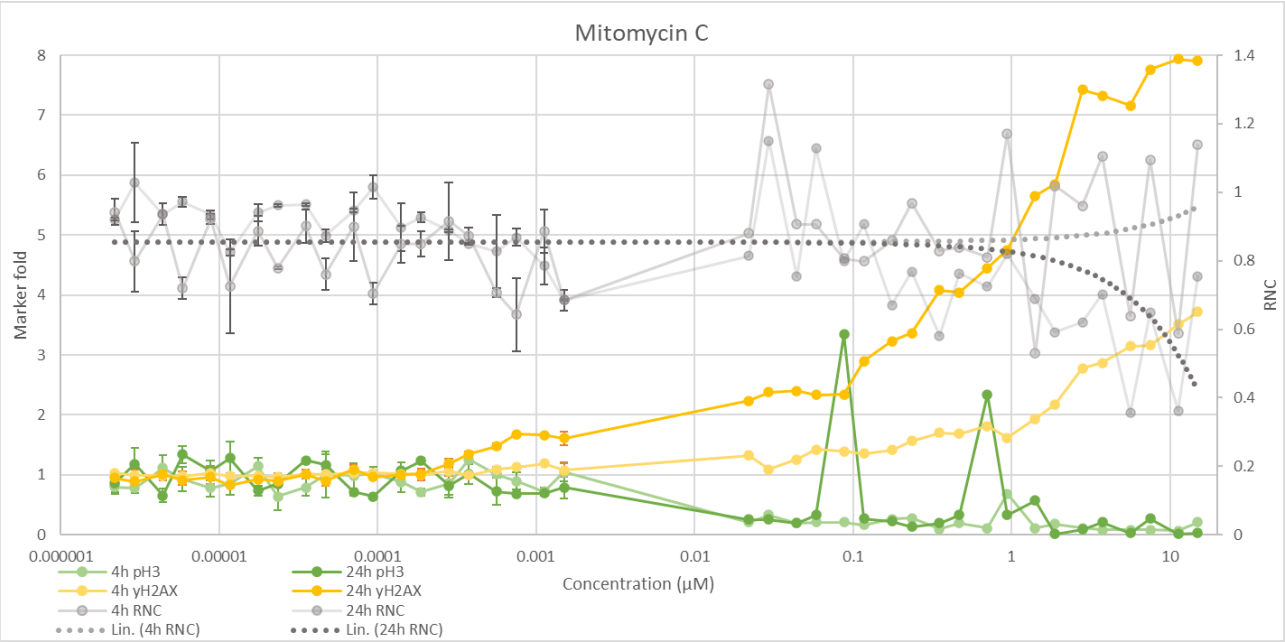
Mitomycin C
Marker fold
RNC
Concentration (µM)
0.000001
0.00001
0.0001
0.001
0.01
0.1
1
10
4h pH3
24h pH3
4h γH2AX
24h γH2AX
4h RNC
24h RNC
Lin. (4h RNC)
Lin. (24h RNC)

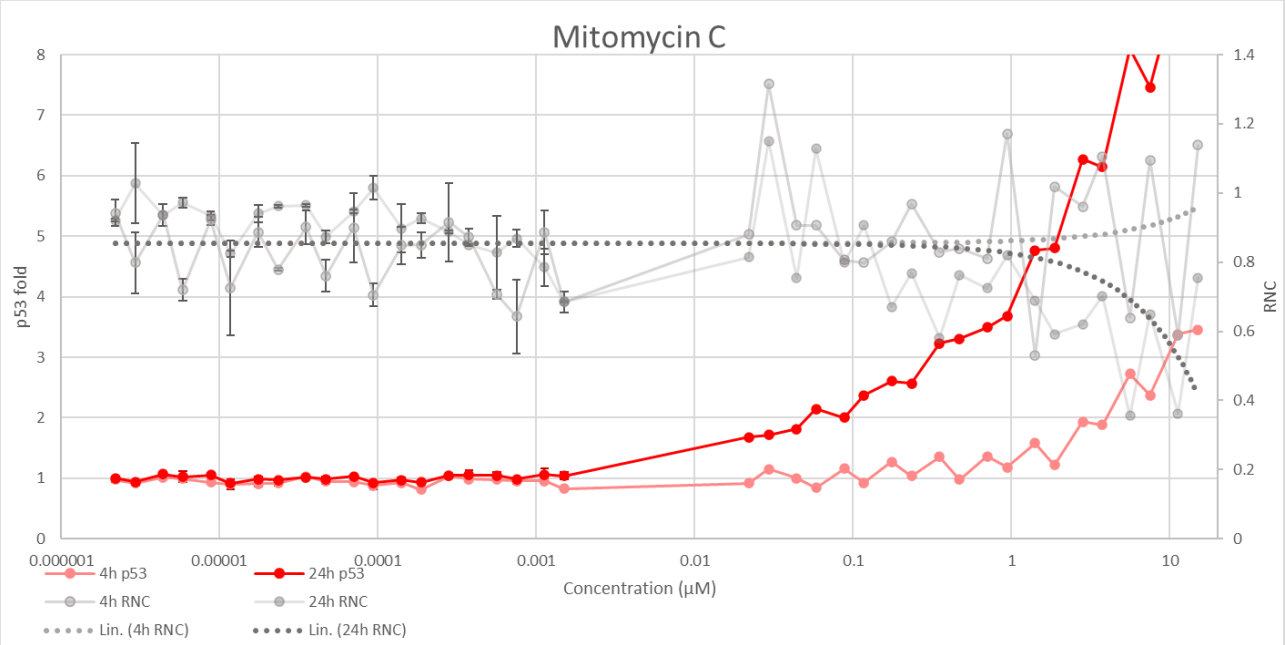
Mitomycin C
p53 fold
RNC
Concentration (µM)
0.000001
0.00001
0.0001
0.001
0.01
0.1
1
10
4h p53
24h p53
4h RNC
24h RNC
Lin. (4h RNC)
Lin. (24h RNC)

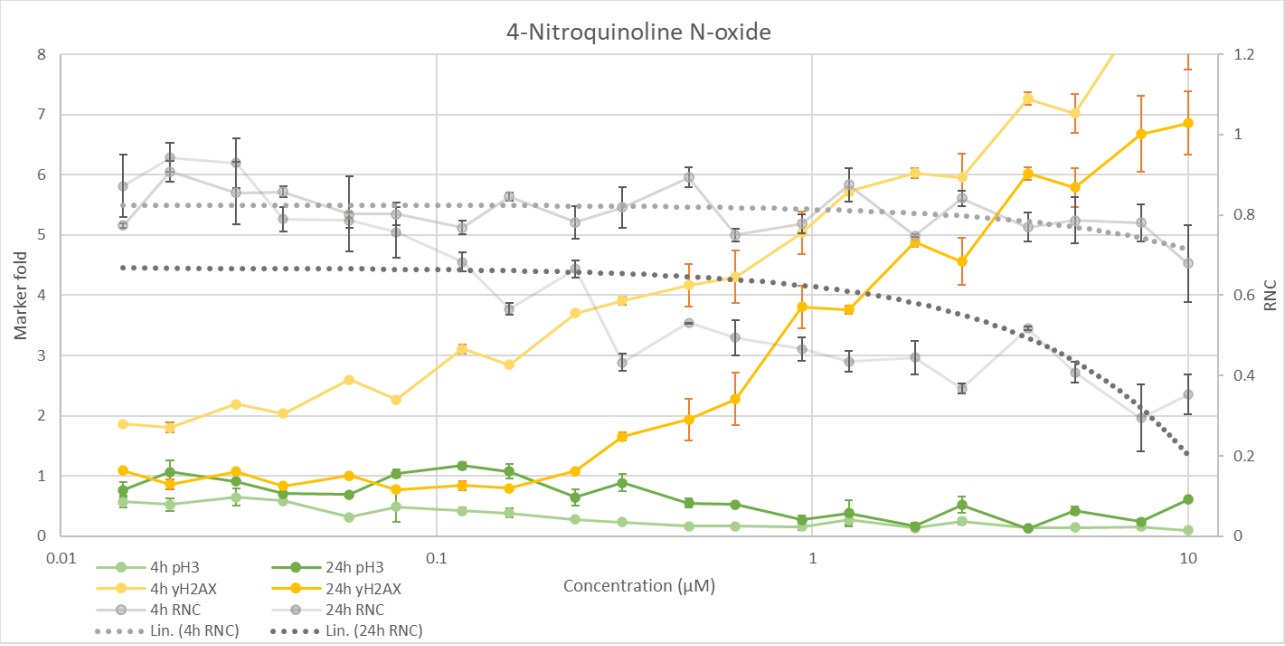
4-Nitroquinoline N-oxide
Marker fold
RNC
Concentration (µM)
0.01
0.1
1
10
4h pH3
24h pH3
4h γH2AX
24h γH2AX
4h RNC
24h RNC
Lin. (4h RNC)
Lin. (24h RNC)

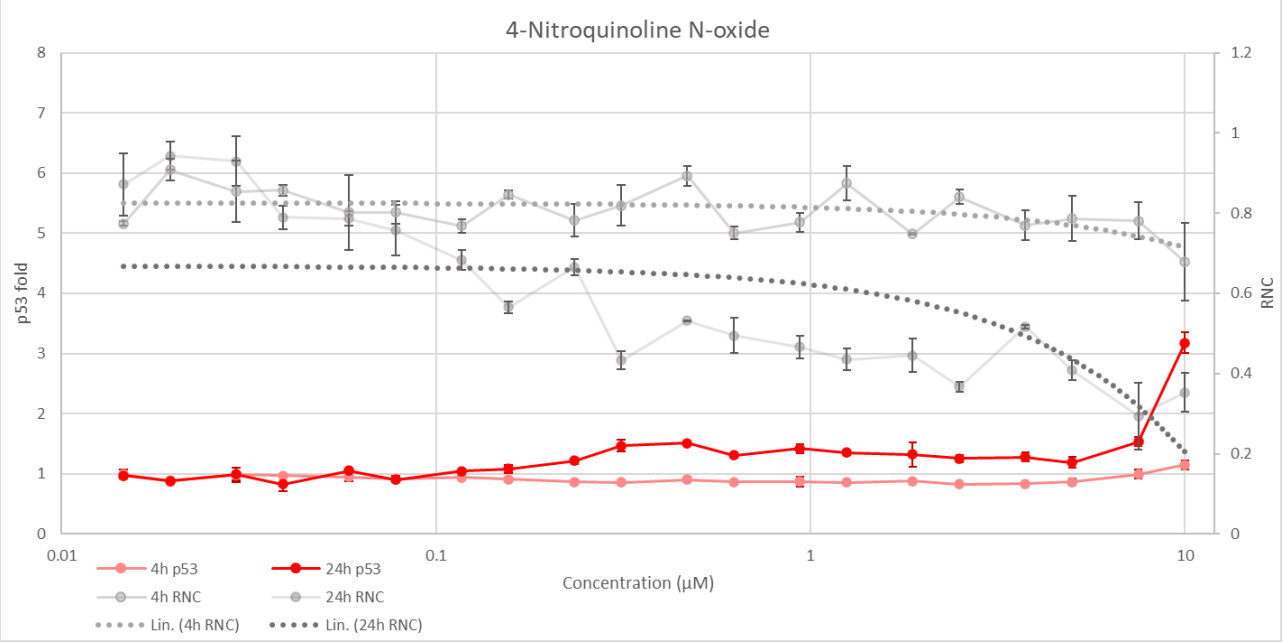
4-Nitroquinoline N-oxide
p53 fold
RNC
Concentration (µM)
0.01
0.1
1
10
4h p53
24h p53
4h RNC
24h RNC
Lin. (4h RNC)
Lin. (24h RNC)

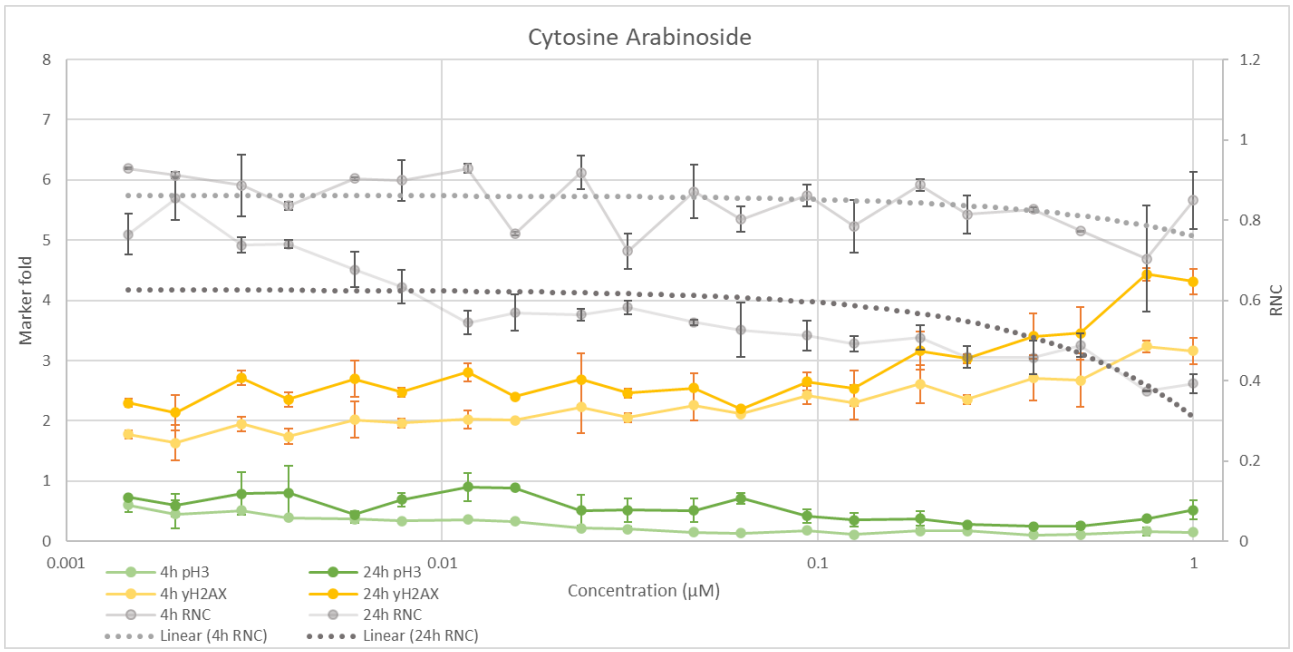
Cytosine Arabinoside
Marker fold
RNC
Concentration (µM)
0.001
0.01
0.1
1
4h pH3
24h pH3
4h γH2AX
24h γH2AX
4h RNC
24h RNC
Linear (4h RNC)
Linear (24h RNC)

,

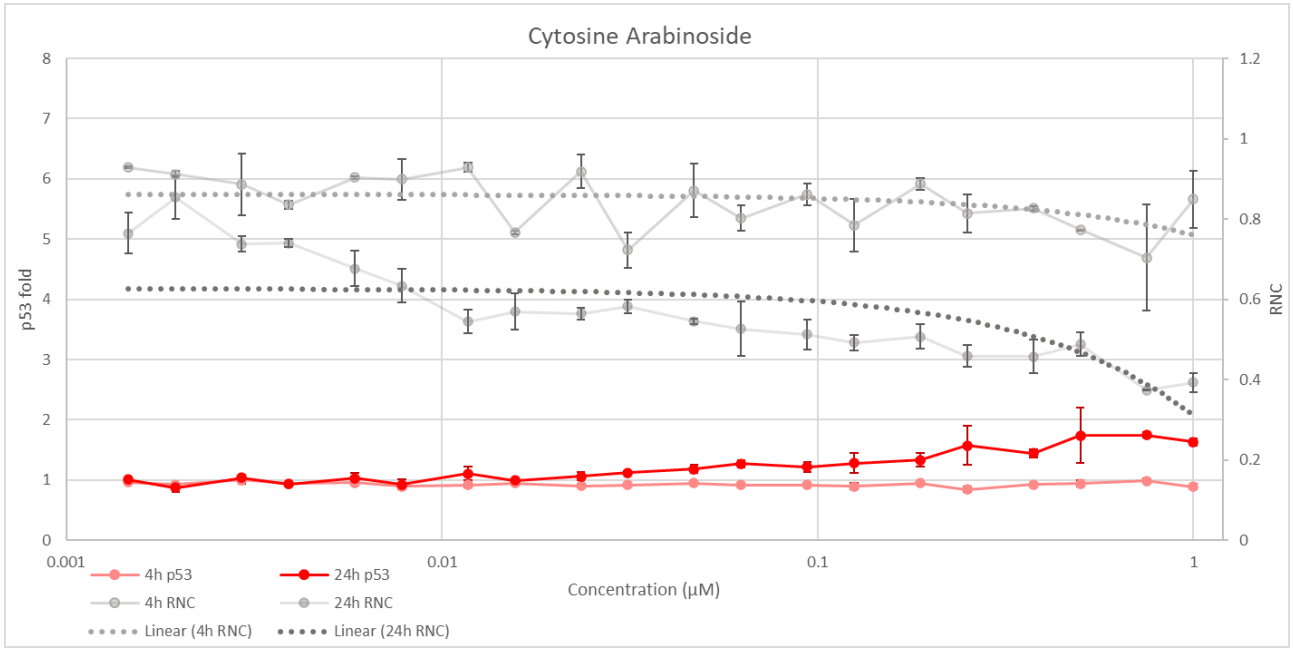
Cytosine Arabinoside
p53 fold
RNC
Concentration (µM)
0.001
0.01
0.1
1
4h p53
24h p53
4h RNC
24h RNC
Linear (4h RNC)
Linear (24h RNC)

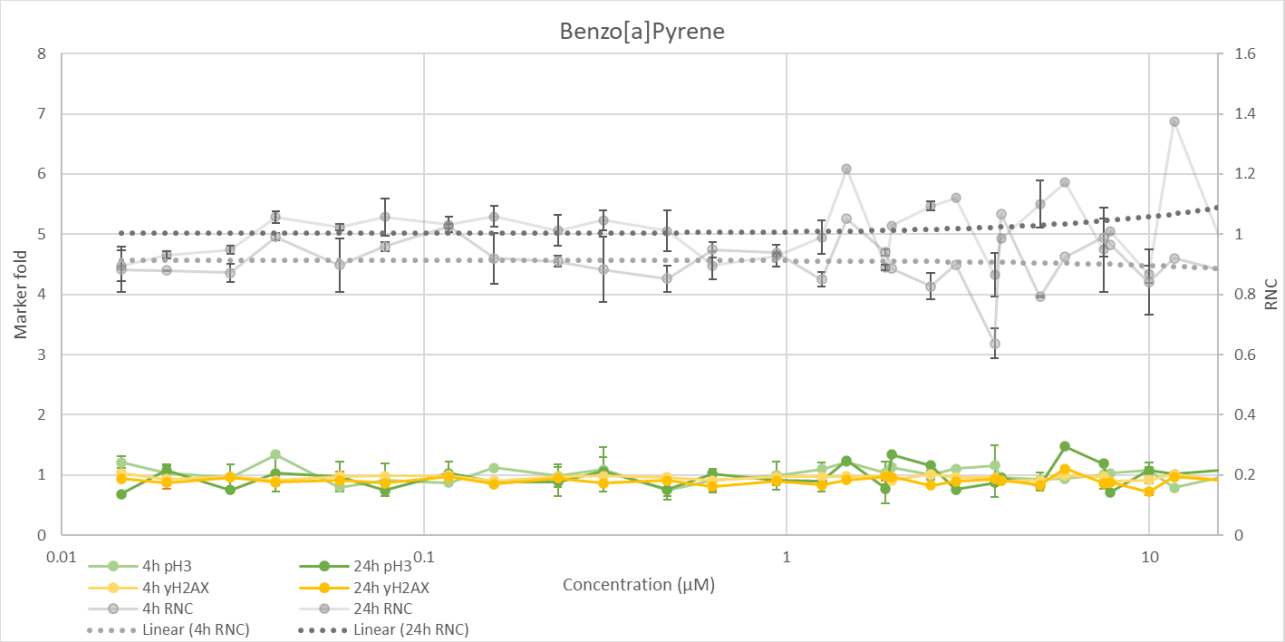
Benzo[a]Pyrene
Marker fold
RNC
Concentration (µM)
0.01
0.1
1
10
4h pH3
24h pH3
4h γH2AX
24h γH2AX
4h RNC
24h RNC
Linear (4h RNC)
Linear (24h RNC)

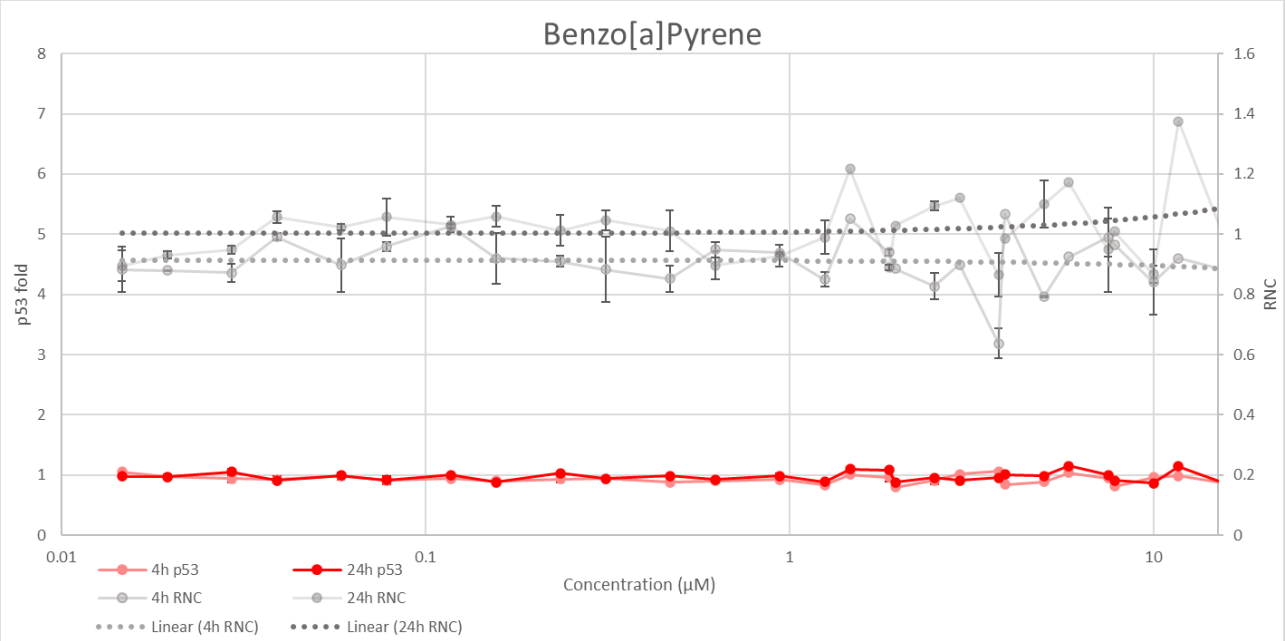
Benzo[a]Pyrene
p53 fold
RNC
Concentration (µM)
0.01
0.1
1
10
4h p53
24h p53
4h RNC
24h RNC
Linear (4h RNC)
Linear (24h RNC)

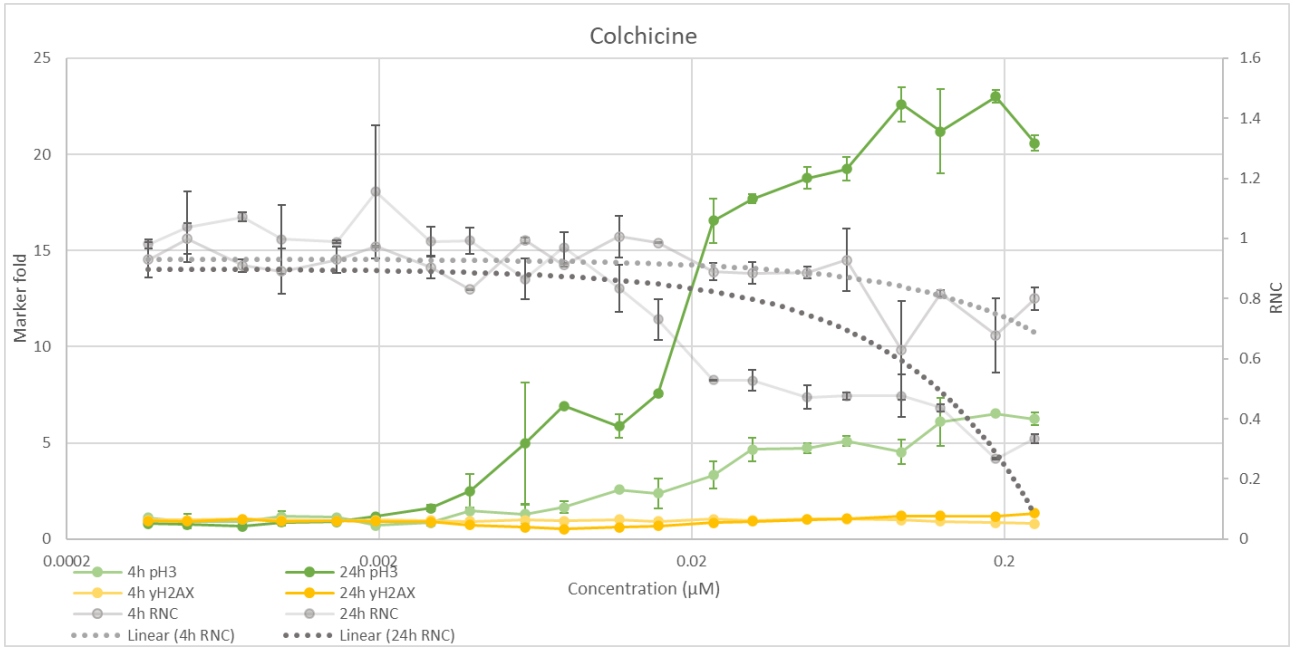
Colchicine
Marker fold
RNC
Concentration (µM)
0.0002
0.002
0.02
0.2
4h pH3
24h pH3
4h γH2AX
24h γH2AX
4h RNC
24h RNC
Linear (4h RNC)
Linear (24h RNC)

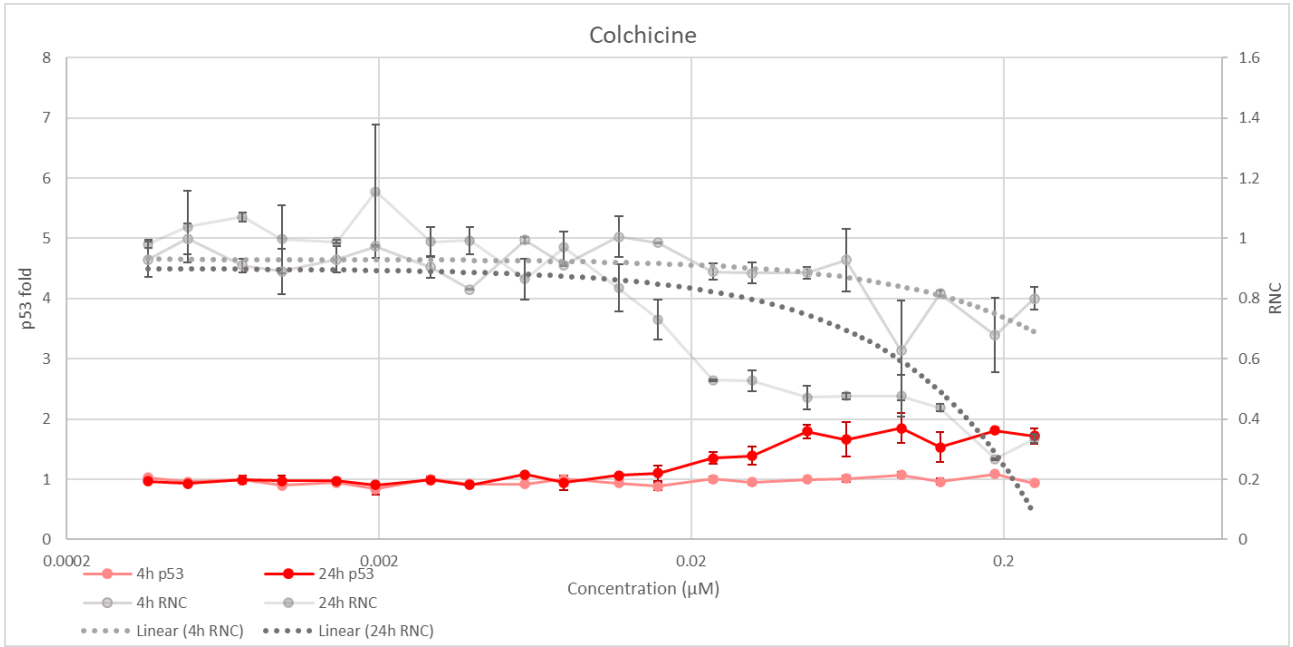
Colchicine
p53 fold
RNC
Concentration (µM)
0.0002
0.002
0.02
0.2
4h p53
24h p53
4h RNC
24h RNC
Linear (4h RNC)
Linear (24h RNC)

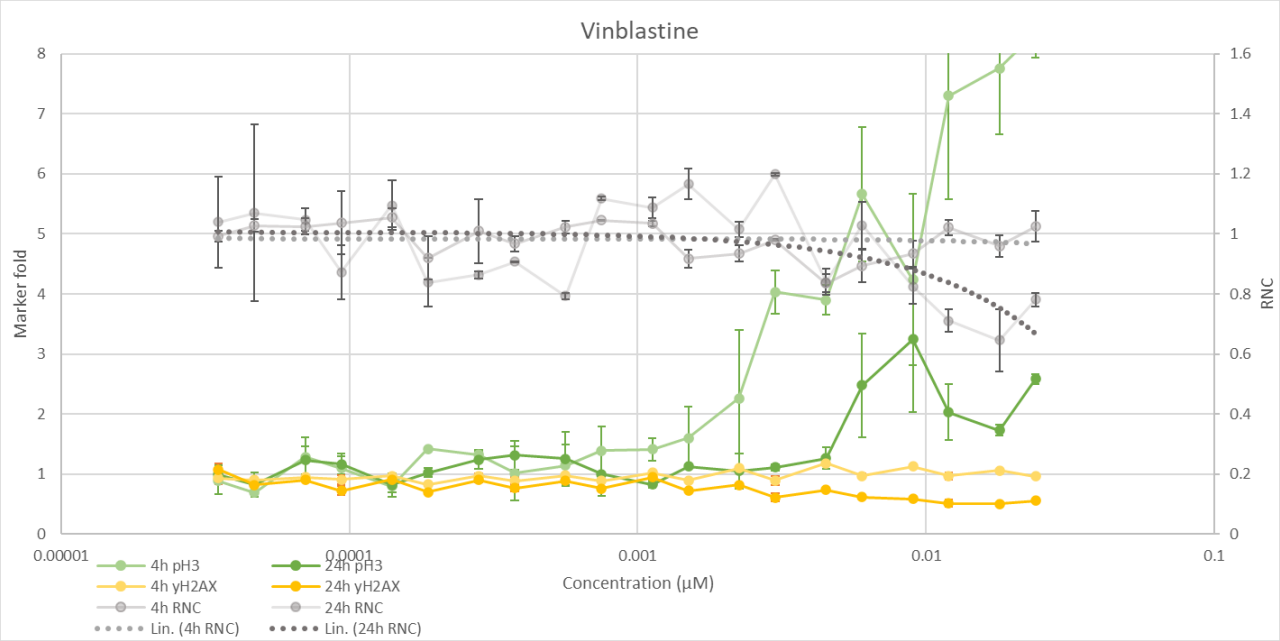
Vinblastine
Marker fold
RNC
Concentration (µM)
0.00001
0.0001
0.001
0.01
0.1
4h pH3
24h pH3
4h γH2AX
24h γH2AX
4h RNC
24h RNC
Lin. (4h RNC)
Lin. (24h RNC)

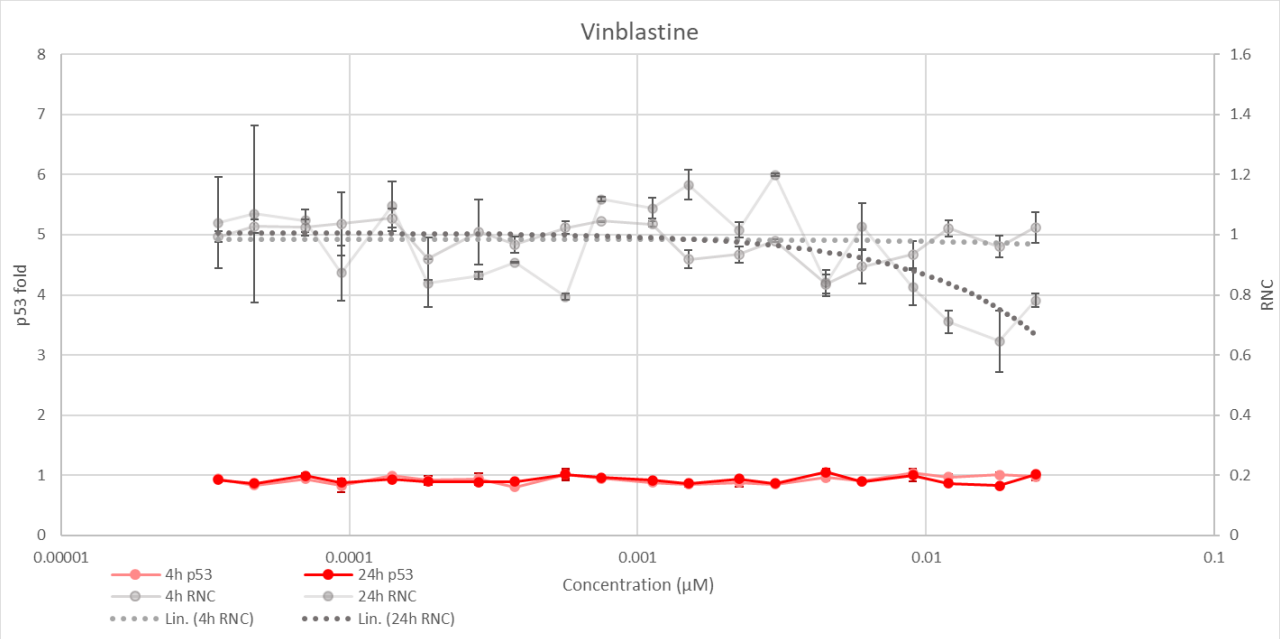
Vinblastine
p53 fold
RNC
Concentration (µM)
0.00001
0.0001
0.001
0.01
0.1
4h p53
24h p53
4h RNC
24h RNC
Lin. (4h RNC)
Lin. (24h RNC)

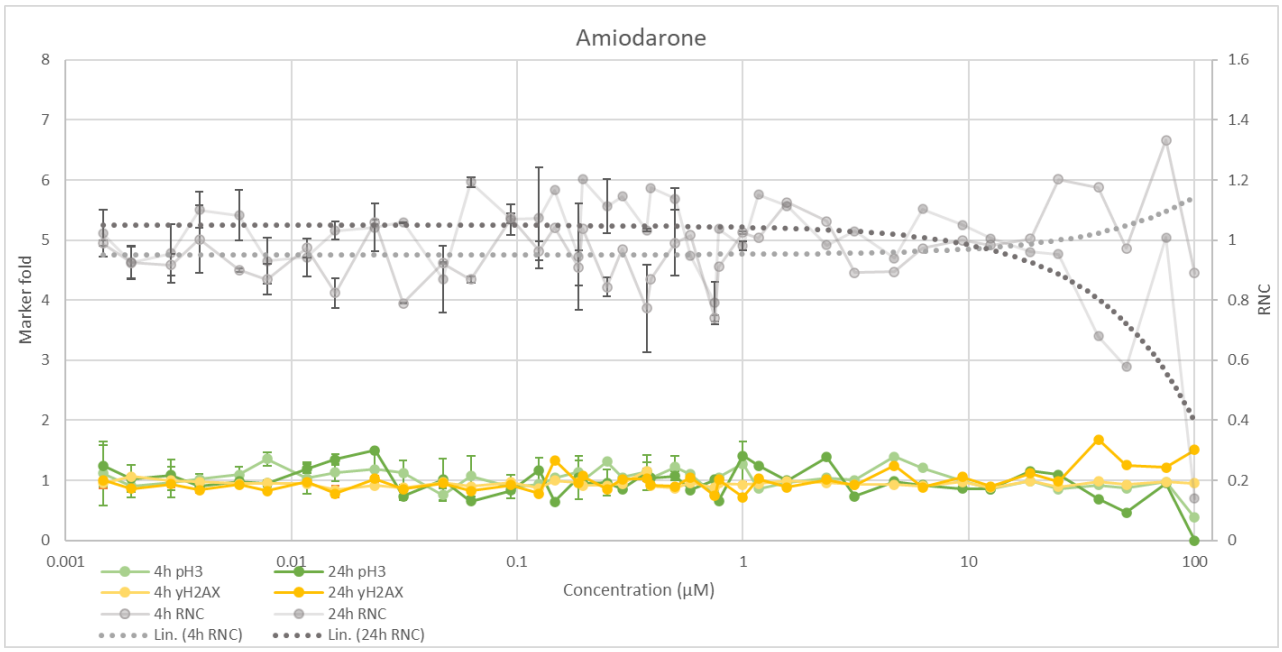
Amiodarone
Marker fold
RNC
Concentration (µM)
0.001
0.01
0.1
1
10
100
4h pH3
24h pH3
4h γH2AX
24h γH2AX
4h RNC
24h RNC
Lin. (4h RNC)
Lin. (24h RNC)

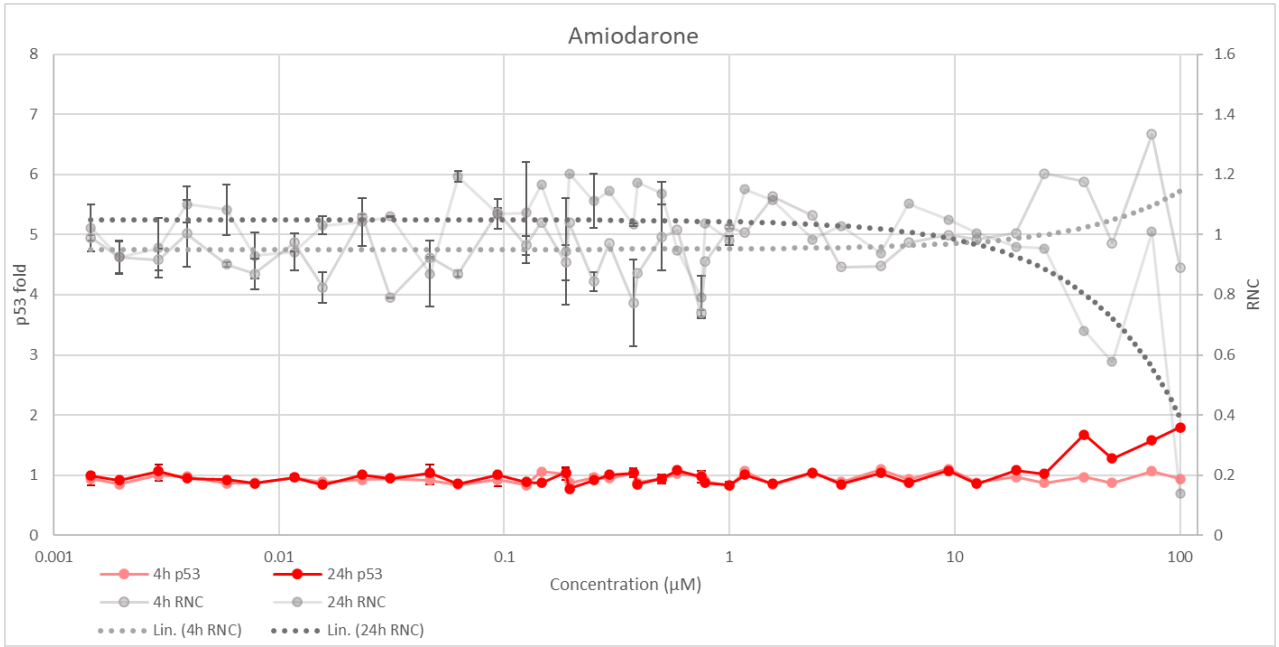
Amiodarone
p53 fold
RNC
Concentration (µM)
0.001
0.01
0.1
1
10
100
4h p53
24h p53
4h RNC
24h RNC
Lin. (4h RNC)
Lin. (24h RNC)

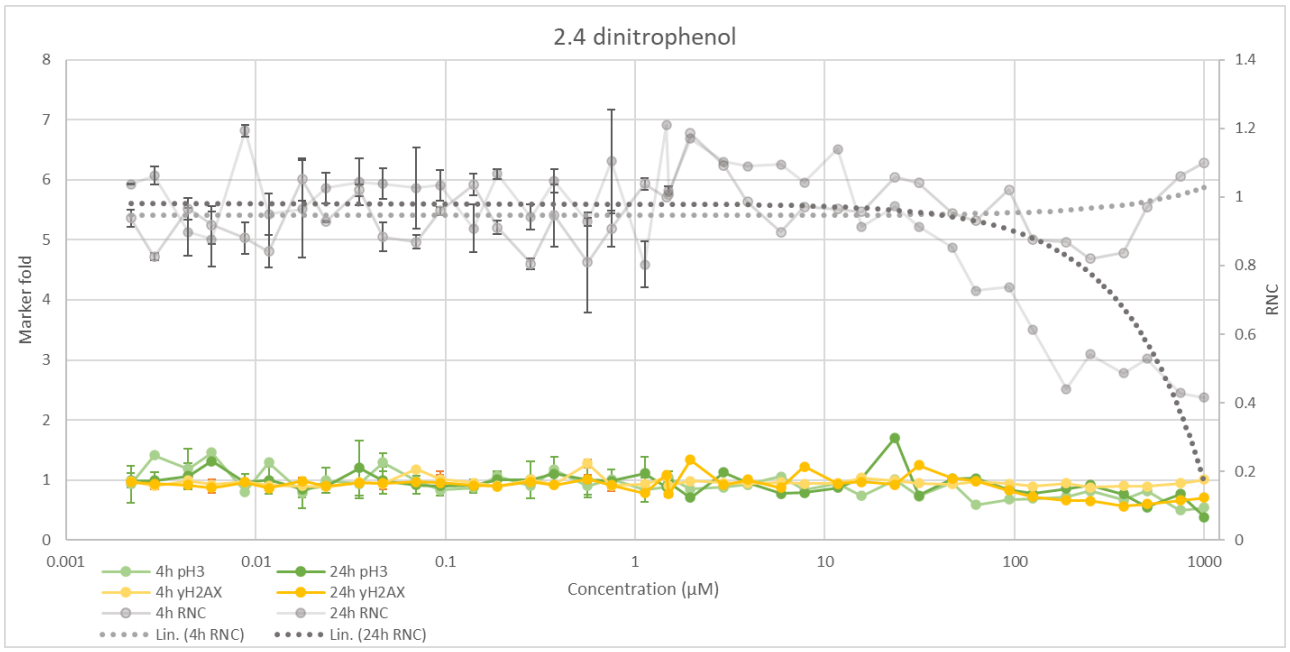
2.4 dinitrophenol
Marker fold
RNC
Concentration (µM)
0.001
0.01
0.1
1
10
100
1000
4h pH3
24h pH3
4h γH2AX
24h γH2AX
4h RNC
24h RNC
Lin. (4h RNC)
Lin. (24h RNC)

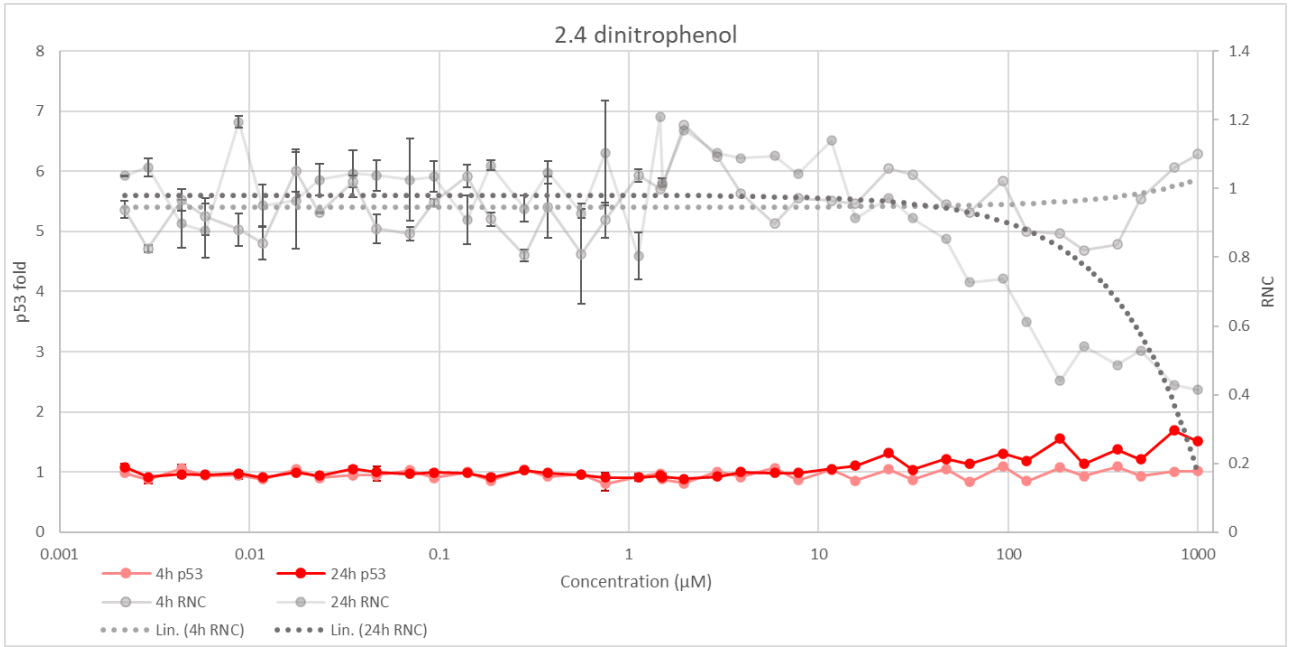
2.4 dinitrophenol
p53 fold
RNC
Concentration (µM)
0.001
0.01
0.1
1
10
100
1000
4h p53
24h p53
4h RNC
24h RNC
Lin. (4h RNC)
Lin. (24h RNC)

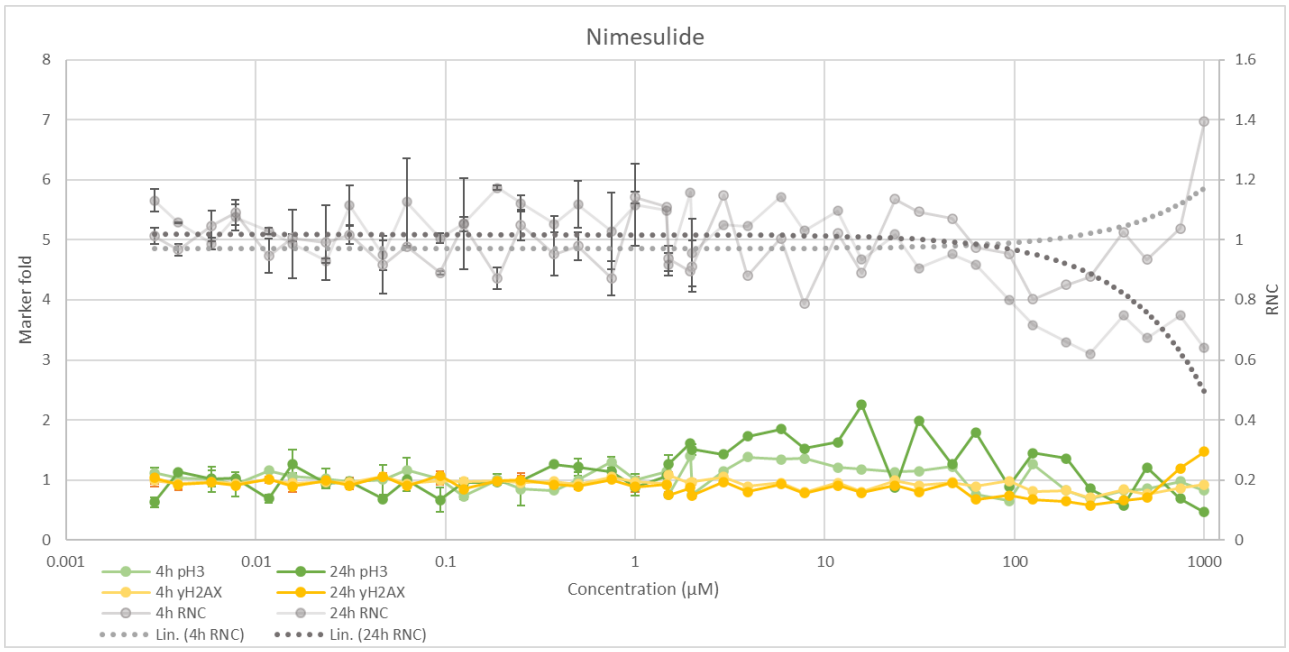
Nimesulide
Marker fold
RNC
Concentration (µM)
0.001
0.01
0.1
1
10
100
1000
4h pH3
24h pH3
4h γH2AX
24h γH2AX
4h RNC
24h RNC
Lin. (4h RNC)
Lin. (24h RNC)

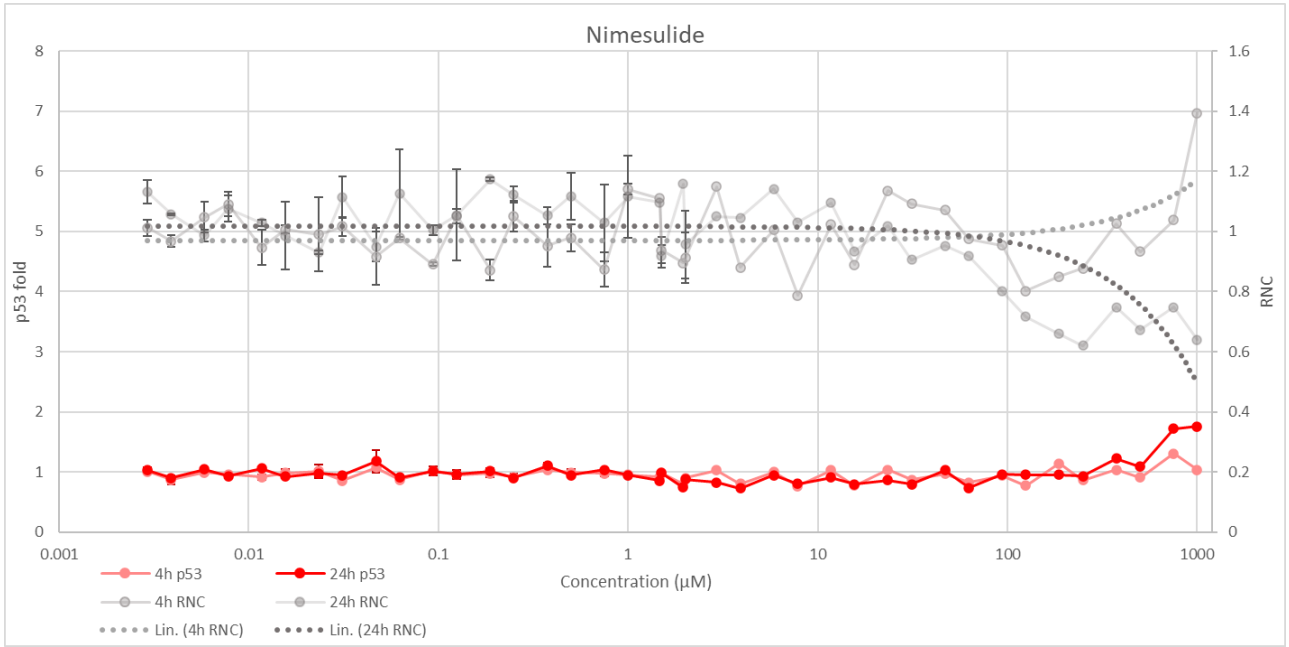
Nimesulide
p53 fold
RNC
Concentration (µM)
0.001
0.01
0.1
1
10
100
1000
4h p53
24h p53
4h RNC
24h RNC
Lin. (4h RNC)
Lin. (24h RNC)

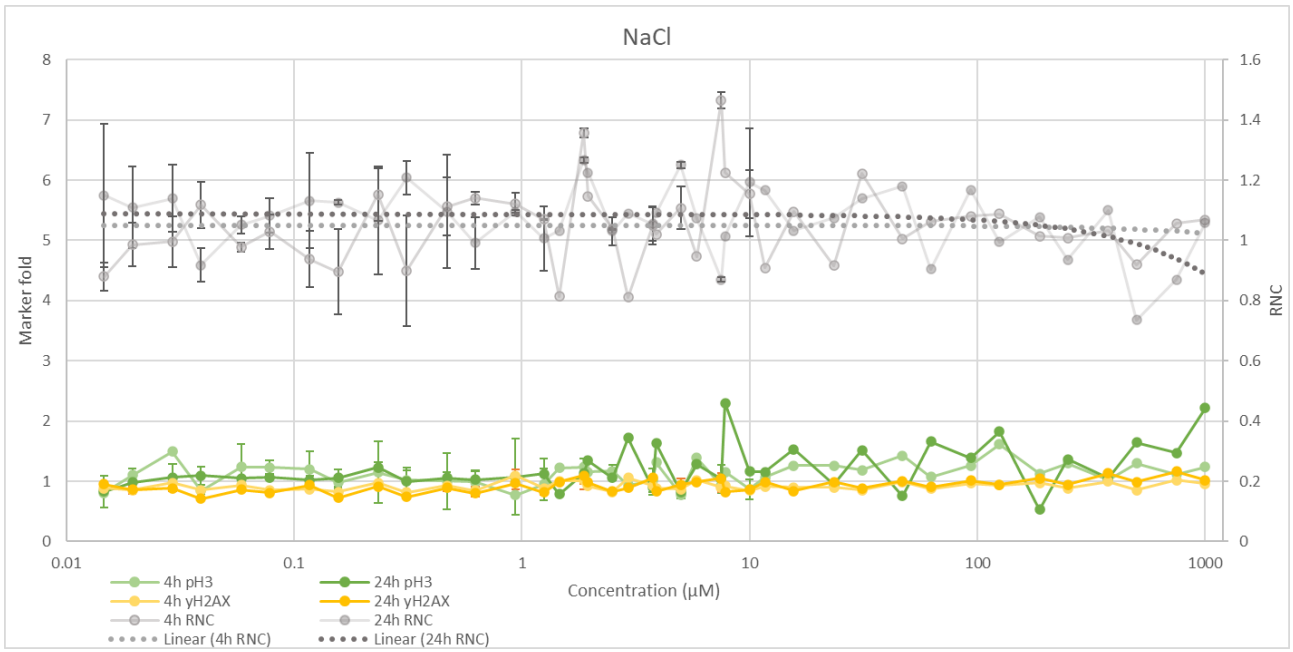
NaCl
Marker fold
RNC
Concentration (µM)
0.01
0.1
1
10
100
1000
4h pH3
24h pH3
4h γH2AX
24h γH2AX
4h RNC
24h RNC
Linear (4h RNC)
Linear (24h RNC)

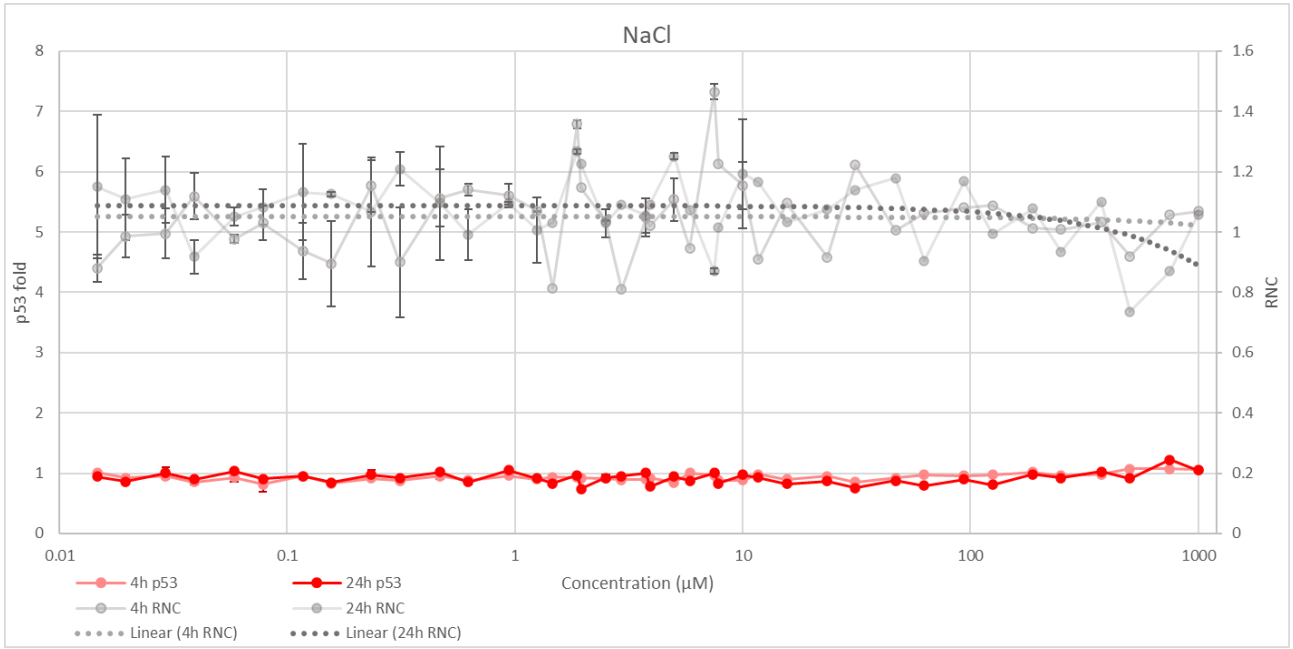
NaCl
p53 fold
RNC
Concentration (µM)
0.01
0.1
1
10
100
1000
4h p53
24h p53
4h RNC
24h RNC
Linear (4h RNC)
Linear (24h RNC)

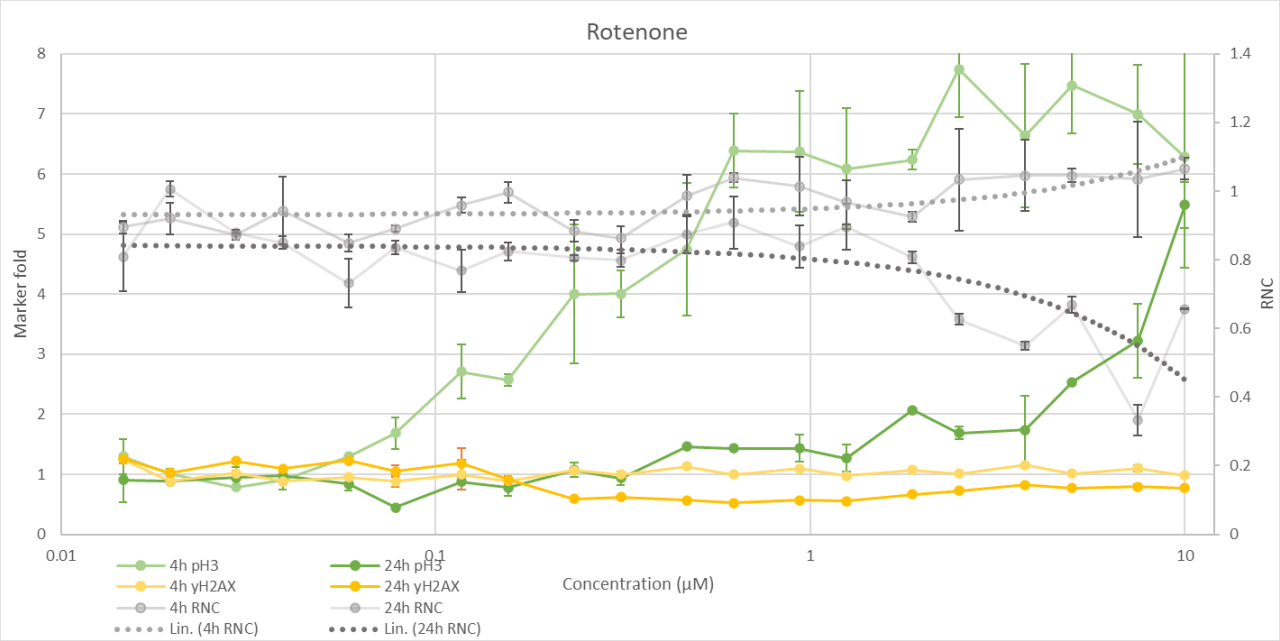
Rotenone
Marker fold
RNC
Concentration (µM)
0.01
0.1
1
10
4h pH3
24h pH3
4h γH2AX
24h γH2AX
4h RNC
24h RNC
Lin. (4h RNC)
Lin. (24h RNC)

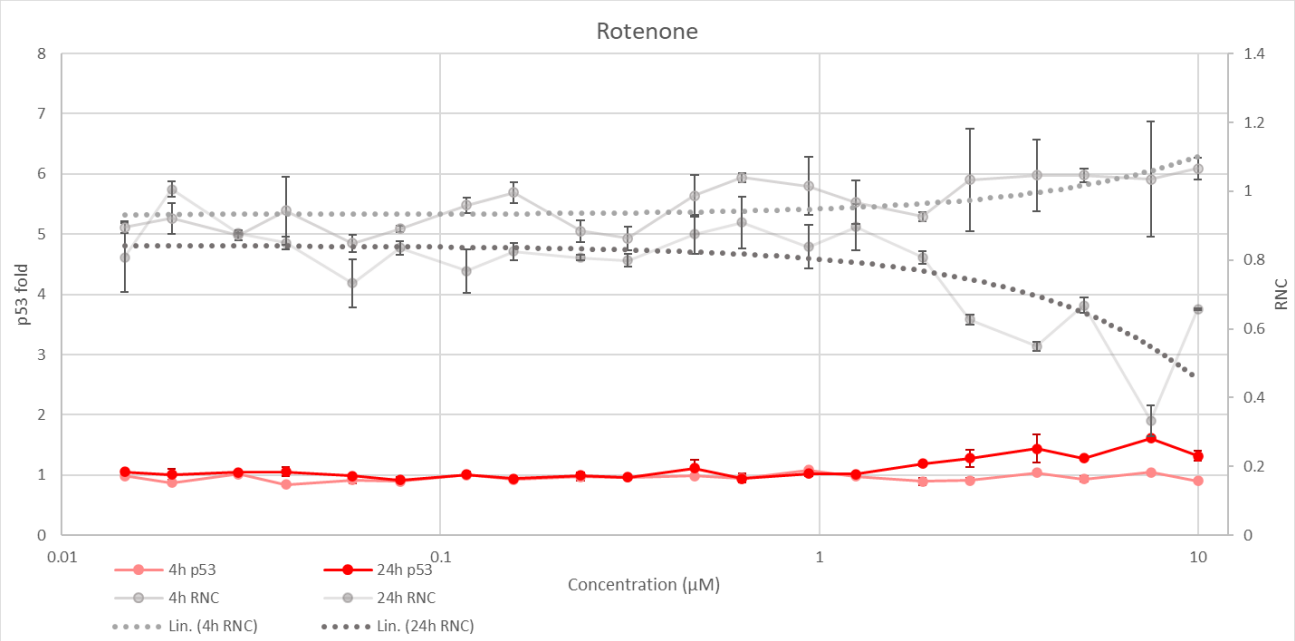
Rotenone
p53 fold
RNC
Concentration (µM)
0.01
0.1
1
10
4h p53
24h p53
4h RNC
24h RNC
Lin. (4h RNC)
Lin. (24h RNC)

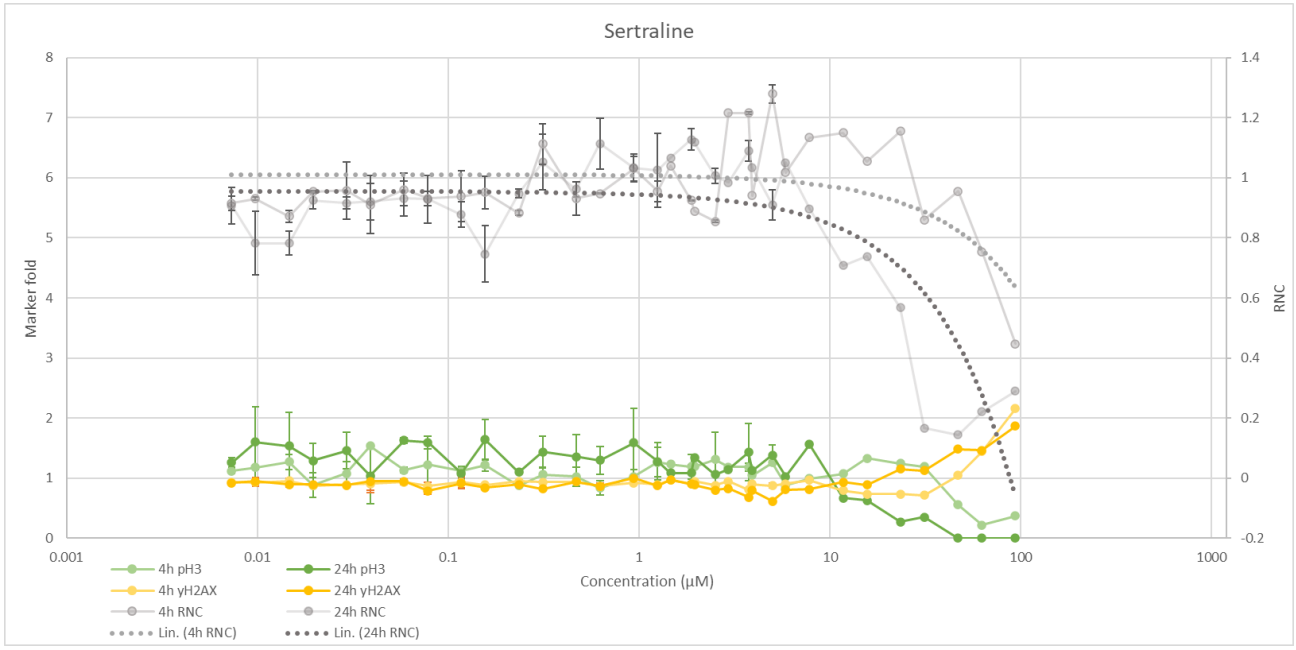
Sertraline
Marker fold
RNC
Concentration (µM)
0.001
0.01
0.1
1
10
100
1000
4h pH3
24h pH3
4h γH2AX
24h γH2AX
4h RNC
24h RNC
Lin. (4h RNC)
Lin. (24h RNC)

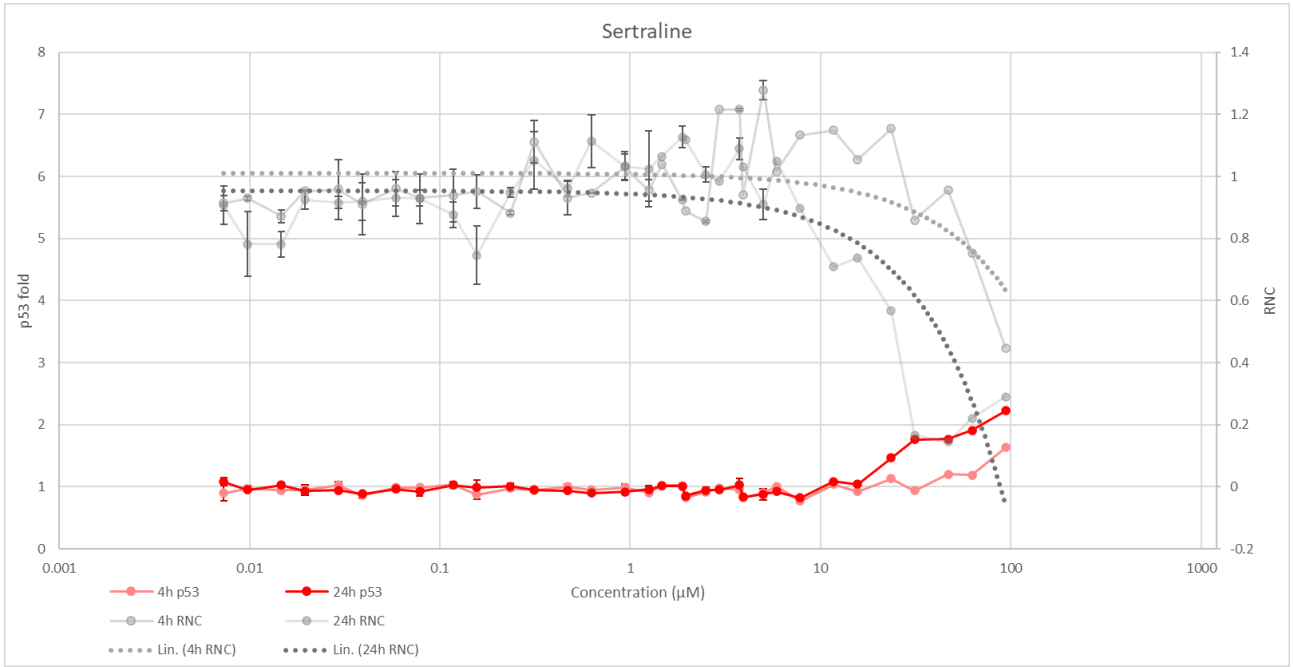
Sertraline
p53 fold
RNC
Concentration (µM)
0.001
0.01
0.1
1
10
100
1000
4h p53
24h p53
4h RNC
24h RNC
Lin. (4h RNC)
Lin. (24h RNC)

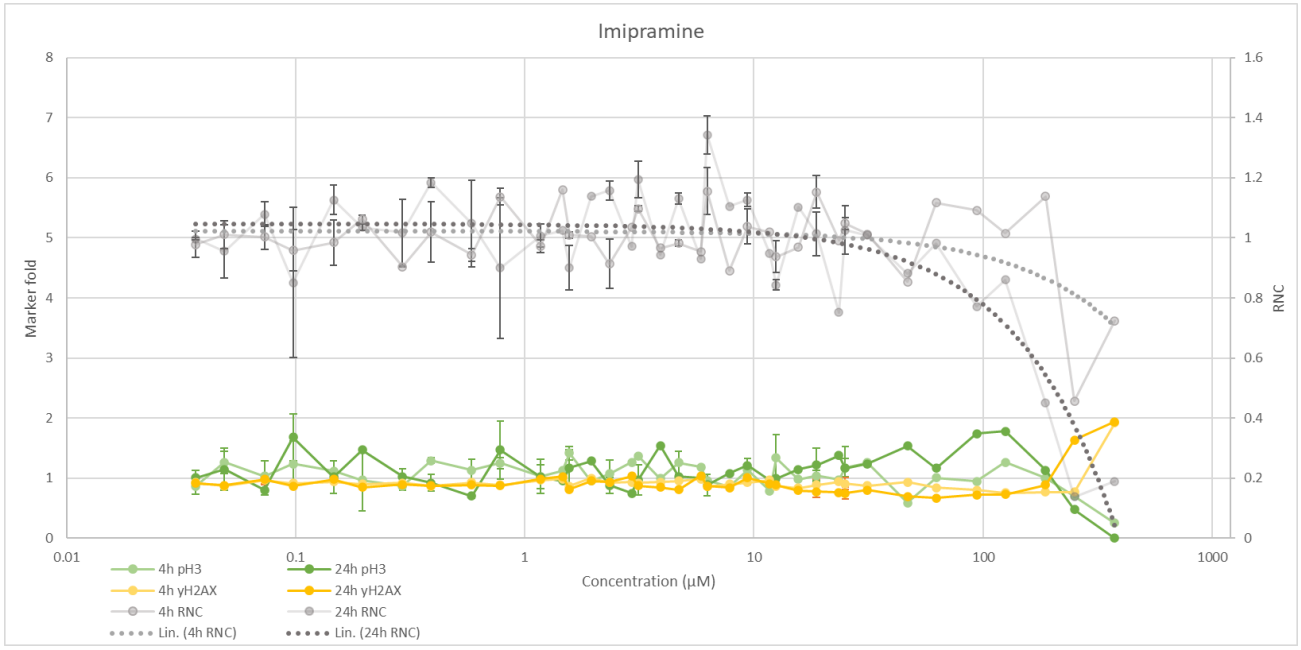
Imipramine
Marker fold
RNC
Concentration (µM)
0.01
0.1
1
10
100
1000
4h pH3
24h pH3
4h γH2AX
24h γH2AX
4h RNC
24h RNC
Lin. (4h RNC)
Lin. (24h RNC)

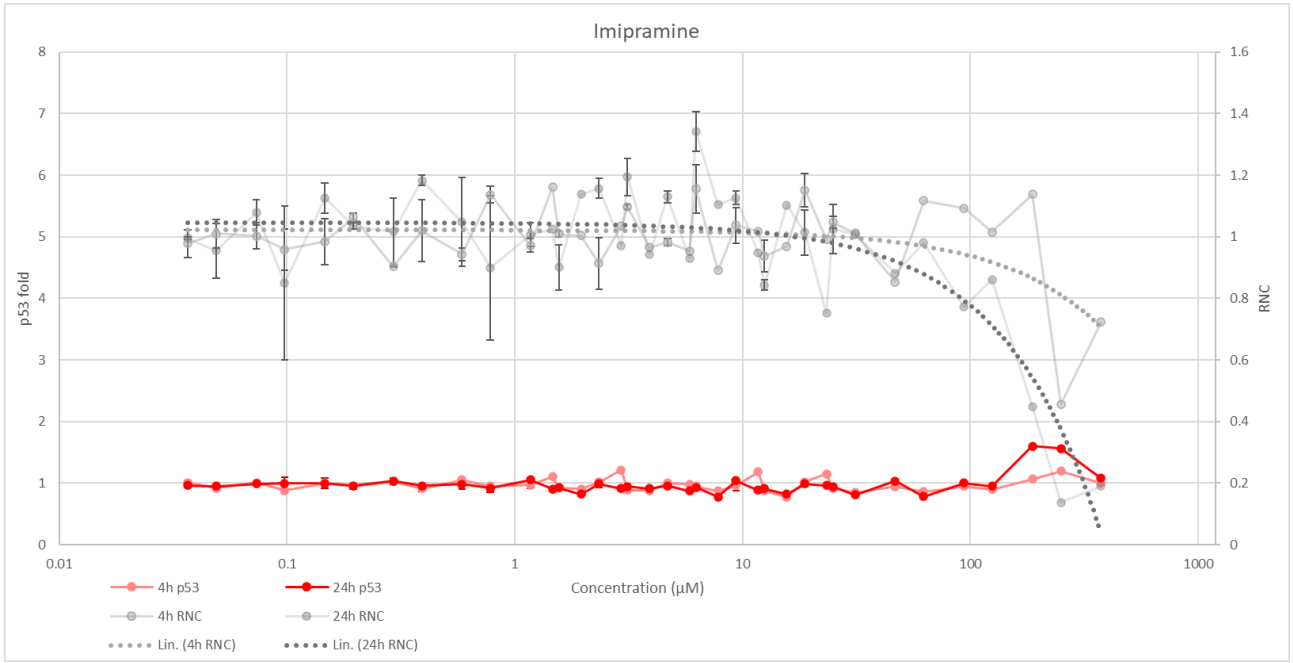
Imipramine
p53 fold
RNC
Concentration (µM)
0.01
0.1
1
10
100
1000
4h p53
24h p53
4h RNC
24h RNC
Lin. (4h RNC)
Lin. (24h RNC)

APPENDIX B

Expression of genotoxicity markers yH2AX, pH3 and p53 in HepG2 cells presented as folds to negative controls. The markekrs for yH2AX and pH3 are presented together with the RNC in one graph, with the scale for the markers on the y-axis on the left-hand side and the scale for RNC on the right-hand side. The green lines represent pH3-folds, the orange lines yH2AX-folds and the grey lines the RNC. Likewise, the marker for p53 and the RNC are shown on the other seprate graph with the same logic and p53-folds as red lines. The concnentration series is presented in µM as a logarithmic scale on the x-axis. The three same-coloured lines represent the three different timepoints measured, after a 4-hour incubation, a 24-hour incubation and a 48-hour incubation. The values presented are the median of all measured values for the same compound at the same concentration. The error bars represent the median absolute deviation (MAD). Results for each compound used in this study is shown on separate pages.

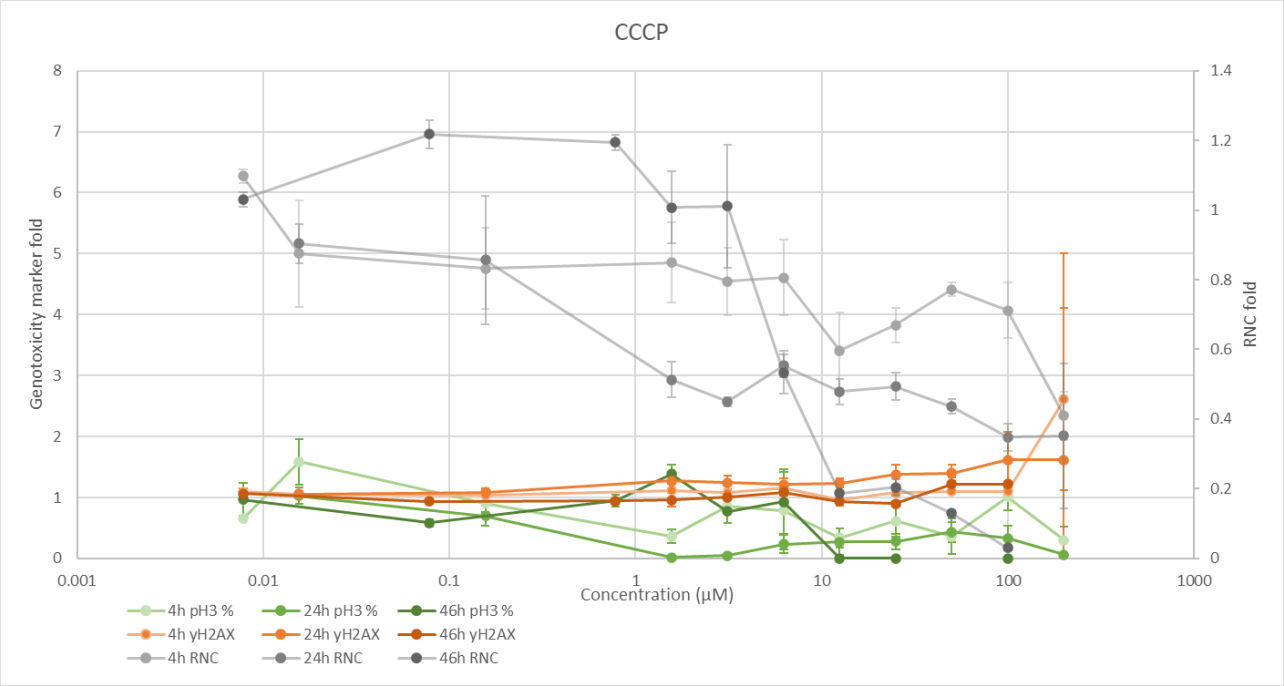
CCCP
Genotoxicity marker fold
RNC fold
Concentration (µM)
0.001
0.01
0.1
1
10
100
1000
4h pH3 %
24h pH3 %
46h pH3 %
4h γH2AX
24h γH2AX
46h γH2AX
4h RNC
24h RNC
46h RNC

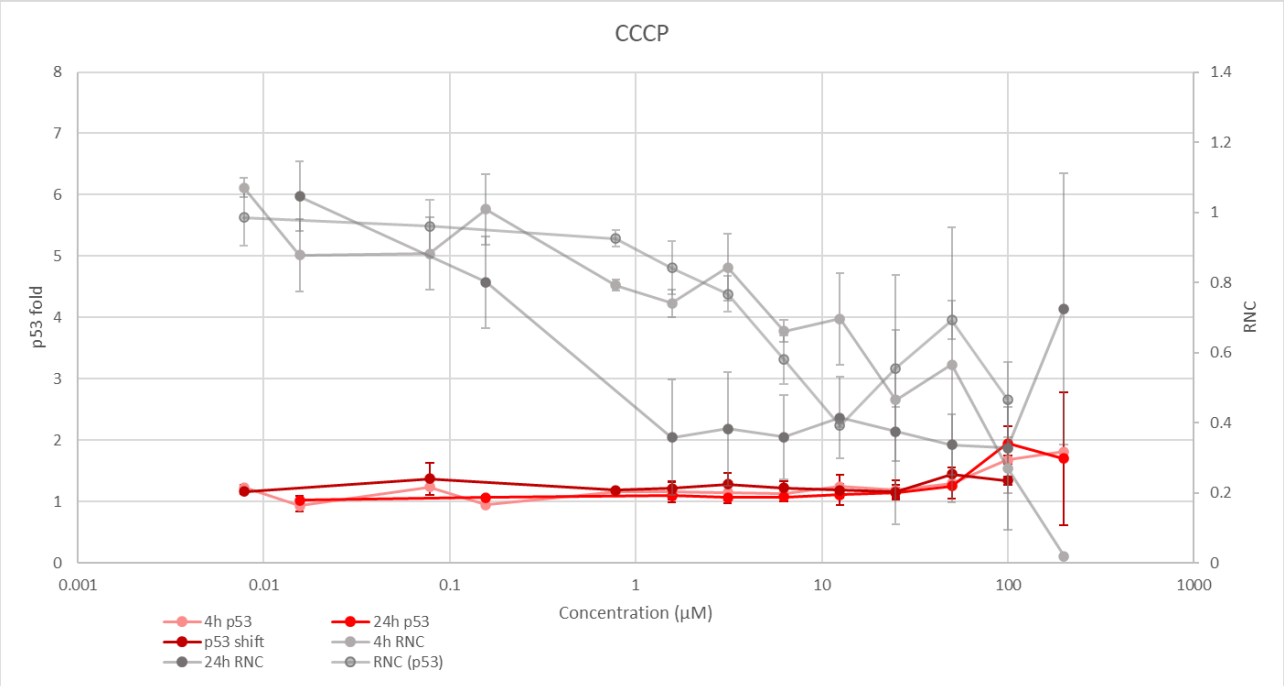
CCCP
p53 fold
RNC
Concentration (µM)
0.001
0.01
0.1
1
10
100
1000
4h p53
24h p53
p53 shift
4h RNC
24h RNC
RNC (p53)

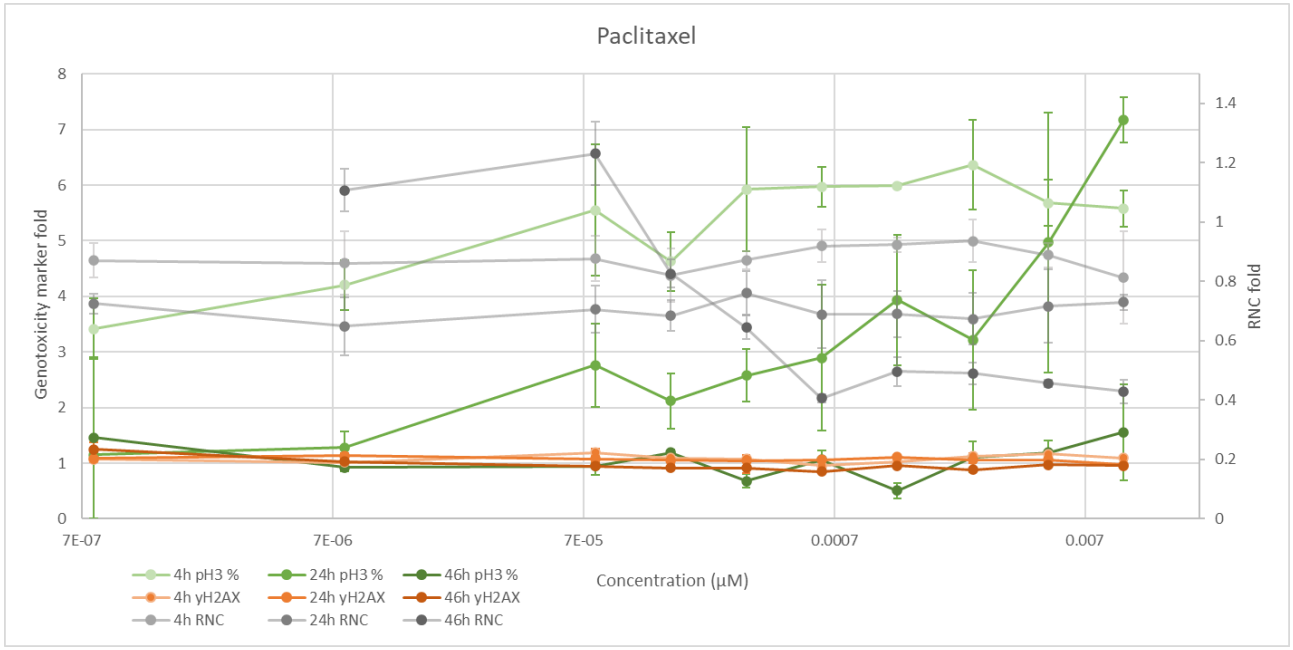
Paclitaxel
Genotoxicity marker fold
RNC fold
Concentration (µM)
7E-07
7E-06
7E-05
0.0007
0.007
4h pH3 %
24h pH3 %
46h pH3 %
4h γH2AX
24h γH2AX
46h γH2AX
4h RNC
24h RNC
46h RNC

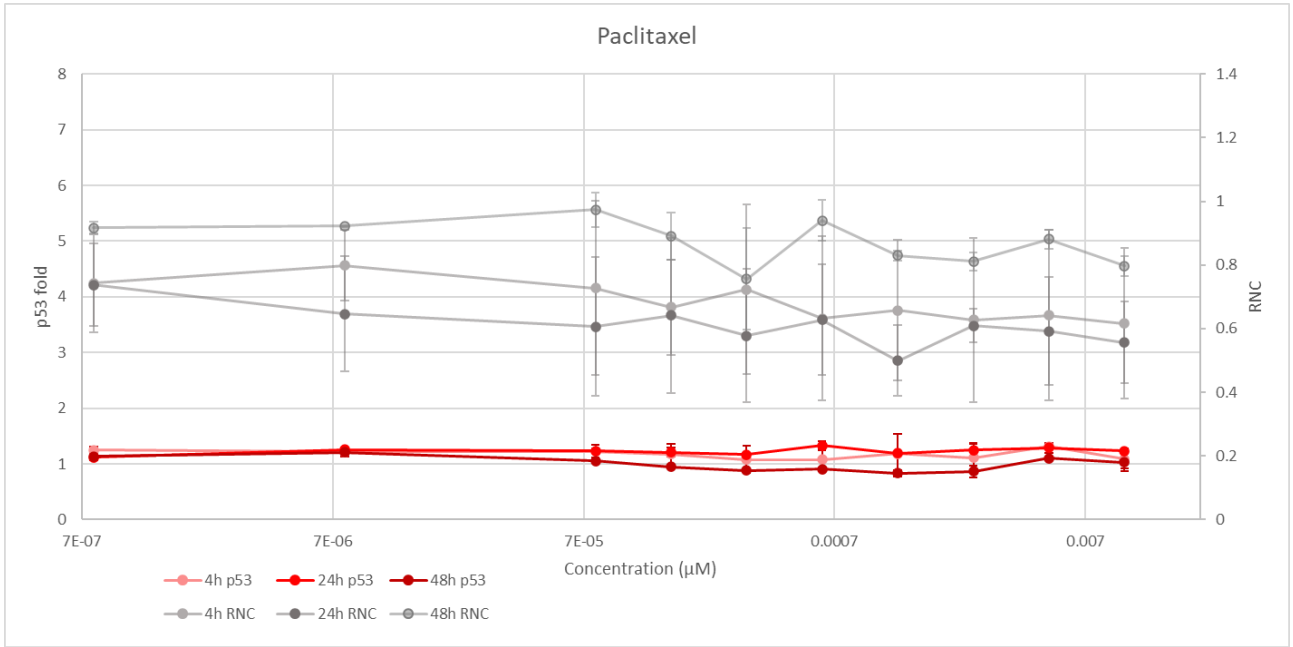
Paclitaxel
p53 fold
RNC
Concentration (µM)
7E-07
7E-06
7E-05
0.0007
0.007
4h p53
24h p53
48h p53
4h RNC
24h RNC
48h RNC

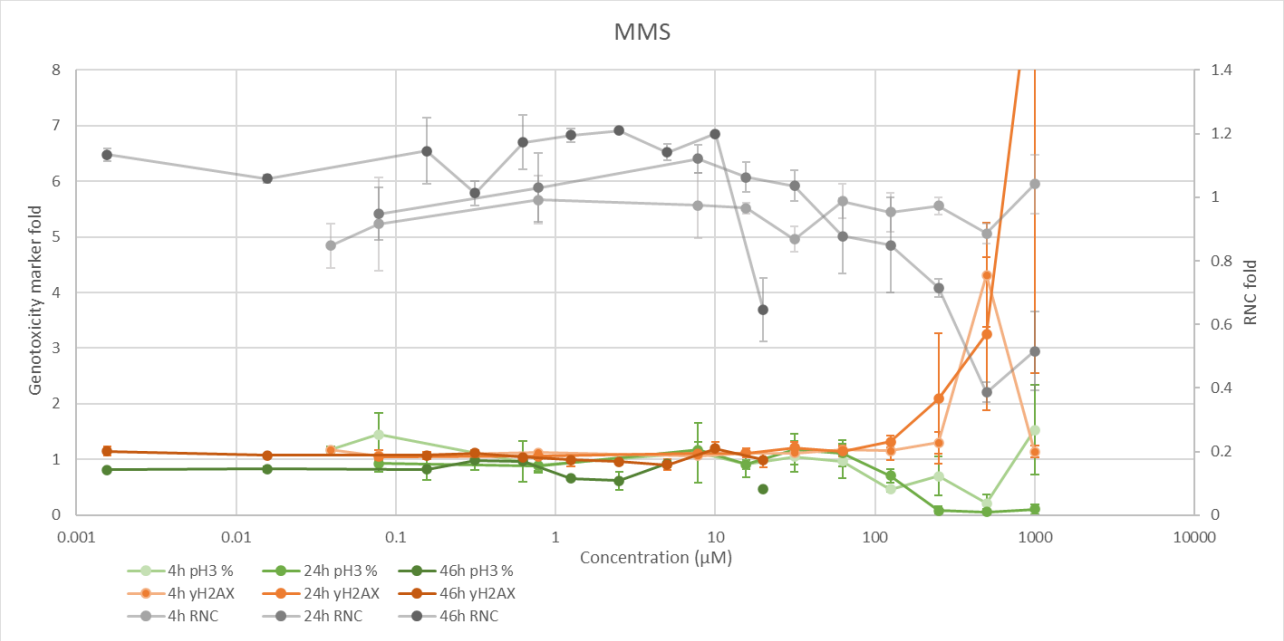
MMS
Genotoxicity marker fold
RNC fold
Concentration (µM)
0.001
0.01
0.1
1
10
100
1000
10000
4h pH3 %
24h pH3 %
46h pH3 %
4h γH2AX
24h γH2AX
46h γH2AX
4h RNC
24h RNC
46h RNC

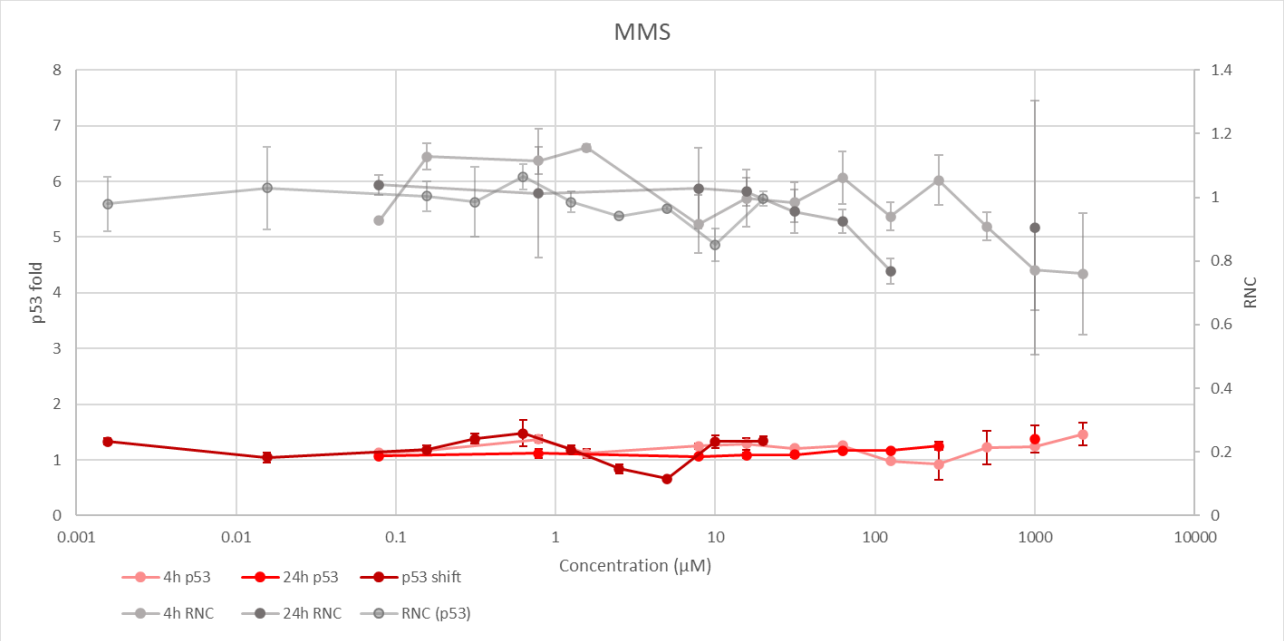
MMS
p53 fold
RNC
Concentration (µM)
0.001
0.01
0.1
1
10
100
1000
10000
4h p53
24h p53
p53 shift
4h RNC
24h RNC
RNC (p53)

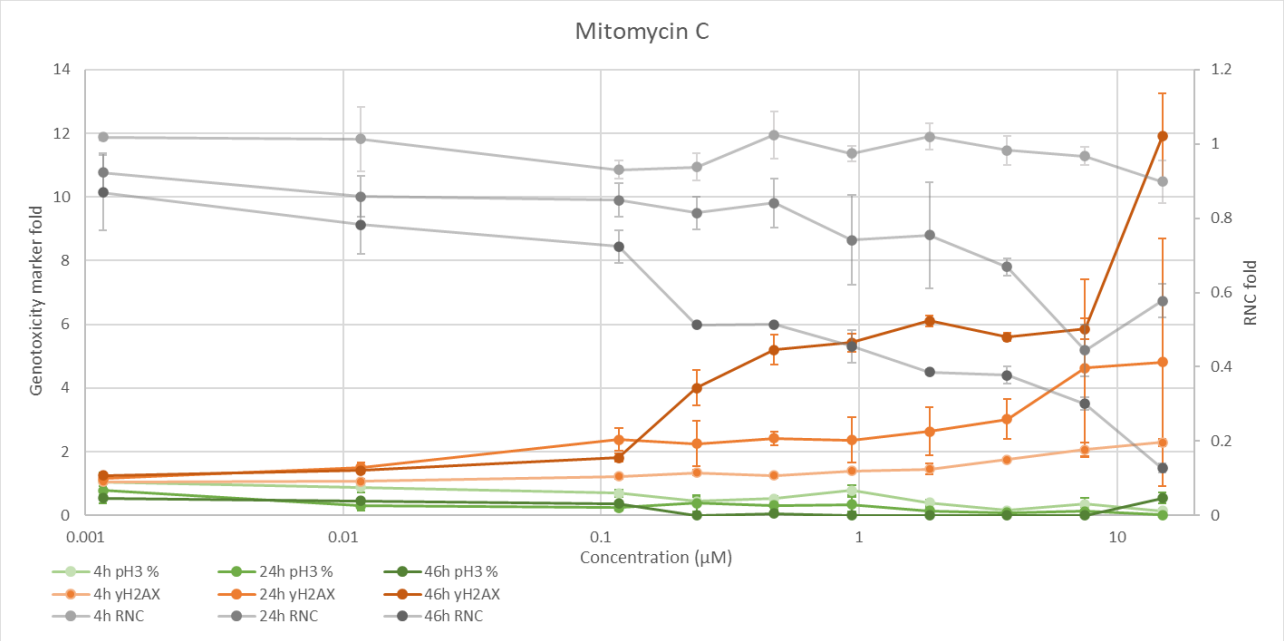
Mitomycin C
Genotoxicity marker fold
RNC fold
Concentration (µM)
0.001
0.01
0.1
1
10
4h pH3 %
24h pH3 %
46h pH3 %
4h yH2AX
24h yH2AX
46h yH2AX
4h RNC
24h RNC
46h RNC

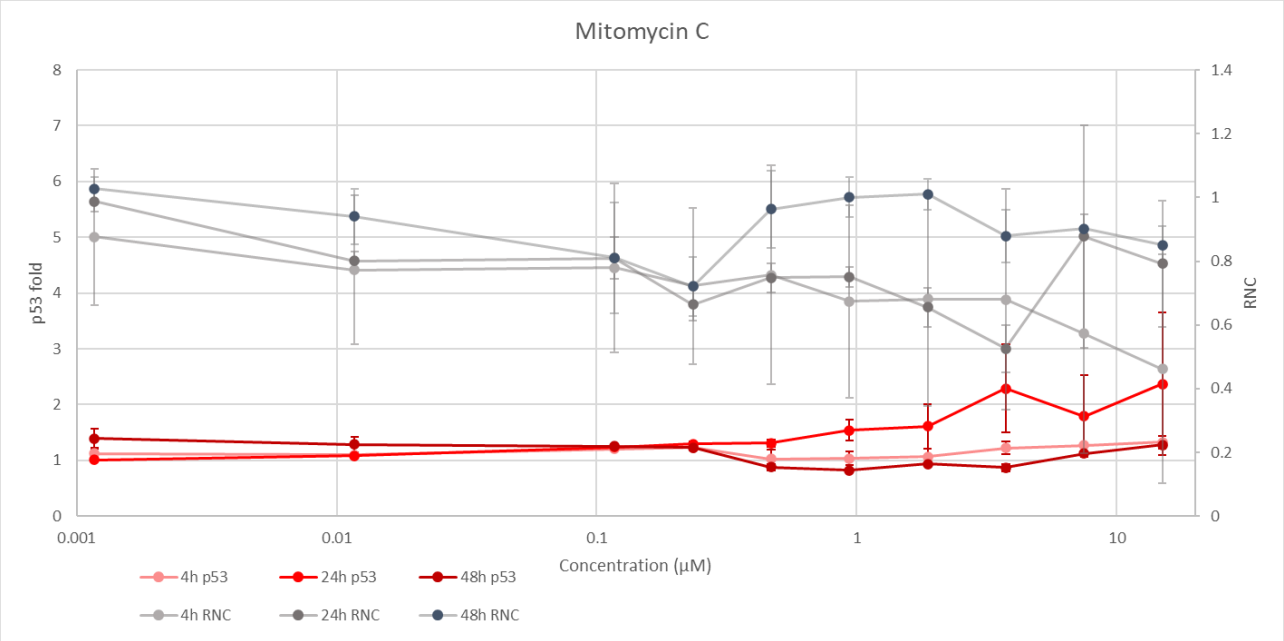
Mitomycin C
p53 fold
RNC
Concentration (µM)
0.001
0.01
0.1
1
10
4h p53
24h p53
48h p53
4h RNC
24h RNC
48h RNC

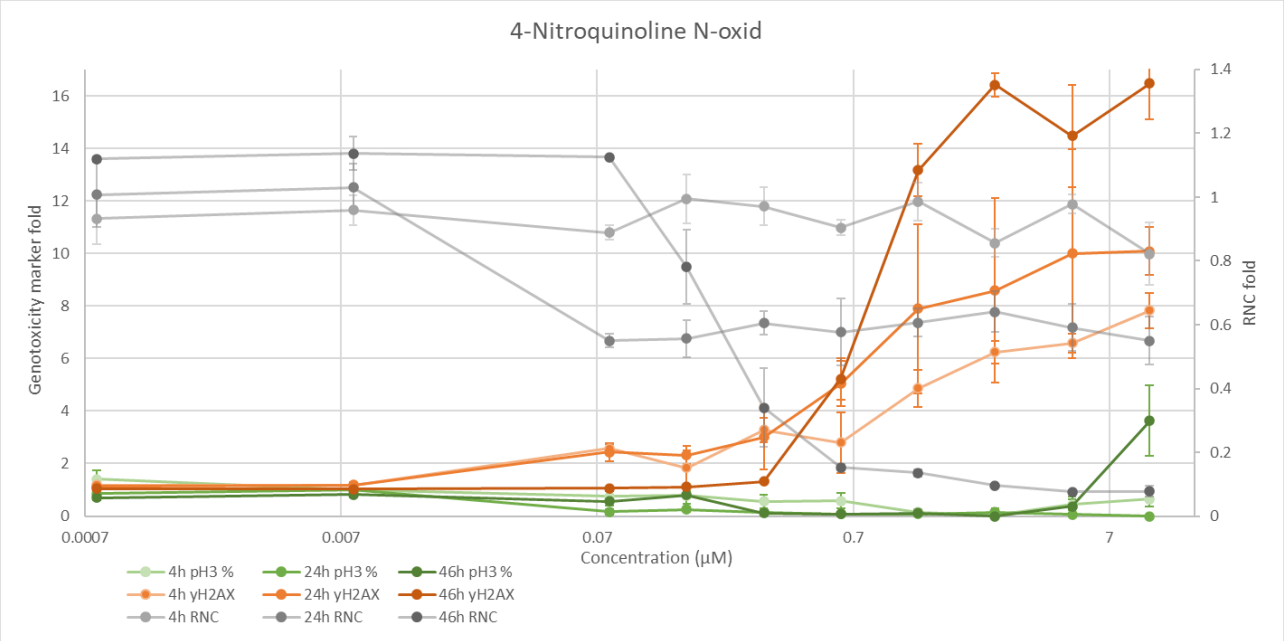
4-Nitroquinoline N-oxid
Genotoxicity marker fold
RNC fold
Concentration (µM)
0.0007
0.007
0.07
0.7
7
4h pH3 %
24h pH3 %
46h pH3 %
4h γH2AX
24h γH2AX
46h γH2AX
4h RNC
24h RNC
46h RNC

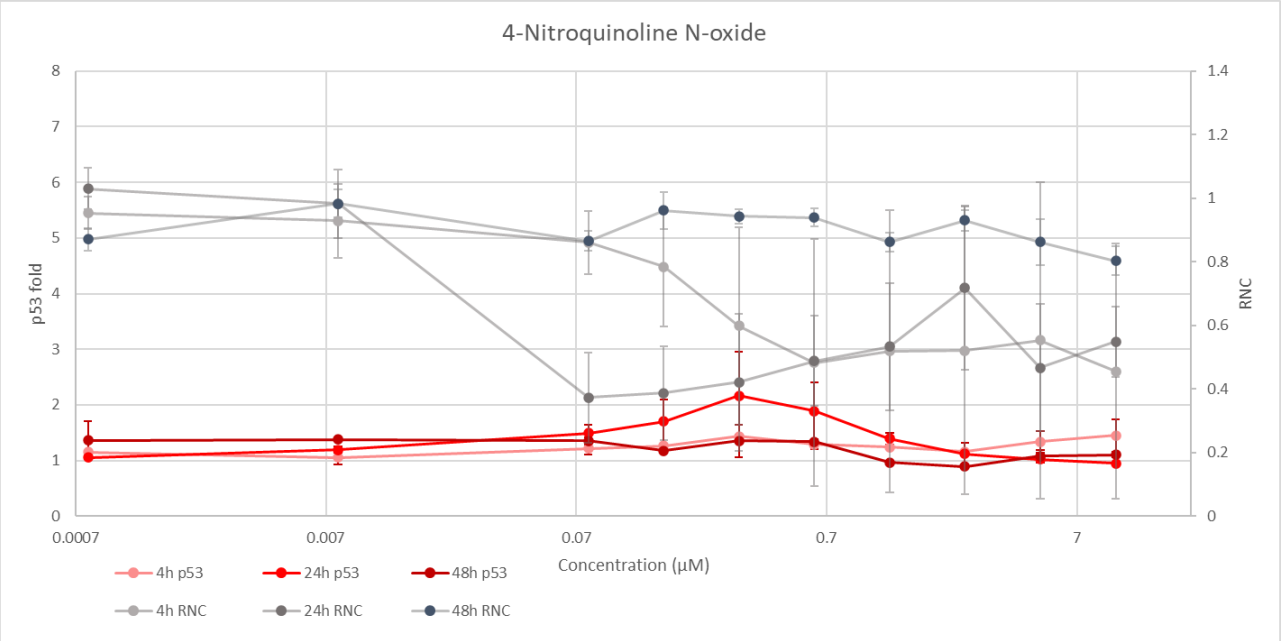
4-Nitroquinoline N-oxide
p53 fold
RNC
Concentration (µM)
0.0007
0.007
0.07
0.7
7
4h p53
24h p53
48h p53
4h RNC
24h RNC
48h RNC

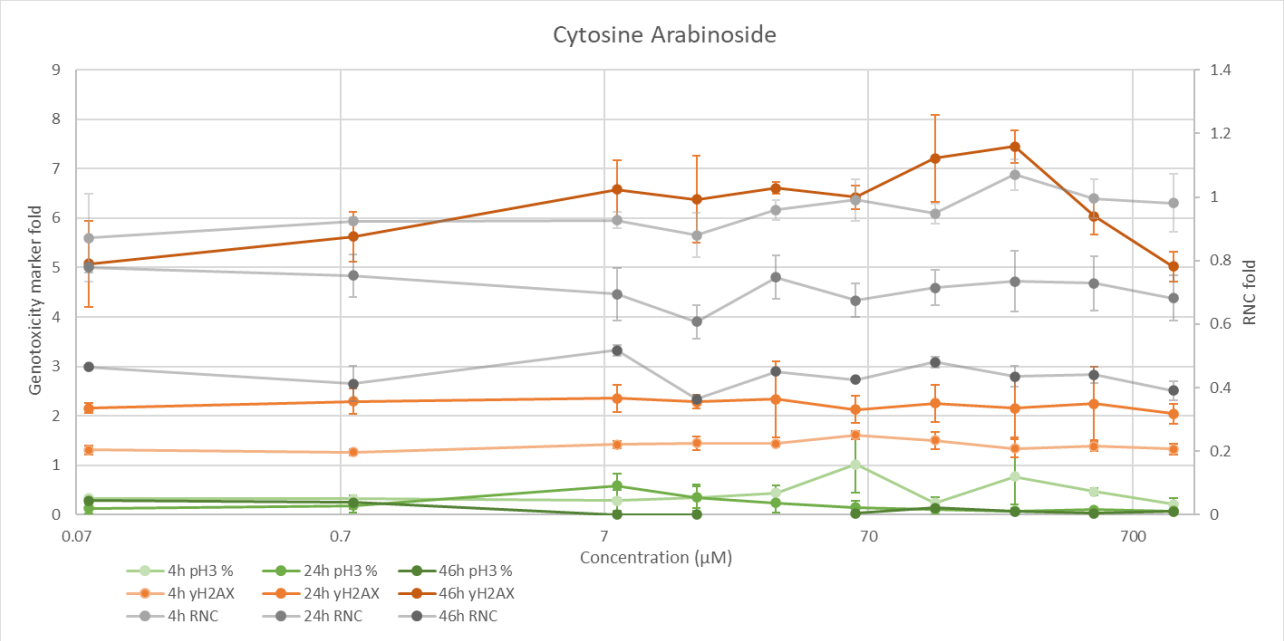
Cytosine Arabinoside
Genotoxicity marker fold
RNC fold
Concentration (µM)
0.07
0.7
7
70
700
4h pH3 %
24h pH3 %
46h pH3 %
4h γH2AX
24h γH2AX
46h γH2AX
4h RNC
24h RNC
46h RNC

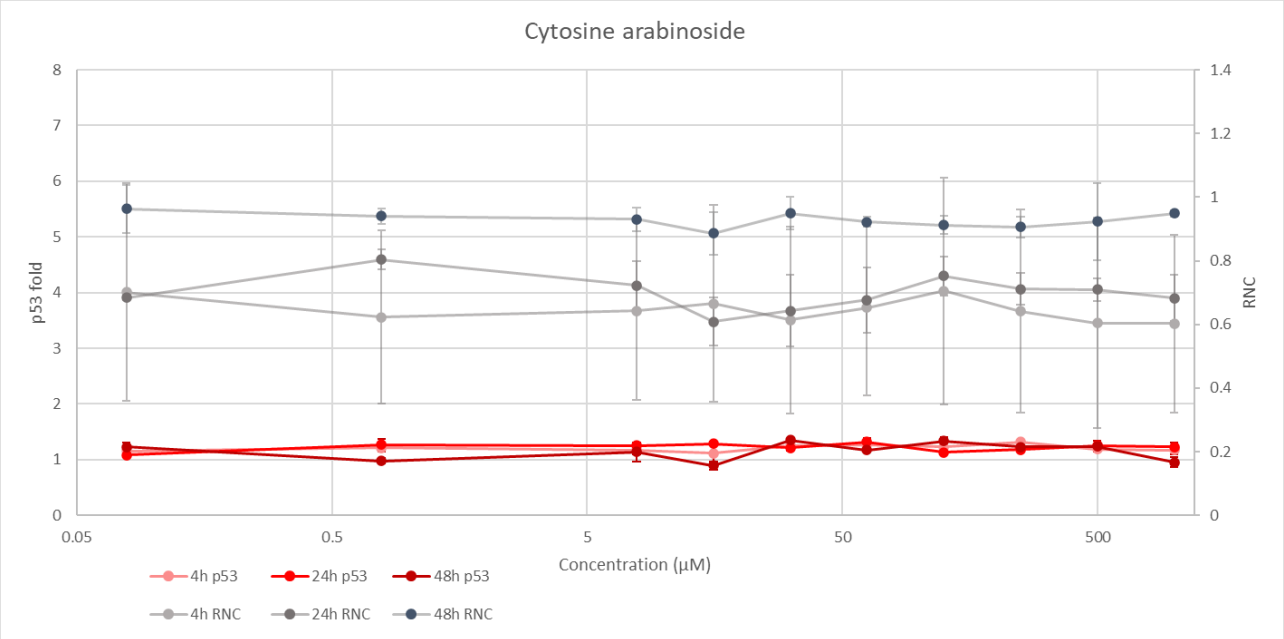
Cytosine arabinoside
p53 fold
RNC
Concentration (µM)
0.05
0.5
5
50
500
4h p53
24h p53
48h p53
4h RNC
24h RNC
48h RNC

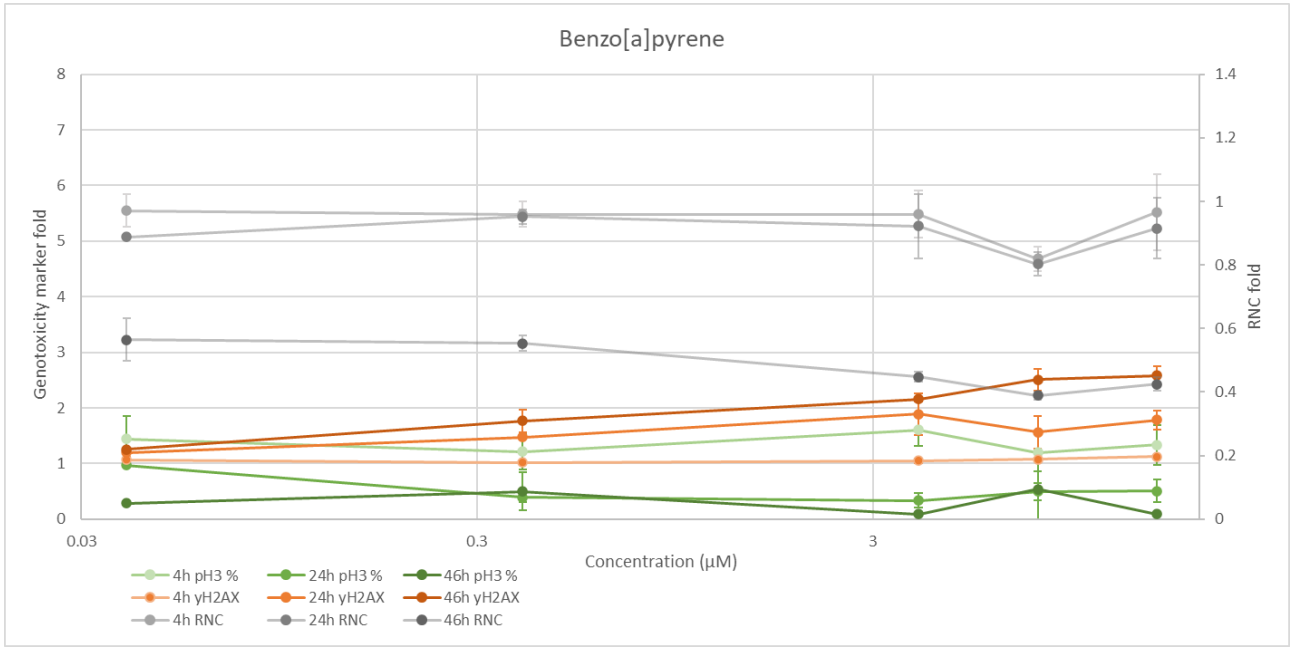
Benzo[a]pyrene
Genotoxicity marker fold
RNC fold
Concentration (µM)
0.03
0.3
3
4h pH3 %
24h pH3 %
46h pH3 %
4h γH2AX
24h γH2AX
46h γH2AX
4h RNC
24h RNC
46h RNC

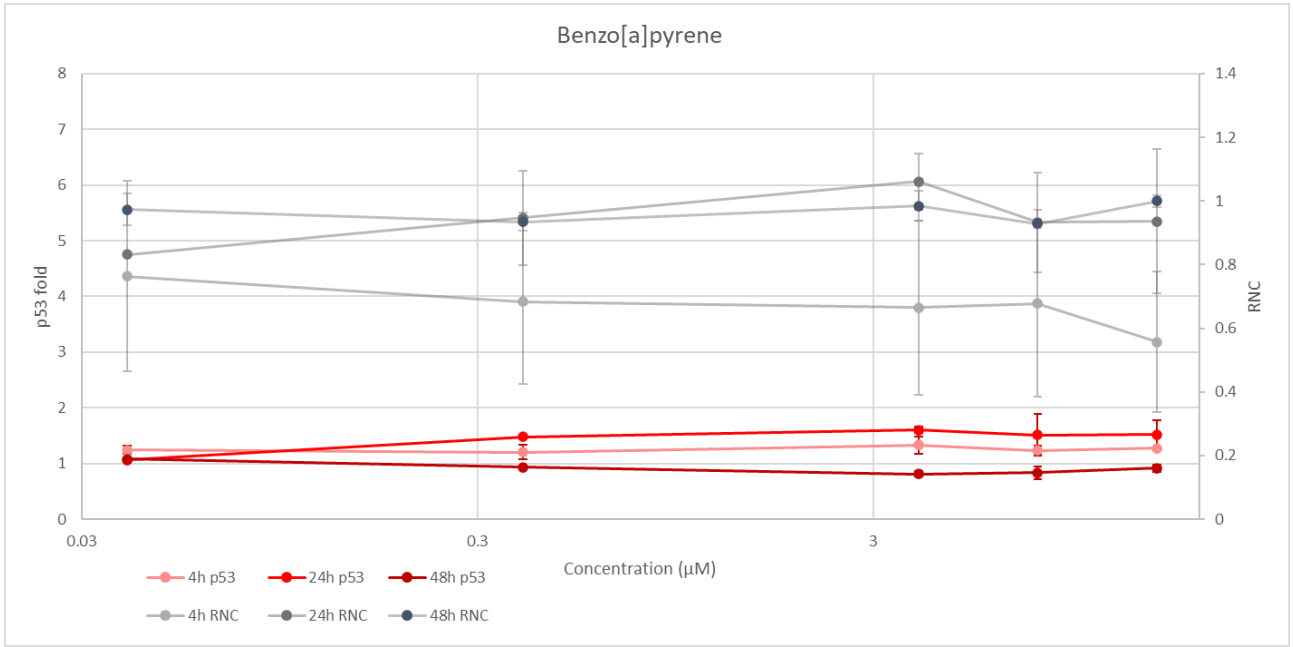
Benzo[a]pyrene
p53 fold
RNC
Concentration (µM)
0.03
0.3
3
4h p53
24h p53
48h p53
4h RNC
24h RNC
48h RNC

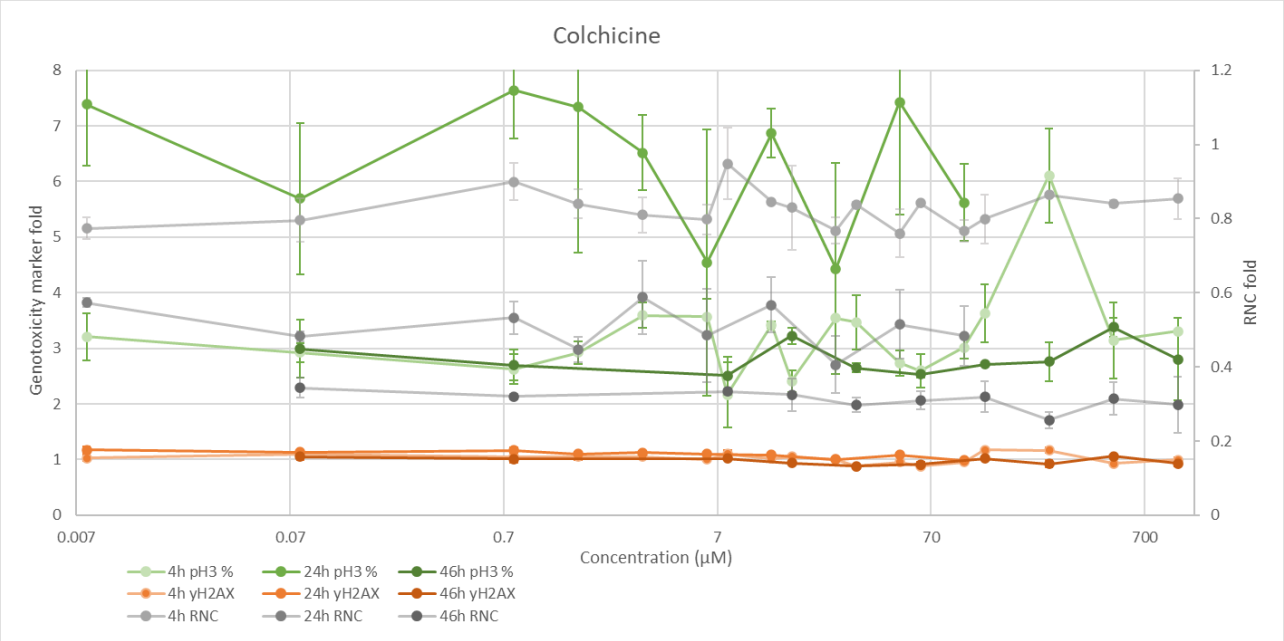
Colchicine
Genotoxicity marker fold
RNC fold
Concentration (µM)
0.007
0.07
0.7
7
70
700
4h pH3 %
24h pH3 %
46h pH3 %
4h γH2AX
24h γH2AX
46h γH2AX
4h RNC
24h RNC
46h RNC

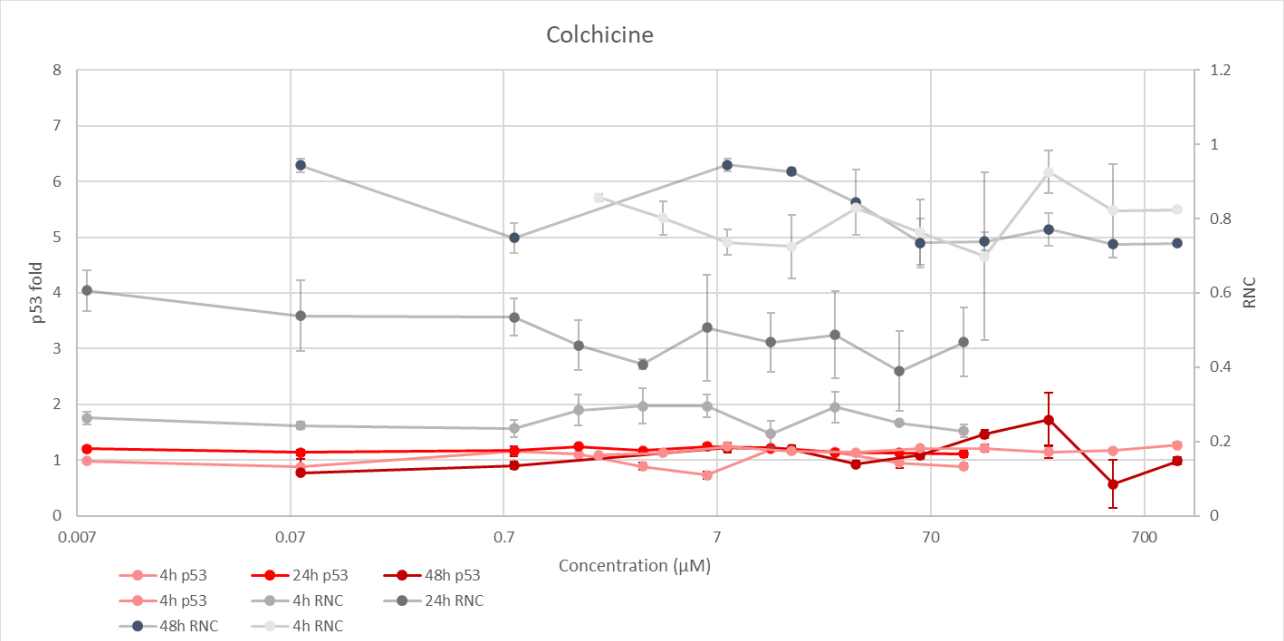
Colchicine
p53 fold
RNC
Concentration (µM)
0.007
0.07
0.7
7
70
700
4h p53
24h p53
48h p53
4h p53
4h RNC
24h RNC
48h RNC
4h RNC

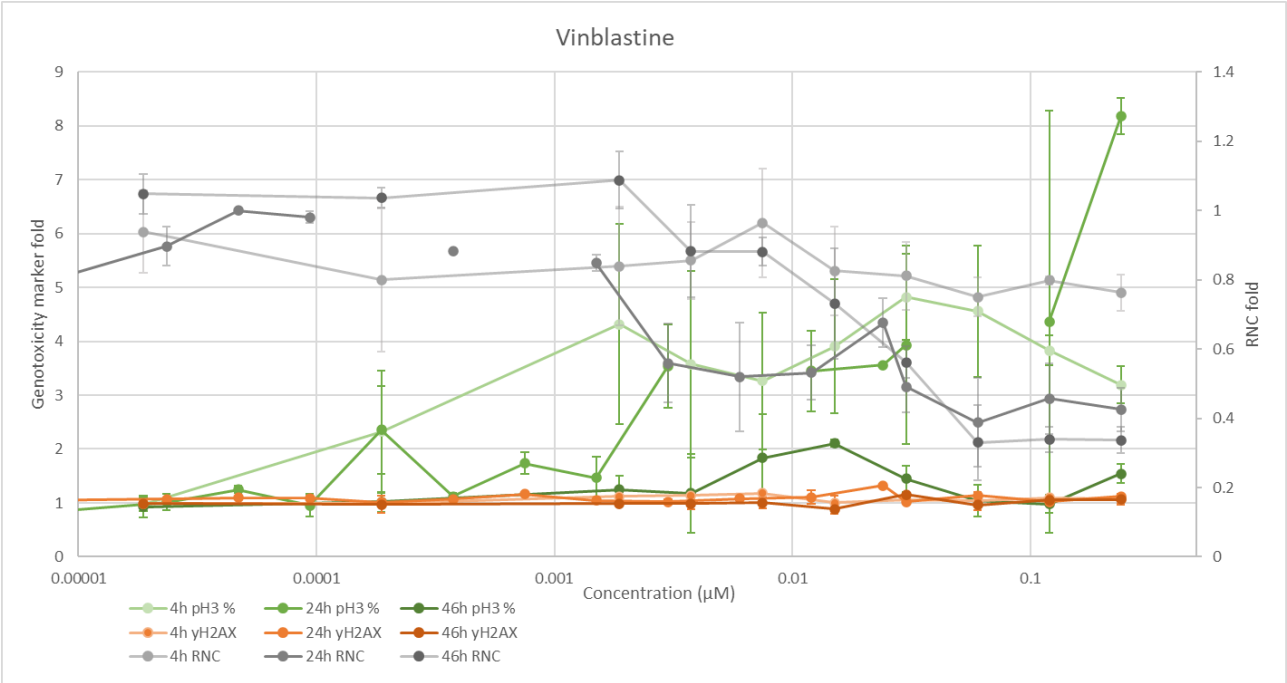
Vinblastine
Genotoxicity marker fold
RNC fold
Concentration (µM)
0.00001
0.0001
0.001
0.01
0.1
4h pH3 %
24h pH3 %
46h pH3 %
4h yH2AX
24h yH2AX
46h yH2AX
4h RNC
24h RNC
46h RNC

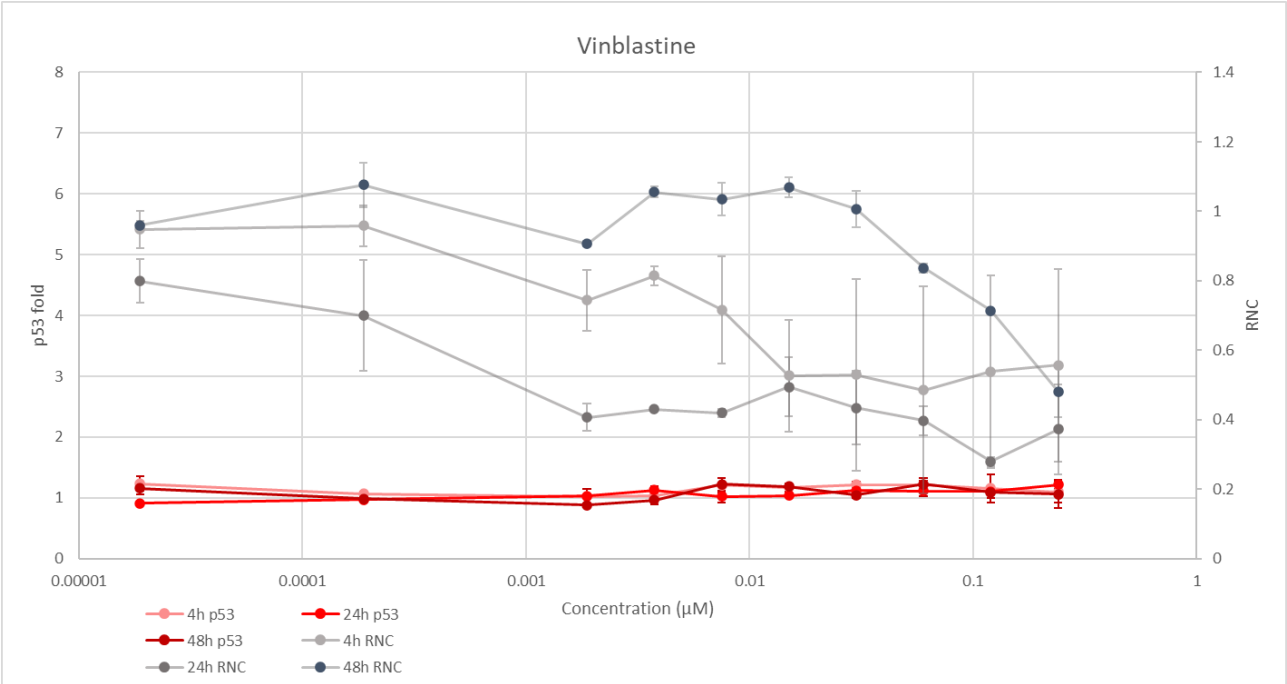
Vinblastine
p53 fold
RNC
Concentration (µM)
0.00001
0.0001
0.001
0.01
0.1
1
4h p53
24h p53
48h p53
4h RNC
24h RNC
48h RNC

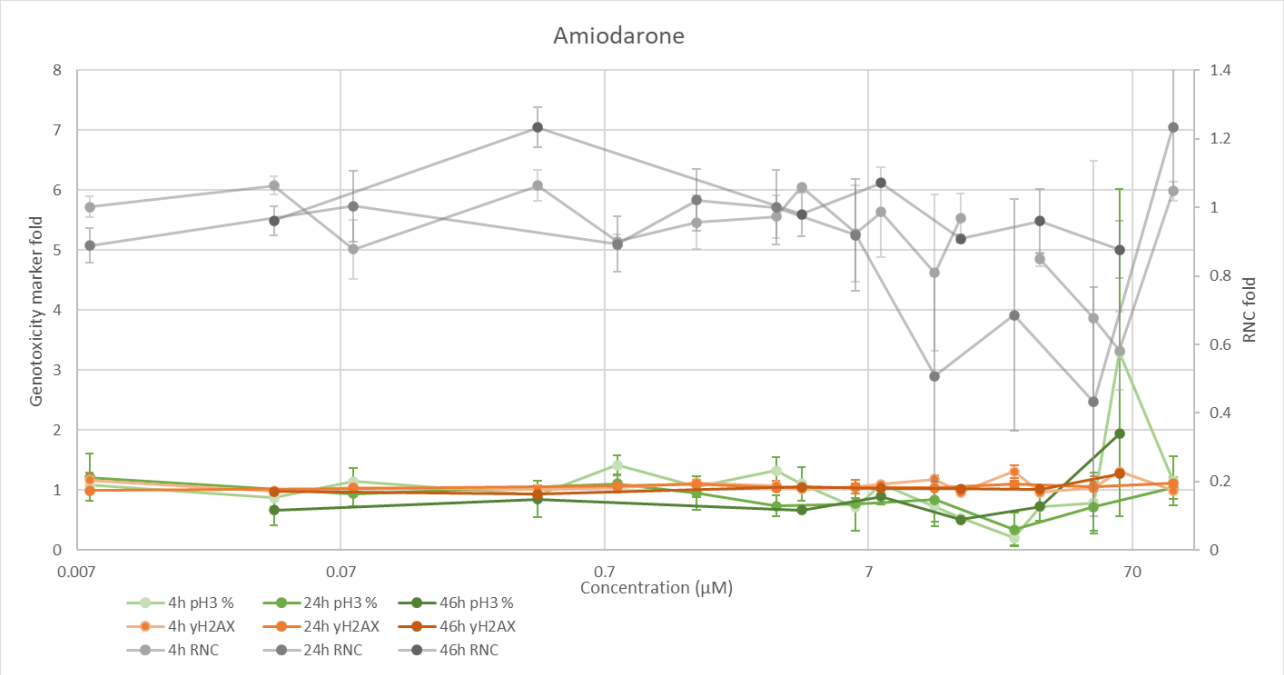
Amiodarone
Genotoxicity marker fold
RNC fold
Concentration (µM)
0.007
0.07
0.7
7
70
4h pH3 %
24h pH3 %
46h pH3 %
4h γH2AX
24h γH2AX
46h γH2AX
4h RNC
24h RNC
46h RNC

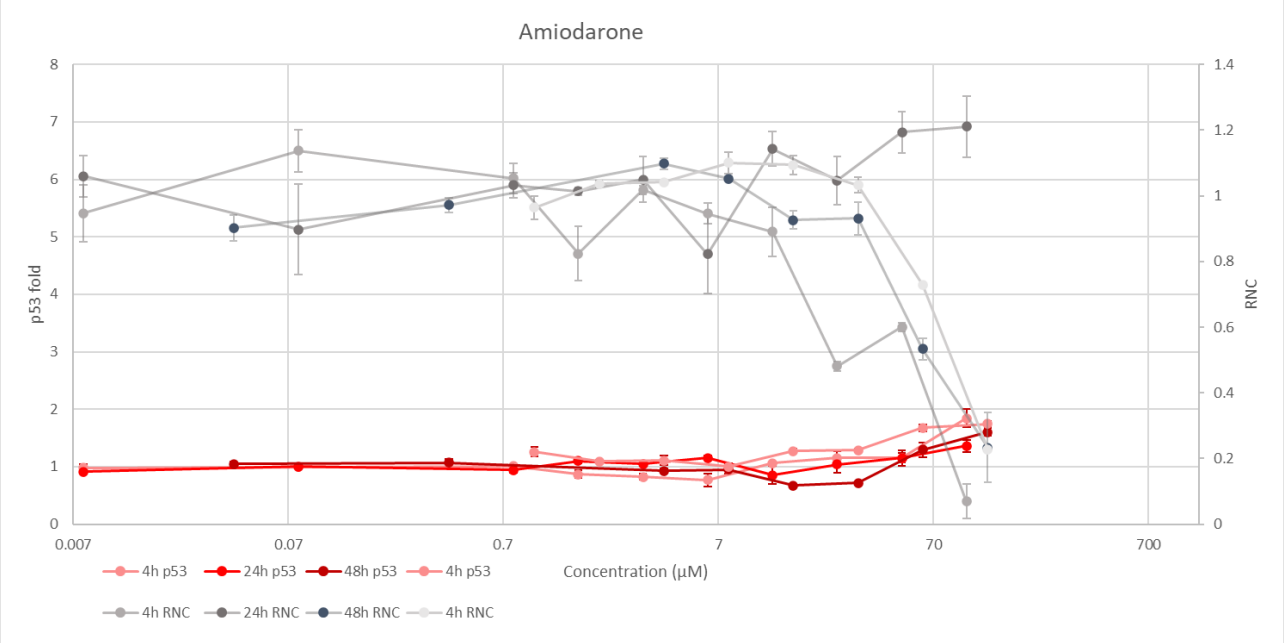
Amiodarone
p53 fold
RNC
Concentration (µM)
0.007
0.07
0.7
7
70
700
4h p53
24h p53
48h p53
4h p53
4h RNC
24h RNC
48h RNC
4h RNC

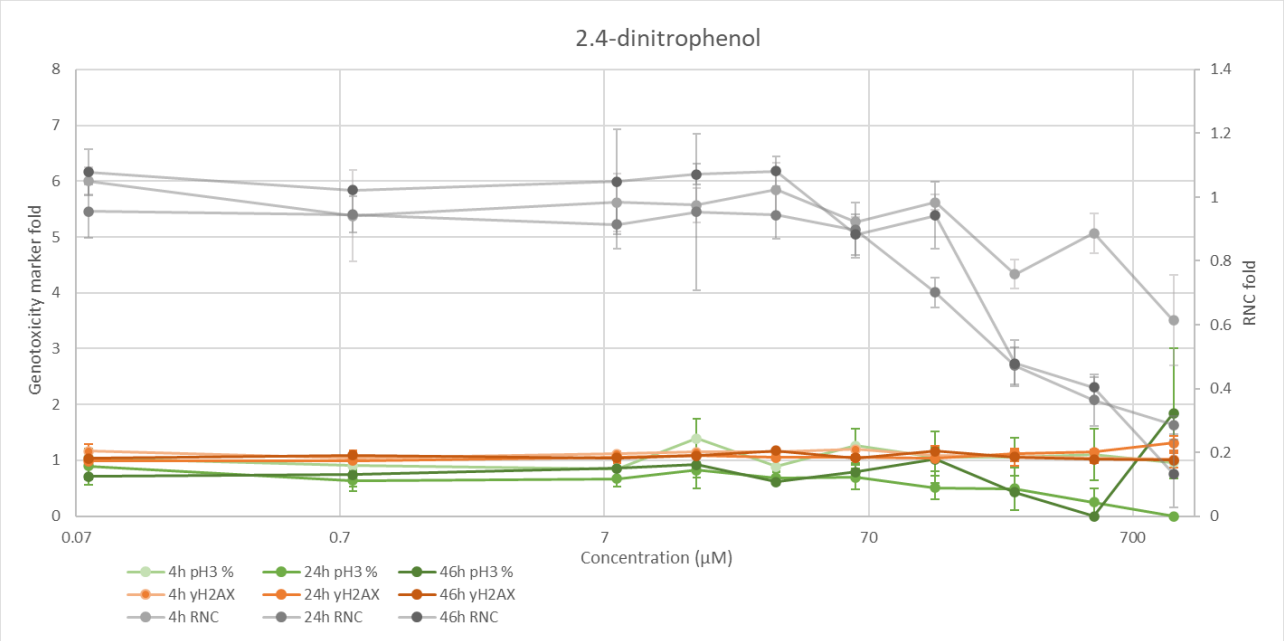
2.4-dinitrophenol
Genotoxicity marker fold
RNC fold
Concentration (µM)
0.07
0.7
7
70
700
4h pH3 %
24h pH3 %
46h pH3 %
4h γH2AX
24h γH2AX
46h γH2AX
4h RNC
24h RNC
46h RNC

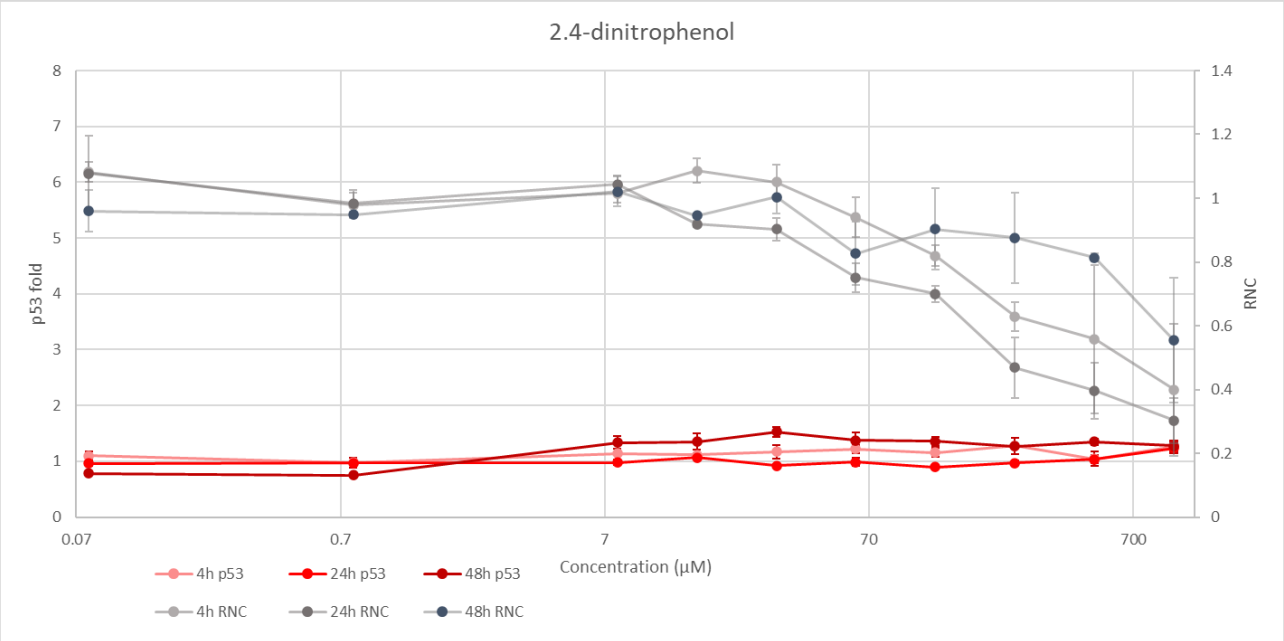
2.4-dinitrophenol
p53 fold
RNC
Concentration (µM)
0.07
0.7
7
70
700
4h p53
24h p53
48h p53
4h RNC
24h RNC
48h RNC

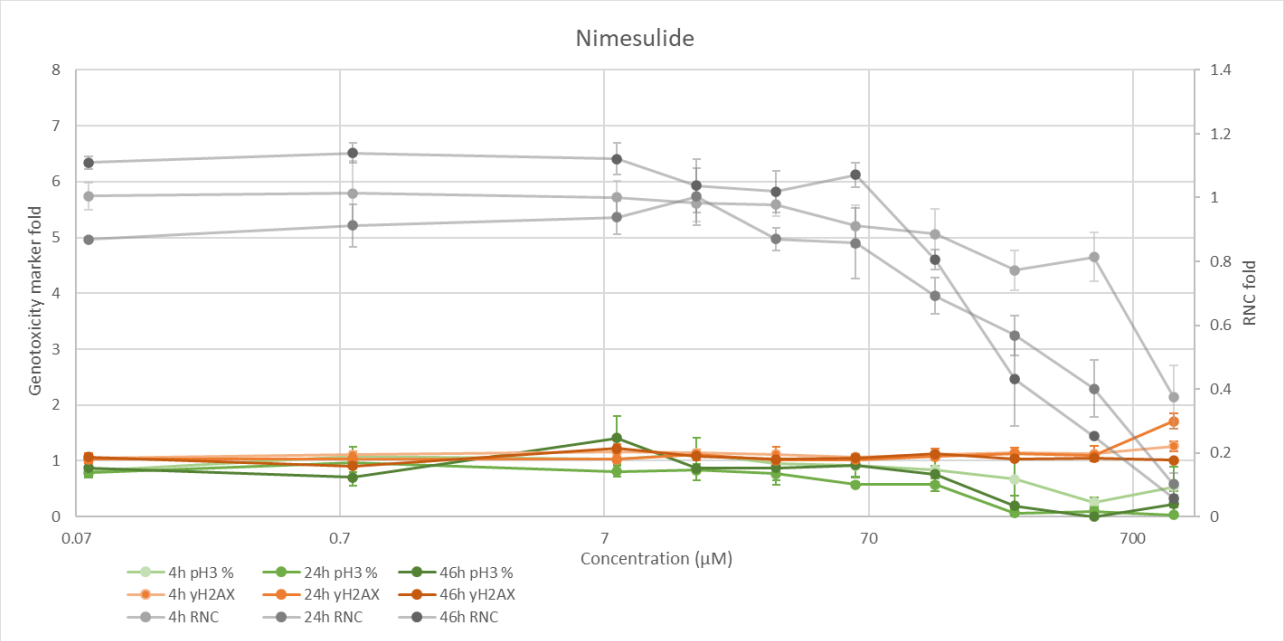
Nimesulide
Genotoxicity marker fold
RNC fold
Concentration (µM)
0.07
0.7
7
70
700
4h pH3 %
24h pH3 %
46h pH3 %
4h γH2AX
24h γH2AX
46h γH2AX
4h RNC
24h RNC
46h RNC

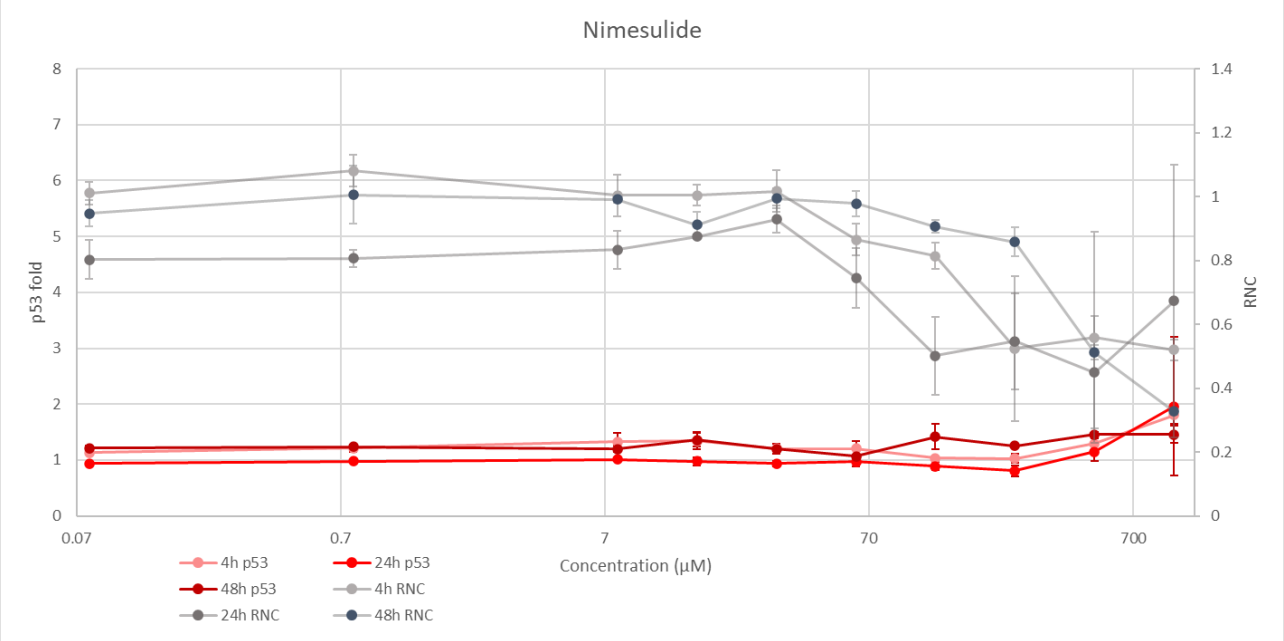
Nimesulide
p53 fold
RNC
Concentration (µM)
0.07
0.7
7
70
700
4h p53
24h p53
48h p53
4h RNC
24h RNC
48h RNC

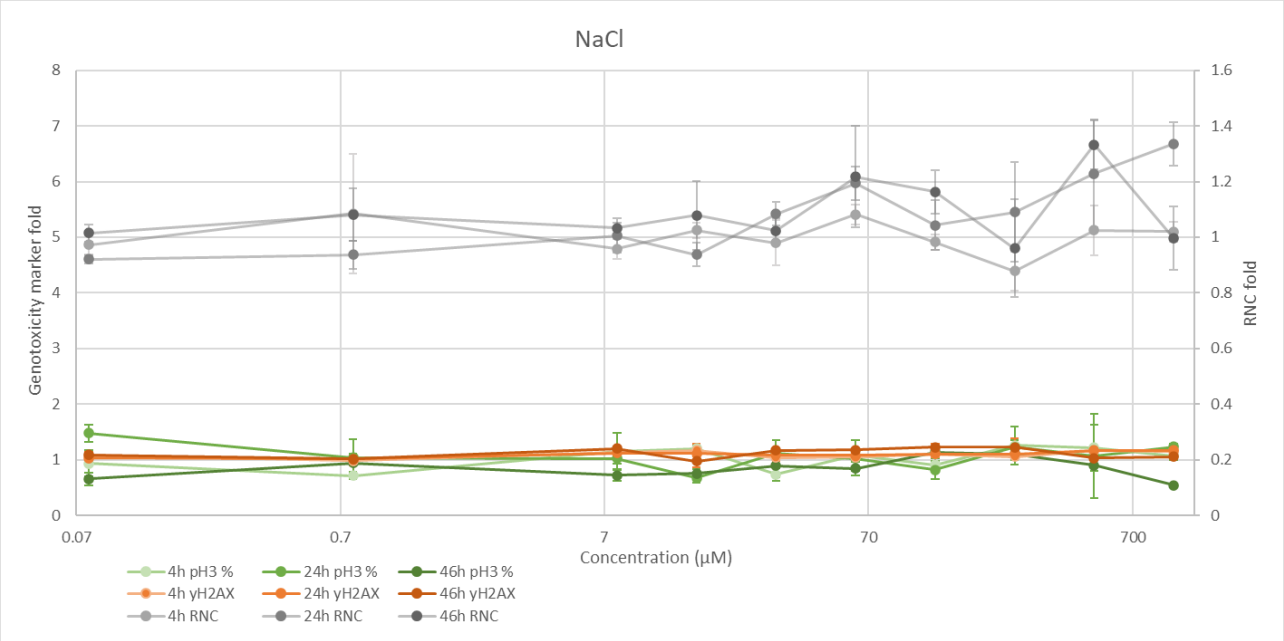
NaCl
Genotoxicity marker fold
RNC fold
Concentration (µM)
0.07
0.7
7
70
700
4h pH3 %
24h pH3 %
46h pH3 %
4h γH2AX
24h γH2AX
46h γH2AX
4h RNC
24h RNC
46h RNC

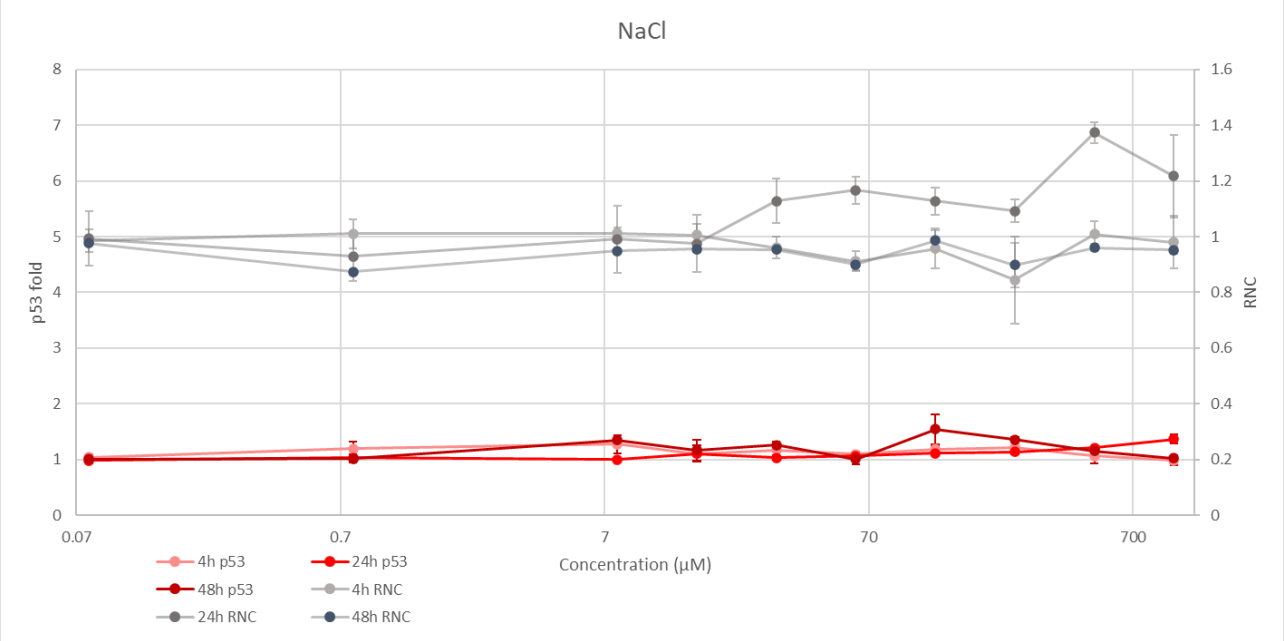
NaCl
p53 fold
RNC
Concentration (µM)
0.07
0.7
7
70
700
4h p53
24h p53
48h p53
4h RNC
24h RNC
48h RNC

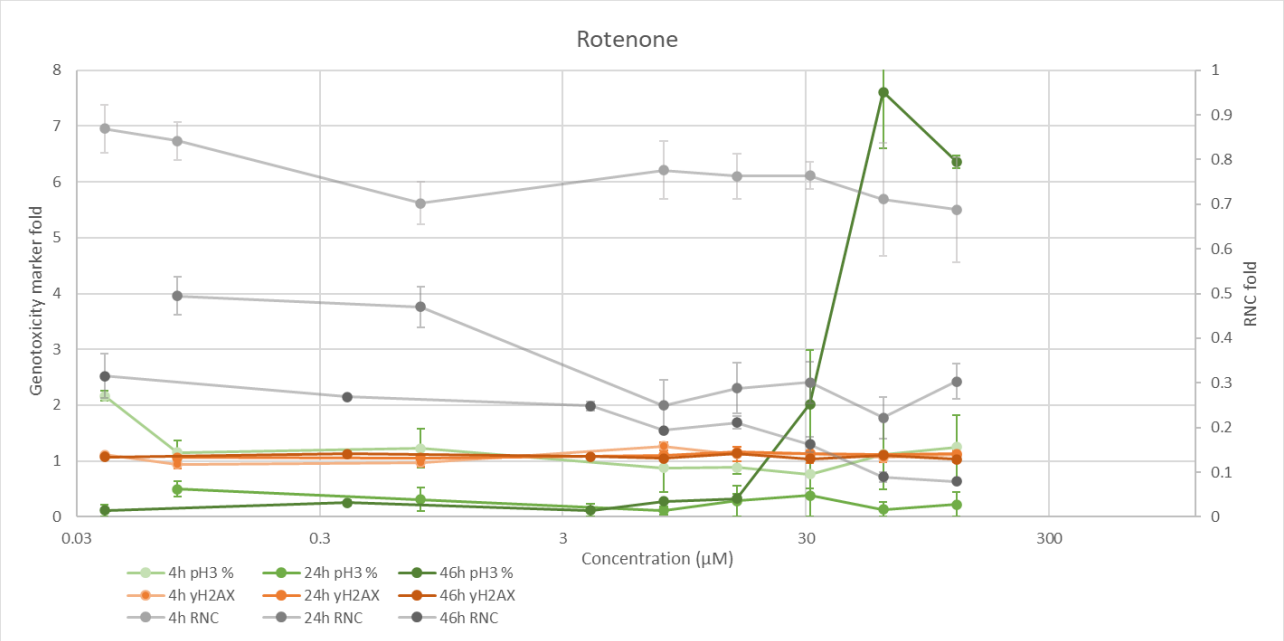
Rotenone
Genotoxicity marker fold
RNC fold
Concentration (µM)
0.03
0.3
3
30
300
4h pH3 %
24h pH3 %
46h pH3 %
4h γH2AX
24h γH2AX
46h γH2AX
4h RNC
24h RNC
46h RNC

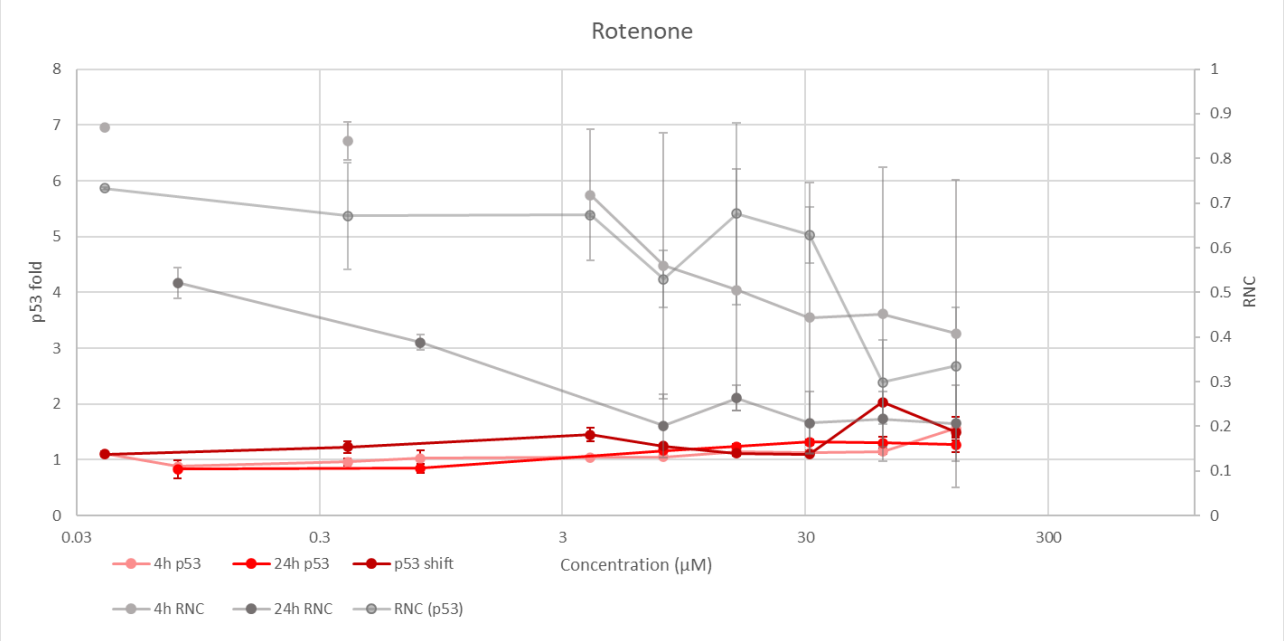
Rotenone
p53 fold
RNC
Concentration (µM)
0.03
0.3
3
30
300
4h p53
24h p53
p53 shift
4h RNC
24h RNC
RNC (p53)

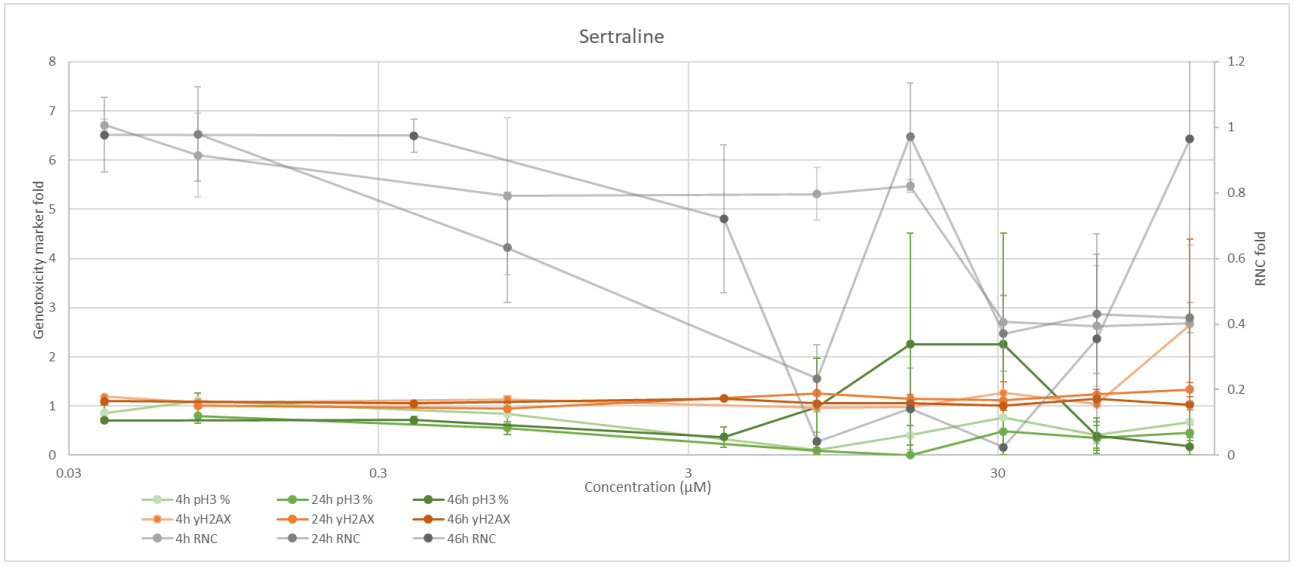
Sertraline
Genotoxicity marker fold
RNC fold
Concentration (µM)
0.03
0.3
3
30
4h pH3 %
24h pH3 %
46h pH3 %
4h γH2AX
24h γH2AX
46h γH2AX
4h RNC
24h RNC
46h RNC

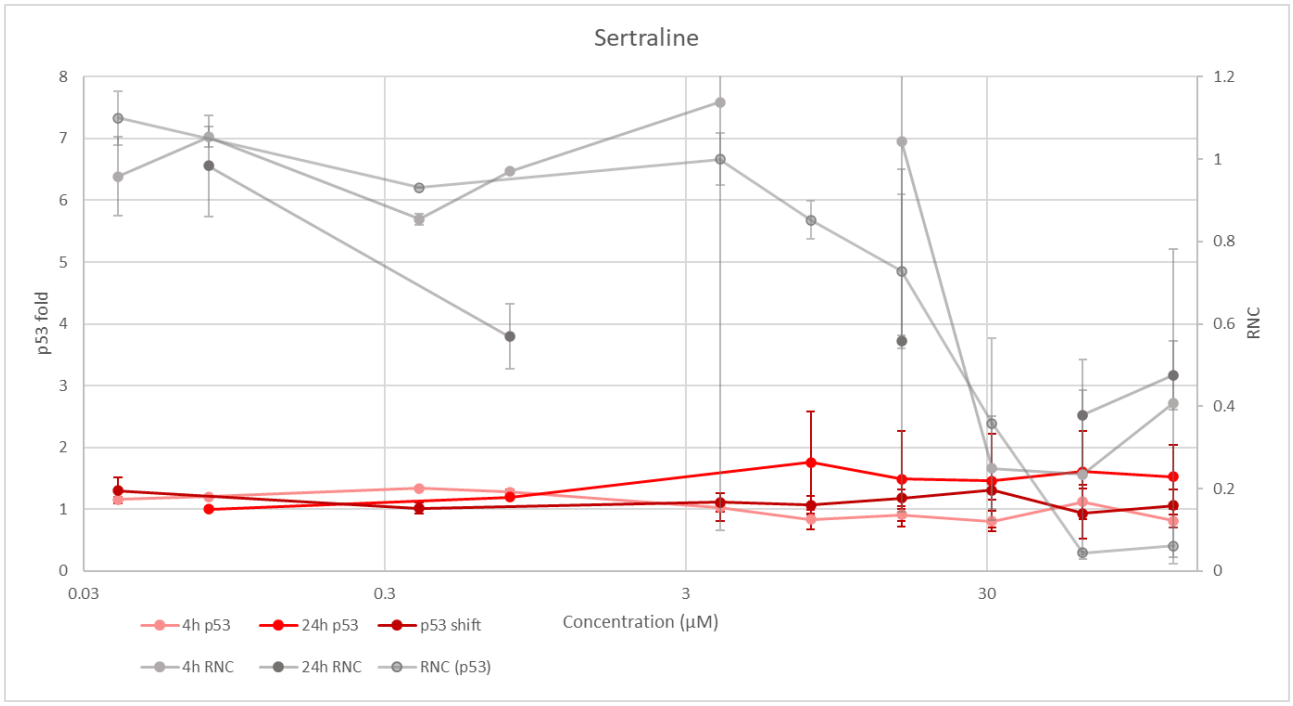
Sertraline
p53 fold
RNC
Concentration (µM)
0.03
0.3
3
30
4h p53
24h p53
p53 shift
4h RNC
24h RNC
RNC (p53)

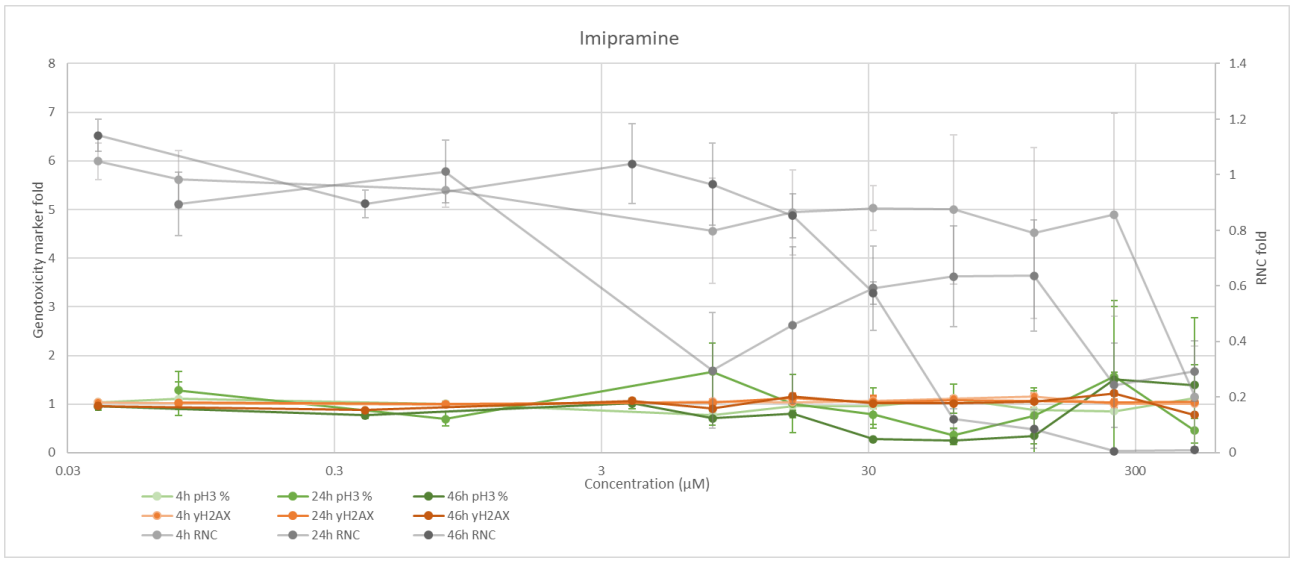
Imipramine
Genotoxicity marker fold
RNC fold
Concentration (µM)
0.03
0.3
3
30
300
4h pH3 %
24h pH3 %
46h pH3 %
4h γH2AX
24h γH2AX
46h γH2AX
4h RNC
24h RNC
46h RNC

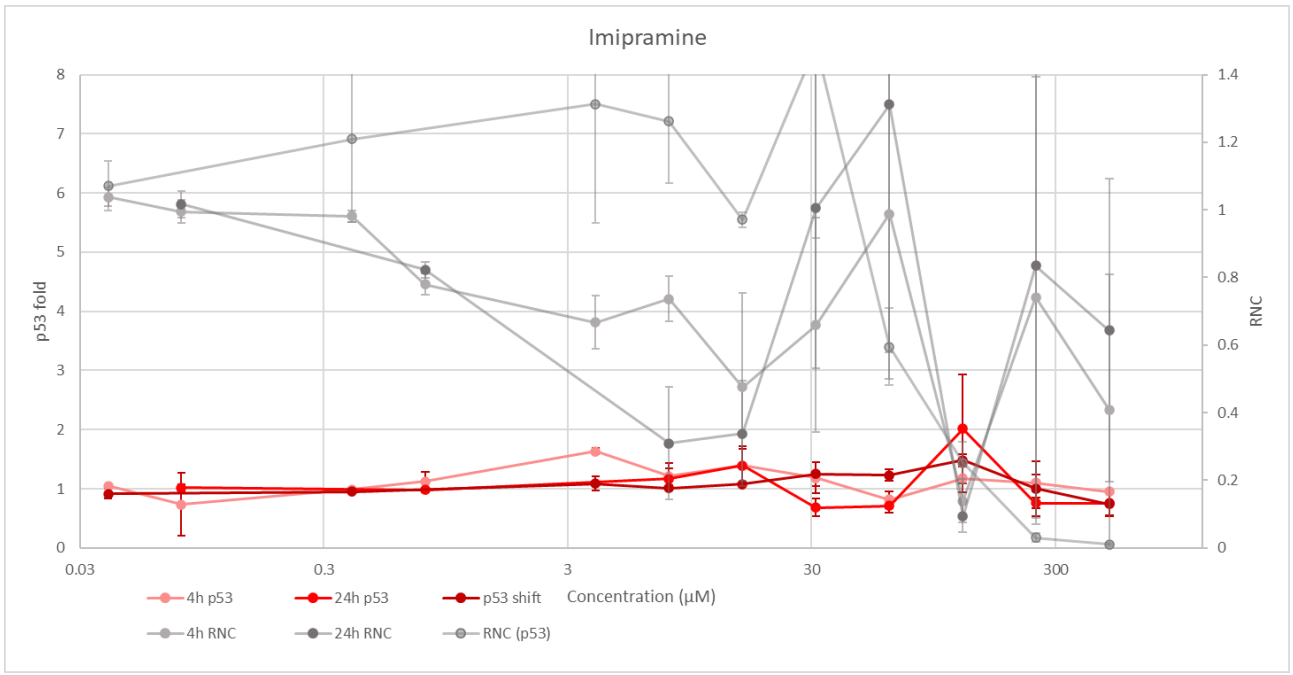
Imipramine
p53 fold
RNC
Concentration (µM)
0.03
0.3
3
30
300
4h p53
24h p53
p53 shift
4h RNC
24h RNC
RNC (p53)